uOttawa

L'Université canadienne
Canada's university

FACULTÉ DES ÉTUDES SUPÉRIEURES ET POSTOCTORALES

uOttawa

L'Université canadienne
Canada's university

FACULTY OF GRADUATE AND POSDOCTORAL STUDIES

Jayson Current

AUTEUR DE LA THÈSE / AUTHOR OF THESIS

M.A.Sc. (Civil Engineering)

GRADE / DEGREE

Department of Civil Engineering

FACULTÉ, ÉCOLE, DÉPARTEMENT / FACULTY, SCHOOL, DEPARTMENT

Development of a Pullout Test Method for Adhesive Applied Roofing Systems

TITRE DE LA THÈSE / TITLE OF THESIS

Dr. H. Tanaka

DIRECTEUR (DIRECTRICE) DE LA THÈSE / THESIS SUPERVISOR

Dr. A. Baskaran

CO-DIRECTEUR (CO-DIRECTRICE) DE LA THÈSE / THESIS CO-SUPERVISOR

EXAMINATEURS (EXAMINATRICES) DE LA THÈSE / THESIS EXAMINERS

Dr. B. Martin-Perez

Dr. D. T. Lau

Gary W. Slater

Le Doyen de la Faculté des études supérieures et postdoctorales / Dean of the Faculty of Graduate and Postdoctoral Studies

Development of a Pullout Test Method for Adhesive Applied Roofing Systems

By

Jayson Current

A thesis presented to the University of Ottawa in partial fulfillment of the requirements for

The Degree of Master of Applied Science

in Civil Engineering

The M.A.Sc. program in Civil Engineering is a joint program with Carleton University administered by the Ottawa-Carleton Institute for Civil Engineering

Department of Civil Engineering
University of Ottawa
Ottawa, Ontario, Canada

April 2009

Your file Votre référence
ISBN: 978-0-494-51643-0
Our file Notre référence
ISBN: 978-0-494-51643-0

Acknowledgments

This research was carried out as a part of a collaborative research project between the National Research Council Canada (NRC) and the University of Ottawa, entitled "Development of wind uplift standard for adhesive applied low slope roof systems", under the support of NSERC CRD grant (CRDPJ 3065819-04). This research was sponsored by four Canadian roofing industry partners and a Special Interest group. It would have been impossible to conduct the research presented herein and their support and contributions are greatly appreciated. They include:

- Bakor Inc.
- IKO Industries Ltd.
- Roofing Contractors Association of British Columbia, Canada
- Soprema Inc. Canada
- Tremco Inc. Canada

I'd also like to thank my research and academic supervisors, Dr. Bas Baskaran & Dr. Hiroshi Tanaka, for their efforts in supervising my thesis.

Through working with Dr. Baskaran, I have a gained an enormous amount of knowledge about roofing and roofing technology. His wealth of experience in this field has provided me with a core roofing backbone that has assisted me in the development of this thesis. He was also very supportive in ensuring that I had adequate financial assistance while I carried out the experimental work for this thesis, wrote this thesis, and fulfilled my academic obligations. Dr. Baskaran also assisted me by providing invaluable guidance and constructive criticism in the final stages of writing this thesis.

I also appreciate the invaluable input from Dr. Tanaka. His years of experience with graduate students provided me with valuable input on how to successfully complete a Master's Thesis. Through his extensive experience in the Civil Engineering Dept at the University of Ottawa, Dr. Tanaka also was able to provide guidance in course selection by helping me to select appropriate classes.

Overall I believe that my working relationship with Dr. Baskaran and Dr. Tanaka have helped to deliver a high quality thesis delivered in a timely manner.

Throughout the time spent conducting research at the NRC, I have had the pleasure of being acquainted with other colleagues of the IRC-NRC and other graduate students at the University of Ottawa and Carleton University.
Dr. Ralph Paroli, Director of the Building Envelope & Structure of NRC-IRC, facilitated a working environment for me to carry out my research work at NRC-IRC. Jun Wu, Bona Murty, and Weihong Li - my labmates, have always made themselves available to help me with problems and to provide me with moral support when things didn't go as planned.
I also would like to thank NRC-IRC technical officers and staff for creating a friendly and positive working environment. They include Steven Ko, Helen Yew, Darcy Boudreau, Amor Duric, Kevin Deeljur, Sebastian Evoniak and, Sudhakar Molleti who provided various types of support throughout the development of this thesis.

I am also grateful to a number of technical colleagues who were able to facilitate construction of specimens, and to answer technical questions when I had difficulties. They include Mr. Dave Miller, Mr. Peter Saunders, Mr. Marcel Lemieux, Mr. Paul Hastings, Mr. Paul Neville, and Mr. Mike Bisson.

Abstract

A review of literature and standards revealed no standardized process exists for the evaluation or characterization of wind uplift resistance of Adhesive Applied Roofing Systems (AARS). It was determined that a pullout test method – a test in which the adhered components of roofing samples were subjected to tensile loading until failure – could be used to quantify wind uplift performance. From the literature study, critical variables were extracted. Among these were the pullout rate, the specimen size and the specimen attachment condition. After conducting a series of extensive pullout tests, data showed that the optimum pullout rate was 6.35mm/min. Additional tests showed that a specimen size of 300 mm x 450 mm with all flutes fastened provided the experimentally consistent data. Based on the investigation outlined above, the present study drafted a standard test method for the determination of the pullout resistance of adhesively applied roofing components. This contribution is being presented to the Canadian Standards Association (CSA) and American Society of Testing Materials (ASTM) for adoption of a standardized test method. The present study also implemented the standardized test procedure to characterize the pullout behaviour of a variety of different configurations. Over 400 specimens were constructed varying the deck type (steel & concrete), insulation facer (paper and acrylic facer) and coverboard (fiberboard and asphalt core board). Experimental results showed that the use of steel deck, paper faced polyisocyanurate, and asphalt core board yielded optimum pullout resistance. Alternative adhesion patterns were also tested and showed a maximum reduction of 60% from the optimized adhesion pattern.

Table of Contents

List of Figures

List of Tables

List of Symbols

AARS	Adhesive Applied Roofing Systems
ACB	Asphalt Core Board
AF	Acrylic Facer
ASTM	American Standardization and Testing Materials
BUR	Built Up Roof
EN	Eurocode
FA	Full Adhesion
FB	Fiberboard
FM	Factory Mutual
ISO	International Standardization Organization
MARS	Mechanical Attached Roofing System
PA	Partial Adhesion
PF	Paper Facer
SPRI	Single Ply Roofing Industry

Chapter 1: Introduction

1.1 Roofing Systems

Roofs are a basic element of shelter and provide the fundamental needs of building inhabitants. Roofing systems perform an integral role by protecting inhabitants from the adverse effects of weather. These include temperature gradients, wind, snow, rain and protection from the sun's ultraviolet rays. The roofing system also performs the role of sealing the top portion of the building envelope. However, different types of buildings require the use of differently designed roofs to meet the specific demands of the overall building's function.

A modern roof design includes several components. There must be a component that can carry dead and live structural loads. There also has to be a barrier to prevent the infiltration of air that carries water vapour. A component must also control the flow of heat and finally an element to prevent the infiltration of water as outlined by (Garcia et al., 1997). Preventing the infiltration of water into the building is a critical role that the roof must perform. Water leakage can lead to the growth of mould, loss of insulation performance, and the onset of corrosion; factors that degrade the structural and thermal performance of the building as well as affect building inhabitants.

One of the most salient differences between residential roofing systems and commercial & industrial roofing systems is the roof slope. Commercial and industrial buildings typically have flat or low-slope roofs while residential roofs generally have steeper slopes (Molleti, 2006). In figure 1.1 an illustration has been provided of some of the common types of roofing systems that are employed for residential use in Canada. Figure 1.2 illustrates the roofing systems that are employed for commercial and industrial use.

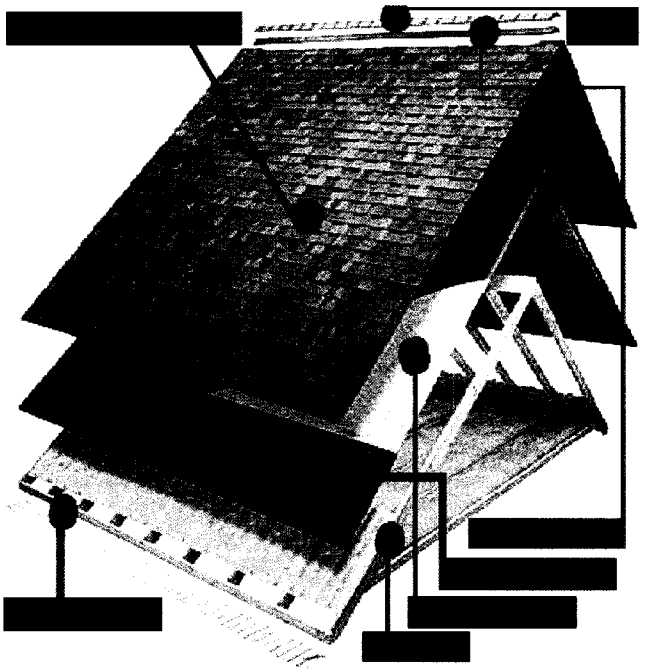

Figure 1.1a: Cross-section of commonly encountered residential roofing system in Canada - Asphalt Shingles (Source: http://cmroof.com/)

Figure 1.1b: Illustration of commonly encountered residential roofing system in Canada – Metal Roofing (Source: www.allsteel-buildings.com)

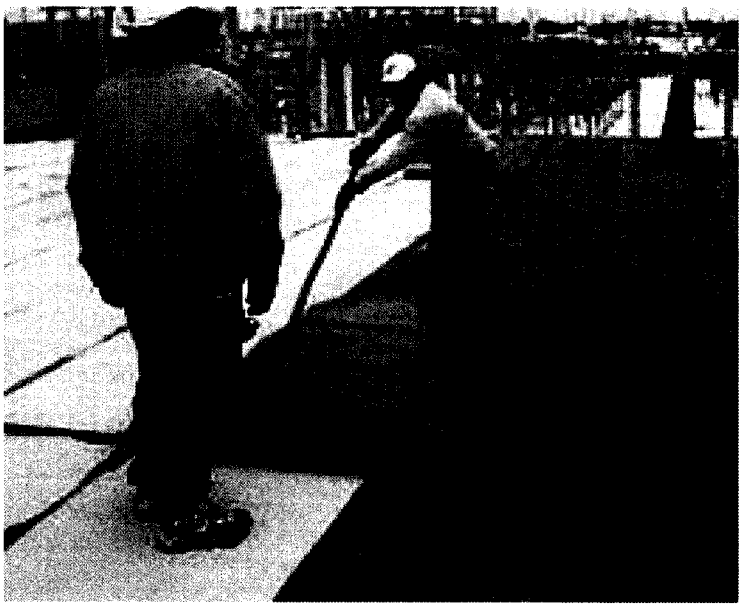

Figure 1.2a: Illustration of Built-Up Roofing System
(Source: www.reliantroofingsystems.com/)

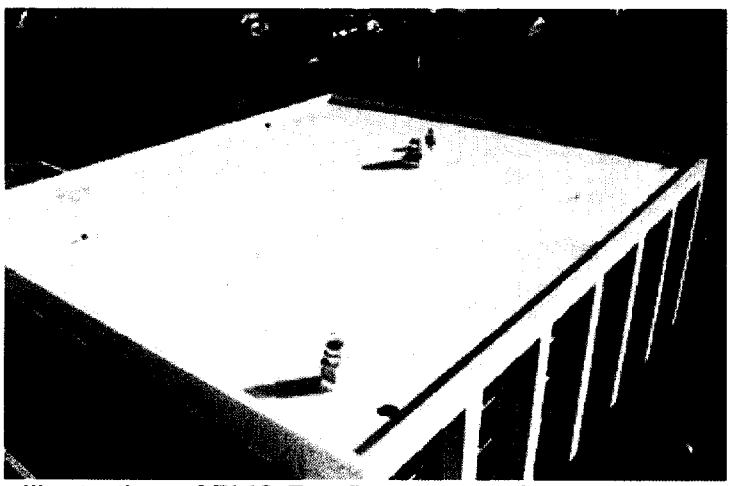

Figure 1.2b: Illustration of PVC Roofing system for commercial application
(Source: www.yourguardianroof.com)

There are an abundant number of roofing systems that are employed for sheathing the top surface of residential roofing systems. These include asphalt and composite shingles, wood shakes, clay and concrete tiles and metal sheets. However for commercial and residential systems, the built-up roof (BUR) is the most common roofing system employed in Canada. The focal point of this investigation is a variation of these types of roofs.

BUR shares similarities with many other roofing systems applied in commercial and residential applications from the structural level (deck) to the heat flux control component (insulation), as shown in Figure 1.3. However, the primary difference in this system when compared to other commercial roofing systems is the method by which exterior waterproofing is performed. After the installation of the insulation, BUR systems are installed by laminating successive layers of roofing felts with a bituminous material or hot asphalt. (Baker, 1964) Typically hot asphalt is mopped over a sheathing material that protects the insulation from the excessive heat of the asphalt. Layers of felt are then laminated together as the asphalt cools. There are several concerns with respect to the BUR systems. Construction of BUR systems are labour intensive processes that drive up the cost of installation. Due to the application of the hot asphalt, there are also concerns with fire propagation. The asphalt also produces toxic fumes that endanger the health and welfare of the workers installing the roof. Figure 1.4 illustrates what one can expect to see on a job-site undertaking the installation of a BUR.

However with the improvement in manufacturing technology and materials research, alternatives to this popular roofing system are being developed.

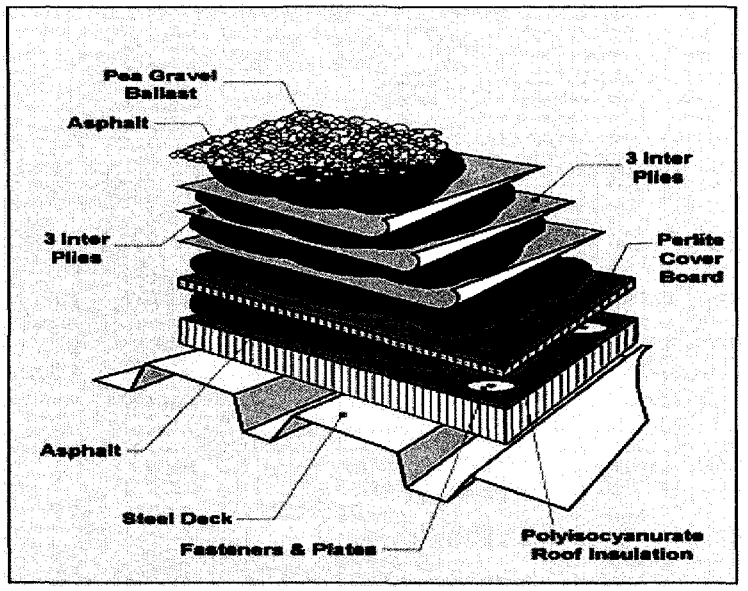

Figure 1.3: Constituent materials of BUR system

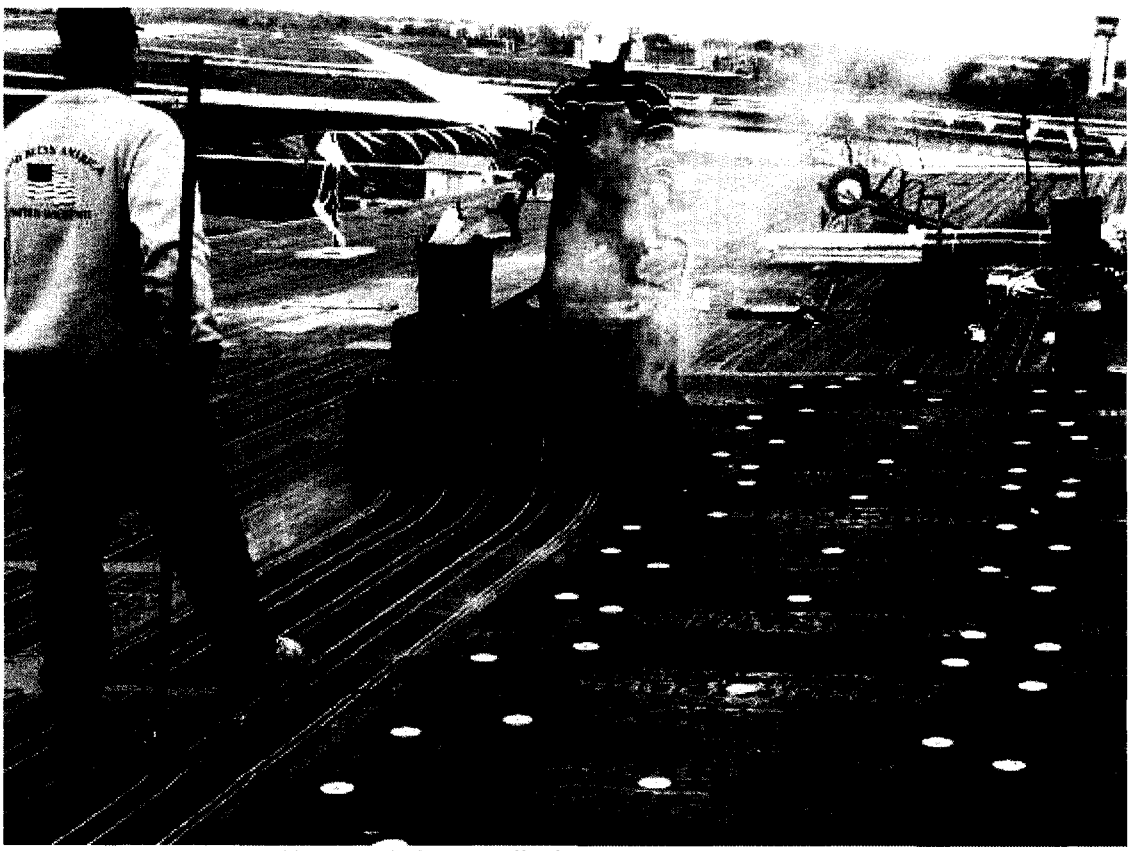

Figure 1.4: Installation of a BUR system
(Source: www.ddinstallations.com)

1.2 Features of Adhesive Applied Roofing Systems.

The application of cold adhesives as a substitute for asphalt is emerging as a popular trend in the roofing construction market. (Kirby, 2006) Cold adhesives eliminate the dangers of fire and toxic fumes that are present in the application of hot asphalt and bitumen. As a result, cold adhesives alleviate some fire and safety concerns.

Adhesive applied roofing systems (AARS) are the next generation of BUR and AARS use cold adhesives to laminate successive layers of roofing components to one another. Figure 1.5 illustrates a cross section of an AARS roofing system and consists of the following components and materials:

- Structural Material: Deck
- Air and Vapour Sheathing: Vapour Barrier
- Thermal Protection: Insulation
- Insulation Sheathing: Coverboard
- Water Tightness: Base & Cap Sheet

The roof deck supports the self weight of the roofing system and provides support for live and dead loading. The vapour barrier is a thin layer that prevents the diffusion of water vapour by preventing the flow of air into the building envelope. Insulation prevents the gain or loss of heat to maintain an ideal ambient indoor temperature. Coverboard does not have a single role but instead fulfills several. It is a material that provides an additional layer to prevent the infiltration of water from the exterior roof surface to the insulation and into the building envelope. It also can enhance the fire rating of the roofing system and provides a barrier for roof constructers to walk on and prevent impact damage to the insulation once it has been placed during construction. Glue or heat laminated base sheet and cap sheet provide the primary waterproofing to prevent leaks over the course of a building's life. Together these components form the backbone of the AARS roofing system and each layer is adhered to the adjacent one with cold adhesives. The installation of an AARS roofing system has been shown in figure 1.6.

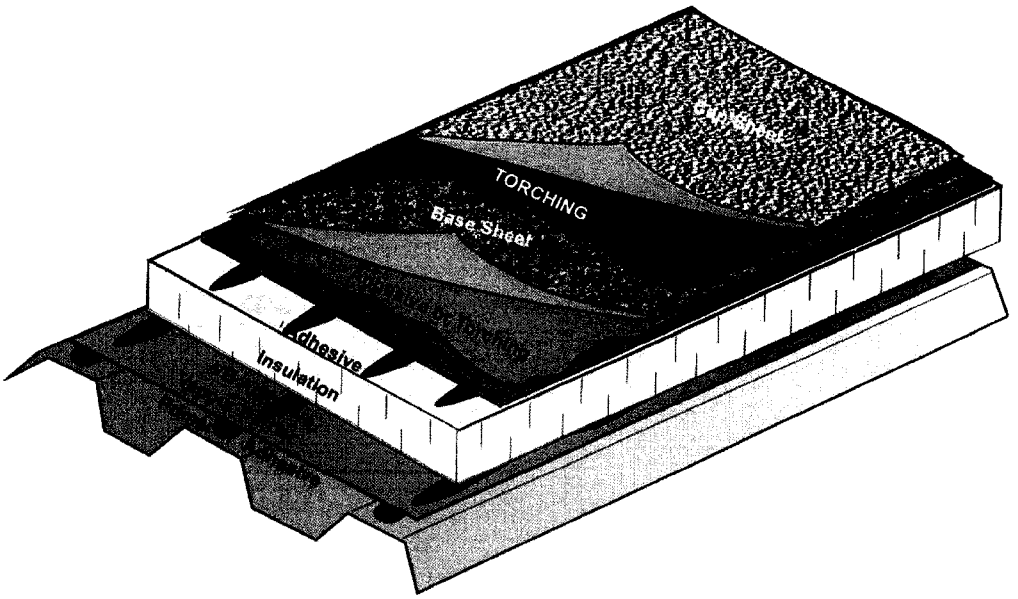

Figure 1.5: Constituent components of AARS

Figure 1.6: Field installation of AARS roofing system

Because of the differences in materials and construction methodology there are distinct advantages and disadvantages associated with the use of BUR and AARS. The salient difference in between the two systems is the presence of fasteners in BUR. Fasteners attach the insulation to the deck and this construction methodology creates two problems that hinder overall roof performance. Fasteners, constructed from steel allow thermal bridging to deteriorate a building's thermal performance by allowing heat flux through the fastener. Fastener holes also create a route that permits water vapour containing air to infiltrate into the building envelope. This usually results in premature corrosion of fasteners. Neither of the problems mentioned above are encountered in AARS because cold adhesives eliminate the need to mechanically attach any roofing components. Although the use of torch and flame can be used to laminate the base and cap sheet in AARS, specific materials have been developed that allow roofers to apply the base and cap sheet with cold adhesives. This is another advantage – the lack of torch and flame improves workers health and safety and benefits the construction companies by decreasing potential job-site disasters. One significant disadvantage of AARS is that it is a labour intensive construction process, more so than BUR. This is because ensuring proper construction depends heavily on the worker's training and of following proper AARS construction protocol.

1.3 Problem Definition

Wind flow around buildings creates both negative and positive pressure fluctuations over a roofing system. Negative pressure on the exterior roof surface is created by the flow separation on the outside of the roof. (Baskaran et al, 2006) The worst suction coefficients on roofs of low buildings are known to occur in the corner caused by the development of conical vortices during cornering winds (Banks, 2000, Banks et al, 2000). As the wind blows over the roof away from the edges and corners, the effects of the wind become less critical. This

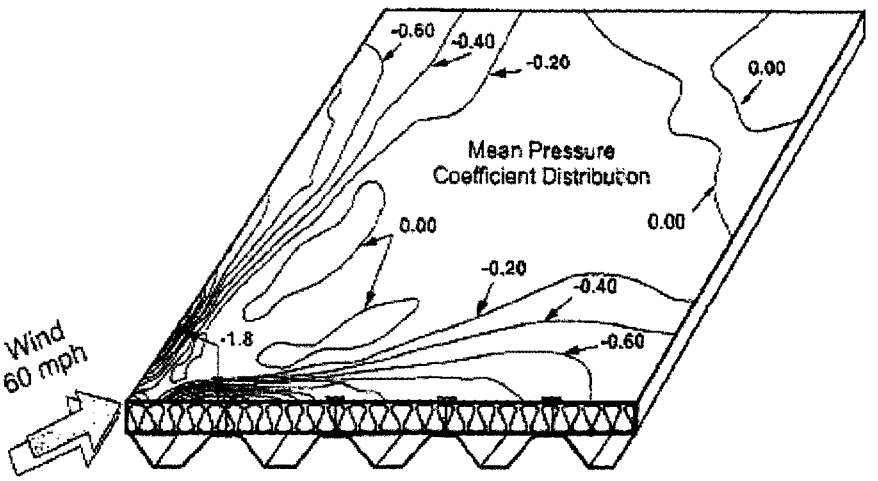

Figure 1.7: Pressure Coefficient Contour Map (Baskaran et al, 2006)

Figure 1.8: Wind Uplift Failure of Roofing System during Hurricane Charley (Baskaran et al, 2006)

Figure 1.9: Wind Uplift Failure of Roofing System during Hurricane Charley (Baskaran et al, 2006)

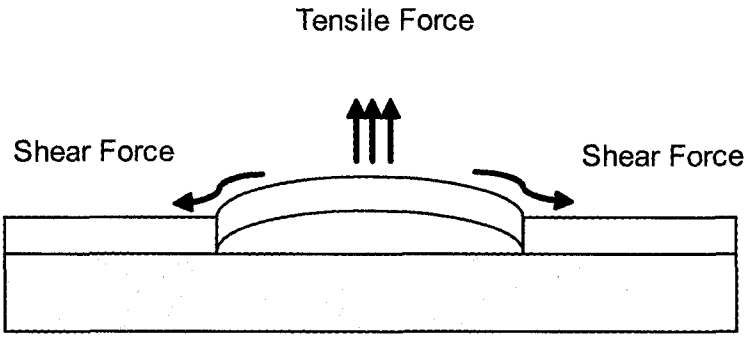

Figure 1.10: Simplified view of driving force causing roof failure due to wind action

phenomenon has been illustrated on a pressure coefficient contour map in Figure 1.7.

Since AARS are bonded together with cold adhesives, naturally AARS materials and adhesives provided resistance to the wind uplift action. The external surface of AARS consists of a flexible roofing membrane, the pressure fluctuations can cause localized failure which can propagate and lead to overall roofing failure. Figures 1.8 and 1.9 show the end result of excessive wind loading and membrane lifting and overall roof failure caused by Hurricane Charley (Baskaran, et al, 2007). Note in Figure 1.8, that wind action caused the exposure of the insulation – demonstrating the amount of damage severe wind action can cause. Blister failure is the most common reason for premature failure of AARS, and it leads to the loss of watertight integrity of AARS membranes (Thomas, 1993). In figure 1.10, a simplified view of the roofing membrane has been shown illustrating the driving forces of roof failure due to wind action. These are the fundamentals forces caused by wind that lead to the failures illustrated in Figures 1.8 and 1.9.

There is a very limited amount of published information about the wind uplift performance of AARS. No existing standards quantify the performance of AARS and many existing wind uplift roofing standards are predicated on fastener pullout performance; which makes previous experimental work irrelevant with respect to AARS. What is required is a test method for evaluating the pullout resistance of AARS. This report proposes the experimental results for the development of a pullout test which will be used for evaluating the wind uplift performance of an AARS.

1.4 Thesis Objectives

Although the extremes of the Canadian climate have provided a niche for AARS in the Canadian roofing market, there is a lack of standard procedures and approved testing methods for evaluating this roofing system with respect to wind loading. The project entitled "Development of wind uplift standard for adhesive

applied low slope roof systems" was carried out by the National Research Council Canada, University of Ottawa and four Canadian roofing industry partners, supported by a NSERC (Natural Sciences and Engineering Research Council of Canada) CRD (Collaborative Research and Development) grant (CRDPJ 3065819-04). Overall, this joint project includes the following five tasks (Current, Murty, Wu, Baskaran and Tanaka, 2008):

- Task I: Pullout testing
- Task II: Peel testing
- Task III: Wind uplift testing
- Task IV: Numerical modeling
- Task V: Development of design guidelines

The present study addresses Task I of the aforementioned tasks. The contribution of this thesis is to provide a standardized test method for determining the pullout resistance of AARS systems. To accomplish this objective, these steps have been followed:

Step 1: Review existing standards for pullout strength, adhesion strength and other relevant standards of this nature with respect to construction materials. From these standards, extract key variables that will require specification in the development of a standardized test.

Step 2: Based on existing standards, develop the scope for a test method and specify the key parameters.

Step 3: Apply the developed test method to conduct experimentation to characterize the pullout behaviour of AARS.

Step 4: Develop a standard test method through the collection of data from Steps 2 & 3. This standard test method will provide the Canadian roofing industry with guidelines for the construction of AARS.

1.5 Thesis Outline

In addition to this introductory chapter, this thesis report contains the following chapters:

- Chapter 2 is a literature review of current pullout standards. These standards are the relevant Canadian, American, and European standards that are currently in practice in these geographic locations. The standards govern the minimum requirements for pullout resistance with respect to building materials and assist in providing starting points as to what are the key variables that require specification for pullout resistance.

- Chapter 3 describes the specimens and the apparatus by documenting the specimen construction process. Based on the literature review of Chapter 2, this chapter will provide the rationale behind the selection of specific variables. This chapter will also illustrate the Instron machine and the necessary modifications that were made in order to conduct pullout testing.

- Chapter 4 describes the experimental setup, and provides definitions of numerical and qualitative observations. This chapter will provide an illustrative step-by-step breakdown for a setup of a pullout test. This chapter will also provide an explanation for the classification of failures as well as a definition of the numerical quantities used for quantifying uplift resistance.

- Chapter 5 presents the results of experimentation that was conducted to determine the variables that required specification for the development of a standard test method for the determination of pullout resistance of AARS specimens. Among these variables are the pullout rate, the specimen size and the fixation condition. Generalized curves of pullout resistance will be developed where applicable by analyzing quantitative results as well as using the failure classifications provided in Chapter 4.

- Chapter 6 presents the experimental results by applying the findings of Chapter 5. The effect of different material combinations were tested, along with different deck types and a different VB-deck adhesion.

- Chapter 7 proposes a draft standard test method for pullout resistance of AARS.

- Chapter 8 summarizes the conclusions of this study and the lessons learned throughout the course of experimentation. It identifies future areas of research, as well as shortcomings of this study.

Chapter 2: Literature Review

2.1 Introduction

As discussed in the preceding chapter, the continued application and popularity of AARS in the Canadian roofing market will require the development of standards related to wind uplift performance. An uplift test, or pullout test would be an effective means to determine uplift strength at the small-scale in order to make projections of the behaviour of the roofing system at full-scale. In order to achieve this objective, a pullout test scope as well as guidelines on how to setup, conduct, and analyze the experimental data are necessary.

Before the proposal of any test method is put forward, an examination of the available literature that characterizes wind uplift must be performed, as well as any pullout tests of a similar nature. Relevant topics include the analysis of:

- Wind performance and applied uplift tests
- The tensile strength of an adhesive
- Pull-off adhesion of coatings
- Adhesive strength tests with respect to external environments

These standards and test methods have been selected because many of the defining characteristics of these tests should be reverse engineered and applied for the development of a pullout test for AARS. As such, an extensive review of the existing standards will reveal slight similarities in the development of the test method proposed in this thesis. All of the standards that will be discussed are currently in practice in North America and Europe. These existing standards were developed by the following organizations:

- American Society for Testing and Materials (ASTM)
- International Standards Organization (ISO)
- European Standards (EN),
- Single Ply Roofing Industry (SPRI)
- Factory Mutual (FM)

In this chapter, a review of the relevant standards published by the preceding standardization organizations will be presented. In section 2.2, a clarification and definition of relevant terms outlined in the proceeding sections will be provided. In section 2.3, a review of relevant ASTM Standards will be presented. In section 2.4, a review of ISO standards will be presented. In section 2.5, a review of EN Standards will be presented. Section 2.6 will review standards from SPRI and section 2.7 will review standards from FM. Section 2.8 will summarize the similarities in these test methods in order to determine the key parameters that will predicate a test method. Finally, Section 2.9 will provide some concluding remarks with respect to how this literature study was able to provide direction in the development of a test standard for the wind uplift performance of AARS.

2.2 Clarification of Terms

ASTM International, or the American Society of Testing and Materials is one of the largest voluntary standards development organizations in the world. Although ASTM was formed originally to improve railroad travel by standardizing the steel used in rail construction, ASTM has evolved to improve the quality and safety of consumer products, as well as to better manufacture these products in a more cost-effective fashion. The ASTM 30 000 member group includes technical experts represented by manufacturers, consumers, government and members of academia. Since ASTM standards originate in the United States many are observed in practice in Canada.

ISO - The International Organization for Standardization is the world's largest developer and publisher of international standards. Many ISO standards are implemented across the globe. At its core, ISO is a non-governmental organization that forms a bridge between the public and private sectors. As a result, it permits a consensus and the development of solutions that meet the diverse requirements of business, manufacturers, testing laboratories,

professional engineering groups, the public, and the government. Since it is a collaborative international agency, these standards satisfy both industry and customers world-wide. As a result of the international nature of these standards, there is no enforcing body that stipulates the implementation of these standards and ISO member bodies follow the guidelines and standards developed on a voluntary basis.

EN, or the European Committee for Standardization is another group consisting of industry, government, and civil society, committed to promoting the development of a coherent European Standardization System. Through it 13-country member association, standards are developed through a consensus process similar to ASTM and ISO. Since there are many partner nations, slight variations from nation to nation are permitted however the European Standards must be transposed in national standards and conflicting standards removed. An example of a European Standard would be BS EN 1348:2007. The "BS" pre-fix would signify that this is a British Standard. The standard is numbered 1348 and was created or updated in 2007. By substituting the "DIN" prefix for the "BS", this would signify that the standard was the same as the original except that the "DIN" standard was applicable to Germany.

SPRI or the Single Ply Roofing Industry is a recognized technical and statistical authority on the single ply roofing industry. SPRI is a trade organization that collectively works within the single ply roofing industry to improve product quality, and installation techniques, and to provide technical guidelines for design, maintenance and repair. SPRI projects include proactively advancing technology, the resolution of technical issues and to impact code and testing issues.

FM or Factory Mutual provides global commercial and industrial property insurance risk managements solutions. As a mutual company, FM provides direct support for client's overall risk management objectives. FM provides sound loss

preventions solutions that safeguard against loss and develops cost-effective insurance and risk transfer solutions.

2.3 Review of ASTM Standards

This section will review relevant ASTM standards, with the relevancy as defined in section 2.1.

2.3.1 ASTM D 2095-96
Standard Test Method for Tensile Strength of Adhesive by Means of Bar and Rod Specimens

This test method covers the relative tensile strength of adhesive by the use of bar- and rod shaped butt-joined specimens under defined conditions of preparation, conditioning, and testing. A minimum of 5 specimens for each test condition are tested on a tensile testing machine, capable of maintaining a specified rate of loading with the error for indicated loads that are to be measured not exceeding +/- 1% and the load indicating mechanism essentially free of inertial lag at a specified rate of loading. The test specimens consist of two separate members adhered to one and other. One of the members will be fixed while the other will be movable. Self-aligning attachment fixtures are required for holding the aforementioned members. These fixtures are illustrated in Figure 2.1. Tests must be performed in a room conditioned to a relative humidity of 50+/-2% at a temperature of 23+/-1°C.

Specimens are placed in the testing machine and loading is applied at a rate of 17-20 MPa/cm^2 of bond area per minute. The maximum load carried by the specimen at failure is recorded along with visual observations that include the percentage of cohesive failure, adhesion failure, contact failure and adherend failure.

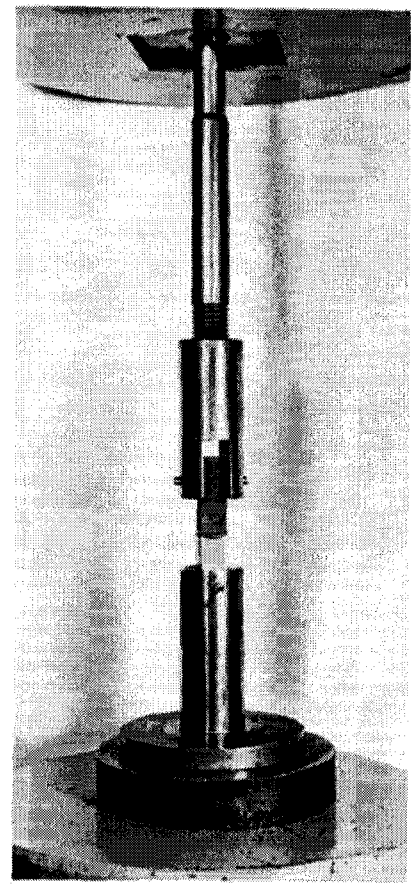

Figure 2.1: Test Specimen with Attachment Fixtures Assembled in Tension Testing Machine (ASTM D 2095 – 96)

2.3.2 ASTM D 7234-05
Standard Test Method for Pull-Off Adhesion Strength of Coatings on Concrete Using Portable Pull-Off Adhesion Testers

This test method covers procedures for evaluating the pull-off adhesion strength of a coating on concrete. This test uses an apparatus that applies concentric loads and counter loads through a loading fixture to a single surface so that coatings can be tested even though only one side is accessible.

The general pull-off adhesion test is performed by scoring through the coating down to the surface of the concrete substrate at a diameter equal to that of the loading fixture. The loading fixtures have a flat surface on one end that can be adhered to the coating and a means of attachment to the tester on the other end. The flat surface on the loading fixture, which represents the contact test area, typically is 50 mm in diameter, but can range on the order of 20-75mm. A selected test area must be a large flat area, with enough space to accommodate the minimum (3) number of test replications. Scoring cuts, will be made normal to the surface being tested and in a manner that does not twist or toque on the test area. The "dummy adhesive" will be applied in a full-coat on a clean surface following the specifications as laid out by the manufacturer.

Once the test sites have been properly prepared, the loading fixture is attached concentrically to the pull-off adhesion tester. The test begins with a fixed rate of loading of 0.2MPa/s, so that failure occurs before 30 seconds has elapsed from the start of the test. The test setup has been illustrated in Figure 2.2.

2.3.3 ASTM D 5179-02
Standard Test Method for Measuring Adhesion of Organic Coatings to Plastic Substrates by Direct Tensile Testing

This test method covers the laboratory determination of organic coating adhesion to plastic substrates by mounting and removing an aluminium mounting fixture from the surface of the coating and measuring the force required to break the coating/substrate with a tensile tester.

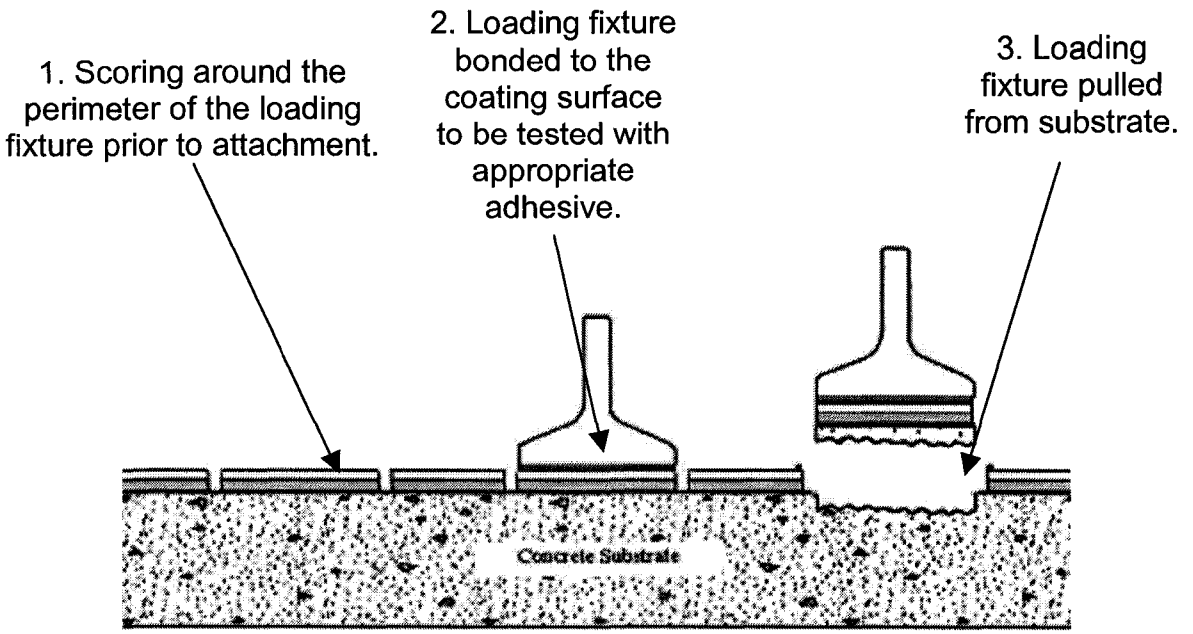

Figure 2.2: General Experimental Setup (ASTM D 7234 – 05)

An adapter is used to attach an aluminium-mounting fixture to the tensile tester. The test method provides specific instructions for the sanding and cleaning of the adhering surface for preparation for testing. A cyanoacrylate adhesive is placed on the aluminium-mounting fixture and immediately pressed onto the coated test substrate. A 2 kg dead load is applied afterward for 2 minutes to ensure proper bonding and the adhesive is left to cure for 2 hours at room temperature.

To start the test a restraining device is installed with the upper adaptor and both are attached to the tensile tester. The specimen is then attached to the restraining device and the tensile tester is jogged so that the upper adaptor can be attached to the test specimen. The tensile test is started and a fixed pull rate of 50 mm/min is applied and stopped when complete failure has been achieved. A minimum of 5 repetitions is performed. In the final report, the maximum stress is reported, along with the planes of failure observed.

2.4 Review of ISO Standards

This section will review relevant ISO standards, with the relevancy as defined in section 2.1

2.4.1 ISO 15509
Determination of the bond strength of engineering plastic joints

This international standard describes a test method for measuring the shear and tensile strength of adhesively bonded plastic/plastic specimens of a specific design.

A hollow cylindrical test specimen of specific design is used for the determination of shear and tensile strengths of the adhesively bonded joint. The circular cross-sectional area permits loading to be in tension, shear and torsion. Plastic moulds are prepared with the bonding area with an outer diameter of 38 mm and inner diameter of 24 mm as shown by the dimensions of the mould

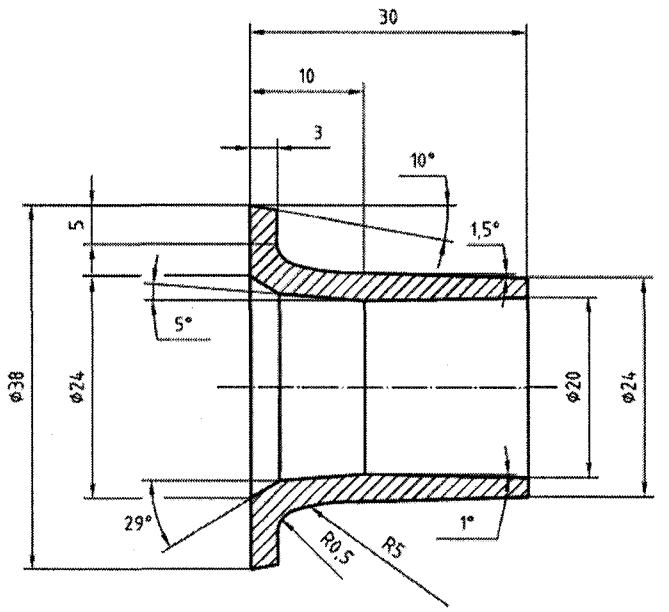

Figure 2.3: Plastic Mould Used to Create a Hollow Cylindrical Test Specimen (ISO 15509)

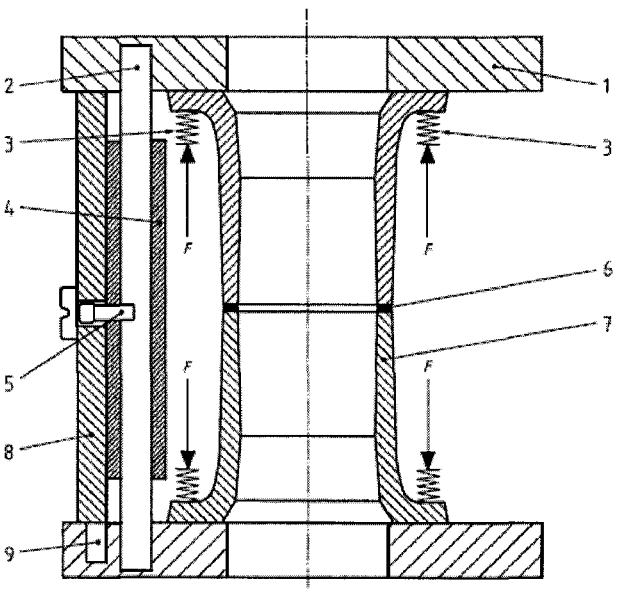

Figure 2.4: Mounting Jig Used for Determining Bond Strength (ISO 15509)

1 Baseplate
2 Guide Pin
3 Fixation holding the adherend on the baseplate
4 Metal Sleeve
5 Screw for fixing spacers on sleeve
6 Gap for adhesive bond
7 Adherend
8 Bond gap thickness spacer
9 Adjustment screw

illustrated in Figure 2.3. The bonding surfaces are to be prepared as per ISO 13895.

A hollow cylindrical test specimen of specific design is used for the determination of shear and tensile strengths of the adhesively bonded joint. The circular cross-sectional area permits loading to be in tension, shear and torsion. Plastic moulds are prepared with the bonding area with an outer diameter of 38 mm and inner diameter of 24 mm as shown by the dimensions of the mould illustrated in Figure 2.3. The bonding surfaces are to be prepared as per ISO 13895.

The two adherends will be placed in a mounting jig, shown in Figure 2.4, and separated by a spacer. The spacer is part of the mounting jig and is required to define a finite bond thickness. Once the mounting jig is adequately prepared, the adhesive is applied and left to cure in accordance with the manufacturer's specifications. A tensile force is applied at a rate of 1 mm/min. If torsional strength was required, a torsional load of 5°/min is required. The ultimate tensile force achieved as well as the failure pattern is reported.

2.5 Review of EN Standards

This section will review relevant EN standards, with the relevancy as defined in section 2.1

2.5.1 BE EN 1348: 2007
Adhesives for tiles – Determination of tensile adhesion strength for cementitious adhesives

This European standard specifies a method for determination of the tensile adhesion strength of ceramic tile adhesives for environments that include both inside and outside of the building envelope.

A concrete slab is prepared prior to testing. This slab will act as the base for test applications. The ceramic tile will be dry with water absorption of < 0.5% by mass, unglazed, matt, adhering surface with square facial dimensions of 50 +/- 1 mm.

The standard specifies a detailed outline for the preparation of the adhesive. A minimum of 2 kg of the dry adhesive is to be prepared and the method specifies that manufacturer's instructions for the amount of water/liquid to be applied should be followed. Once adhesive preparation is complete, it is applied to the concrete slab in 50 mm x 50 mm areas, with areas separated by 50 mm gaps. After 5 minutes ten ceramic tiles are placed on the adhesive and a 20.00 +/- 0.05 N load is applied to the top surface of the tiles for 30s.

This is where the test method diverges. The test method specifies four separate tests with each characterizing tensile adhesion under different environmental conditions. One test is for the initial adhesion strength, and another tests for the tensile adhesion strength after water immersion, another test specifies the tensile adhesion after heat ageing. The final test is an adhesion strength test after a freeze-thaw cycle. The test of particular interest here is the initial adhesion strength test. After 27 days of storage under ambient conditions, pull-head plates with dimensions that match those of the ceramic tiles (Squares with side of 50+/-1 mm) are adhered with a high strength adhesive like epoxide. The pull-head plates require a physical mechanism by which they can attach to a tensile tester apparatus. Once the pull-head plates have been attached and the entire assembly is installed, a tensile force with a constant rate of pull of 250 N/s is applied until failure. The failure load is observed and is reported along with the plane in which failure. Ten repetitions of the test are performed, and values that deviate by more than +/- 20% of the mean are rejected, and repeated until a minimum of five statistically relevant observations are observed.

2.6 Summary of SPRI Standards

This section will review relevant SPRI standards, with the relevancy as defined in section 2.1

2.6.1 SPR IA-1

Standard Field Test Procedure for Determining the Mechanical Uplift Resistance of Insulation Adhesive over Various Substrates

This test method specifies a field testing procedure to determine the mechanical uplift resistance of a specific roof insulation/adhesive combination using portable pull testing instrumentation. The test area and specimen will include:

- Substrate: Bare Deck of the existing system
- Vapour Retarder
- Insulation Layer
- Plywood Attachment Board

A sample size of 610 mm x 610 mm will be employed and all materials will be sized to these dimensions. Adhesive is applied to subsequent layers of materials as per manufacturer's specifications and allowed to cure for a period of time as provided by the adhesive manufactuer. A 50 mm wide strip through the roof covering around the test panel is to be cut to isolate the specimen from the rest of the roofing assembly. The pull-testing instrument is then connected to the plywood plate. Loads are applied perpendicular to the plywood plate. The test begins when the load equals 0.5338 kN plus the tare weight. This load is held for 60 seconds and then increased in 0.2669 kN increments for 60 seconds until catastrophic failure is observed. The maximum sustained load is recorded and a minimum of 4 repetitions are performed for the first 4650 m^2 of roof area and an additional 2 pull tests are performed for each additional 4650 m^2 of roof area. For different roofing conditions, such as different elevations or different deck substrate, testing shall be performed separately. A roof plan is also required showing the locations of the tests as well as a description of the failure.

2.6.2 SPRI FX1
Standard Field Procedure for Determining the Withdrawal Resistance of Roofing Fasteners

This test method specifies a field testing procedure to determine the withdrawal resistance of roofing fasteners using a portable pullout tester.

All roofing materials are removed from the test area to expose the deck and fasteners are installed using the same methodology and tools as will be used during actual construction. Fasteners will be pulled out perpendicular to the deck at a fixed and constant loading rate. This rate is not specified in the test procedure. A minimum of 10 pullout tests are performed for each 4650 m^2 and in various locations over the surface of the roof including the corners, the edge region and the field. The test must be performed by an individual trained by the manufacturer of the fasteners being tested and additional tests are performed for different roofing conditions, such as different elevations or different deck substrate.

2.7 Summary of FM Standards

This section will review relevant EN standards, with the relevancy as defined in section 2.1

2.7.1 FM I52
Field Uplift Testing

This test method covers the determination of the resistance of adhered membrane roofing systems to direct uplift pressure. This is performed by creating a negative pressure over the roofing membrane by means of a chamber fitted with a pressure measurement device and vacuum equipment.

In order to execute this test, a square dome chamber 1500 +/- 15 mm in size made of polycarbonate sufficiently strong to withstand the necessary negative pressures is used to create the vacuum. A dial indicator within the test chamber must also be installed in order to monitor membrane deflections. This

rigid bar is installed 50 mm above the roof surface. A manometer is used to measure the pressure. It must be able to indicate negative pressure measurements in increments of 360+/-20 Pa. A compressor is used and must be able to create pressure increments of 360 +/-20 Pa.

The dial indicator is installed on the roof surface and the dome chamber is centered overtop of the dial indicator. The pressure measuring device is installed and calibrated and the vacuum equipment is installed. Increment the negative pressure to 720+/- 20 Pa for 60 seconds and increase 360 +/- 20 Pa after every 60 seconds. The end of test occurs when one of the following conditions is met:

- The test pressure (the pressure that was agreed upon prior to testing as the target for successful completion) has been sustained for 60 seconds,
- Roof deflection exceeds 25 mm as measured by the dial indicator.
- Catastrophic failure has occurred.

Report the location of the test, characterization of the roofing materials, atmospheric conditions at the time of the test, the test pressure attained as well as observations from each incremental increase in test pressure. Repetitions will be performed along the perimeter and in the field of the roofing system.

2.8 Summary of Existing Pullout & Adhesive Tensile Strength Standards

Based on the literature review conducted in sections 2.3 - 2.7, the similarities and dissimilarities can be compared based on the test parameters discussed in the following section. When developing the standard for AARS, the similar variables and conditions from these test methods may be transferred over to the new standard, while experiments will have to be performed where there are dissimilarities between these test methods.

- Scope:
  - All standards evaluated in this chapter propose to quantify the performance of an adhesive joint when loading occurs normal to the plane of adhesion.

- Nature of Test
  - Testing consists of one fixed member (or a cut substrate) and one "moving" or "floating" member which is to be "pulled-off"
- Specimen Cross-Sectional Shape & Size:
  - Circular, ∅ =12.75 mm
  - Circular, ∅ = 50 mm
  - Circular, ∅ = ¾ in
  - Annulus, Inner ∅ = 24 mm, Outer ∅ = 38 mm
  - Square, L = 50 mm (2 Observations)
  - Square, L = 610 mm
  - Square, L = 1500 mm
- Number of Specimens:
  - All methods specify a minimum of 2-10 repetitions for each test
- Curing Time
  - Typically a curing time of 24 hours is recommended, however the test methods include the disclaimer that the curing time should be reflective of the manufacturer's specifications, and can be changed but must be decided prior to the beginning of testing.
- Curing Condition
  - Most specimen are to cured at 23 ±2°C at a relative humidity of 50±2%
  - When performed as a field test, specimens are to cure under ambient outdoor air humidity and temperature
- Loading Criteria:
  - 17-20 MPa/cm^2/minute (/cm^2 – refers to cm^2 of bond area)
  - 0.2MPa/s
  - 1 mm/min
  - 50 mm/min
  - 0.15+/- 0.01 MPa/s
  - 250+/-50N/s
  - 0.2669 kN / 60 seconds

- 360 +/- 20 Pa / 60 seconds

- Calculation:
  - All methods specify that at minimum, the global maximum load from the test should be reported
- Failure Location
  - All methods require a qualitative description of the plane in which failure occurs. In some cases failures have already been categorized based on a pre-existing standard.

2.9 Concluding Remarks

This chapter presented a survey of the various existing standards for pullout resistance tests of adhesive joints. From these existing standards, it is evident that there are some common similarities – all of these tests consist of a fixed and floating member. They require minimum numbers of repetition for statistical accuracy. They all require a common curing time and curing condition and all tests require the report of the peak load attained during testing as well as a description of the plane in which failure occurs. However, there are two areas in which all these methods differ. The test shape and area are different for almost all methods. Also the loading criteria or deflection rate, or more specifically, the mechanism which leads to failure, is different or dissimilar in each one of these test methods. In the development of a test method, these will be two key variables that will require experiments to be conducted in order to determine optimal parameters for these variables.

Chapter 3: Experimental Setup

3.1 Introduction

This chapter presents an experimental setup and procedure that has been developed by the present study to quantify the pullout resistance of AARS specimens. This experimental setup is aimed at characterizing the behaviour of AARS specimens when subjected to simulated laboratory wind uplift tensile loading.

Section 3.2 discusses the specimens that were constructed for the present study. This section will address the issue of what constitutes an AARS specimen, as well as the process taken to construct a specimen. It is important to note that there were four companies assisting in the construction of test specimens and although the materials used in the construction of roofing systems are similar, these companies employ different methodologies in the specimen construction. Similarities and differences will be outlined in section 3.2

Section 3.3 explains more thoroughly the selection of AARS test variables with reference to the overall objectives of this study. This section will be broken up into two. The first section will address variables that needed specification with respect to the development of a standardized test method. The second section will apply the standardized method and address variables that deal with applications of the test method and general characterization of AARS pullout behaviour.

Section 3.4 describes the experimental apparatus. The pullout tests on the AARS specimens were conducted using a 4502 series Instron frame. This section provides a description of the apparatus that was used to accommodate AARS specimens in the Instron frame.

3.2 Experimental Specimens

The following section provides a description of how AARS roofing specimens are constructed by all four companies that collaborated to complete this experimental investigation. Before getting into specifics of specimen construction, a clarification of terms that will be used in this and the following sections is required.

For the sake of intellectual property rights, the four partner companies will be referred to as Sources 1, 2, 3, & 4. When testing a variable, a source will construct a sample which consisted of 6 to 8 identically constructed specimens with identical parameters. The term "specimen" refers to what was actually constructed and tested. Multiple repetitions of specimens within a sample are required to provide statistical legitimacy to measurements taken in this investigation.

Another clarification is required to differentiate between the terms "component" and "material". A component would refer to something used in AARS construction that fulfils a defined specific purpose. For example, a component that is used to control the infiltration of water vapour into the building envelope is a vapour barrier. The material refers to the specific item that performs the role. In returning to the example, an adhered kraft paper vapour barrier controls the infiltration of water vapour into the building envelope.

Where possible, all materials were precut prior to the days of construction to facilitate an assembly line style of construction of experimental specimens. Under this format, a large volume of specimens could be constructed efficiently. The following sections will outline the steps that were taken for specimen construction.

3.2.1 Overview of Specimen Construction

This section will provide an overview of the steps taken to construct AARS specimens. Figure 3.1 shows a schematic of six different components that constitute AARS specimens and the locations of the adhesive within a specimen. There are nine steps that need to be completed in order to construct an AARS specimen as shown in Figure 3.1. These nine steps are illustrated with pictures from the actual specimen preparation that was undertaken during the course of this study in Figures 3.2a to 3.2i. In the following paragraph, a description has been provided of these specimen construction steps and is annotated with an alphanumeric code corresponding to the figure number illustrating this step of the construction process.

The first step of specimen preparation was to prime the deck. (Figure 3.2a), however, this was an optional step and was performed only if this was a procedure reflective of what was performed in the field. The next step was to adhere the vapour barrier (3.2b) to the primed or unprimed deck. Figure 3.2b illustrates a self-adhering vapour barrier. Following the application of the vapour barrier, vapour barrier-insulation adhesive was applied (3.2c) as per the specifications of the manufacturer and the insulation was adhered. (3.2d) Insulation-cover board adhesive was then applied (3.2e) and coverboard was adhered (3.2f). The next step was to apply the coverboard-base sheet adhesive (3.2g) and to adhere the base sheet (3.2h). Finally, after allowing some time for the adhesive to set, the cap sheet was torched to the base sheet. (3.2i) In some cases, membranes can also be adhered. In the following sections, more detailed information will be provided about the components that were used.

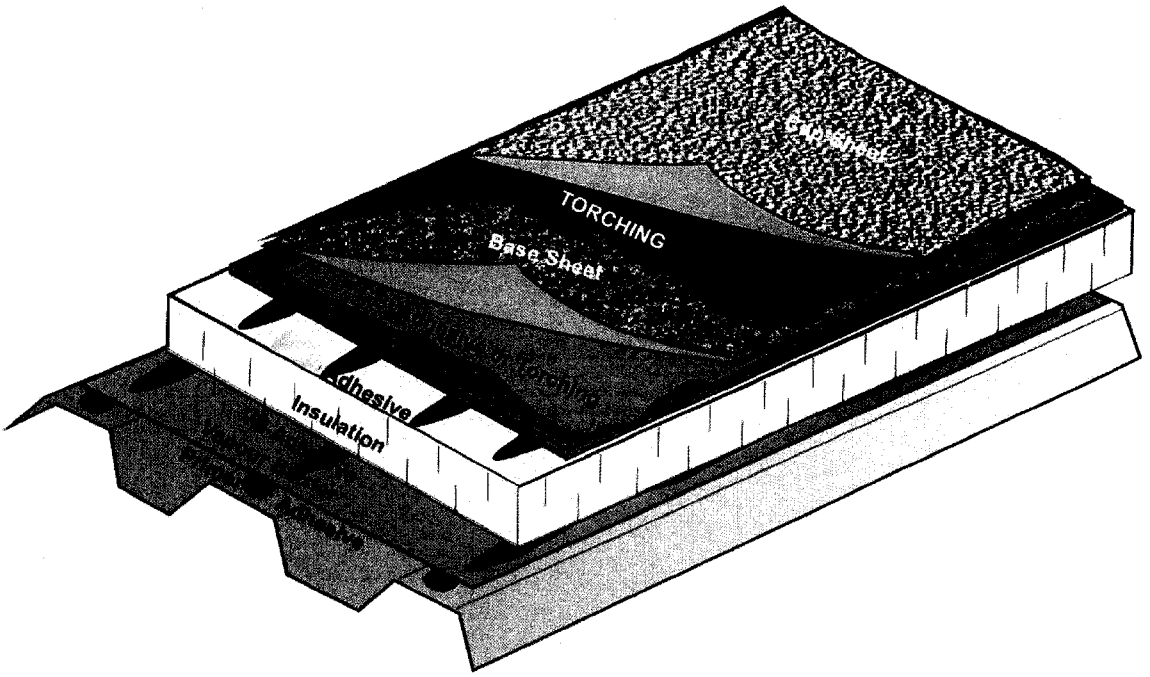

Figure 3.1: Overview of roofing components in AARS

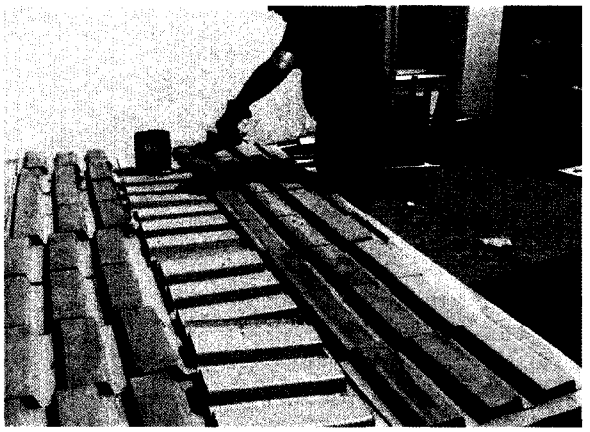

Figure 3.2a: Deck layout & priming

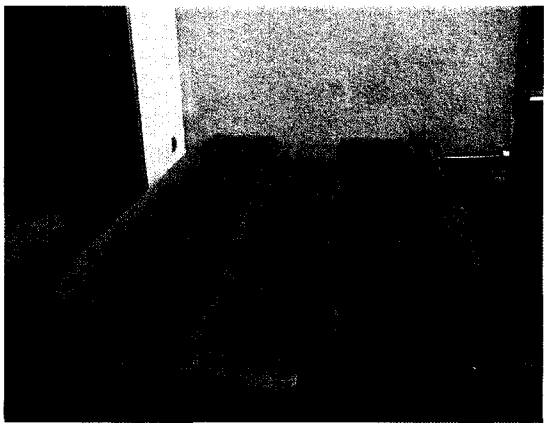

Figure 3.2b: Adhering vapour barrier

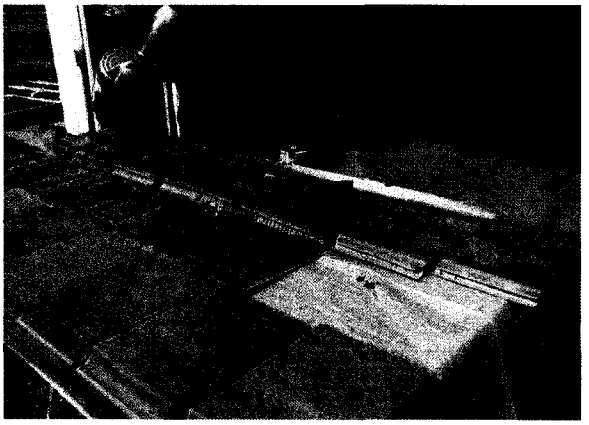

Figure 3.2c: Application of vapour barrier-insulation adhesive

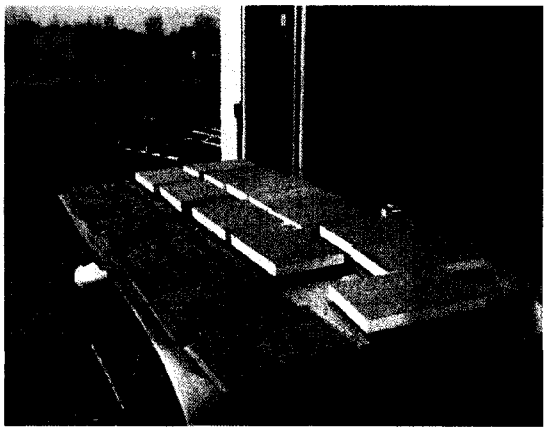

Figure 3.2d: Adhering insulation

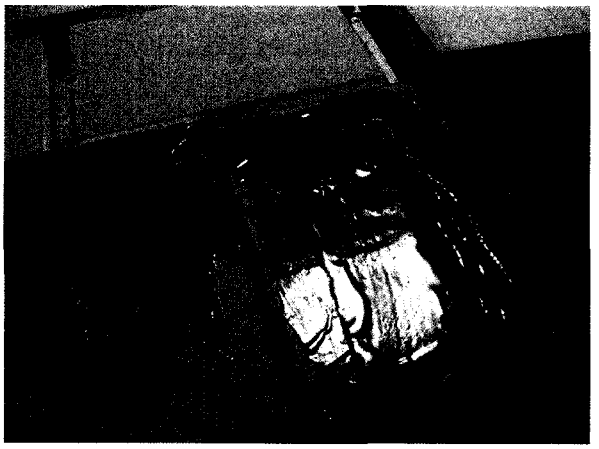

Figure 3.2e: Application of insulation-coverboard adhesive

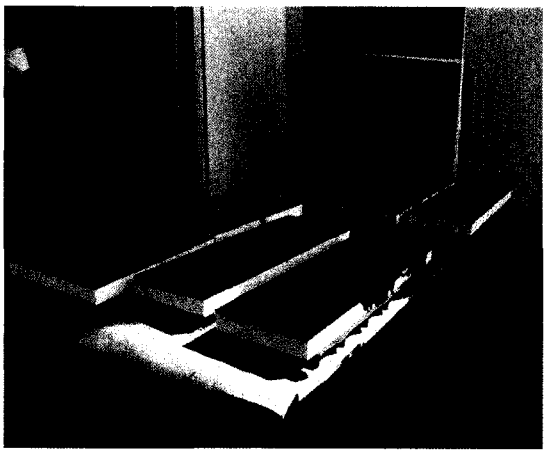

Figure 3.2f: Adhering coverboard

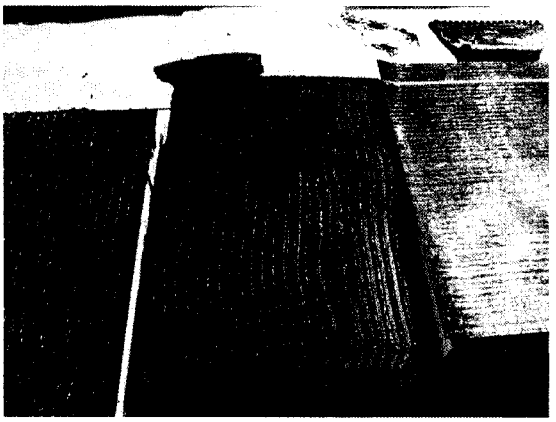

Figure 3.2g: Application of coverboard-base sheet adhesive

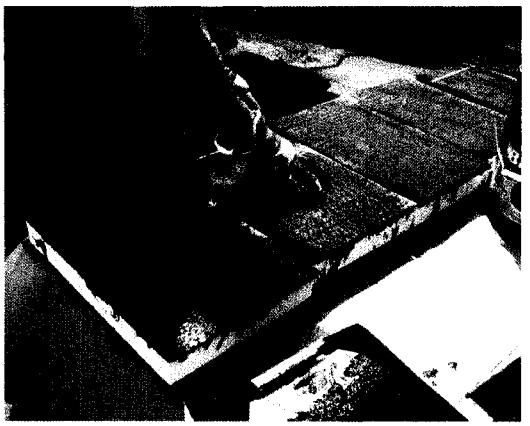

Figure 3.2h: Adhering base sheet

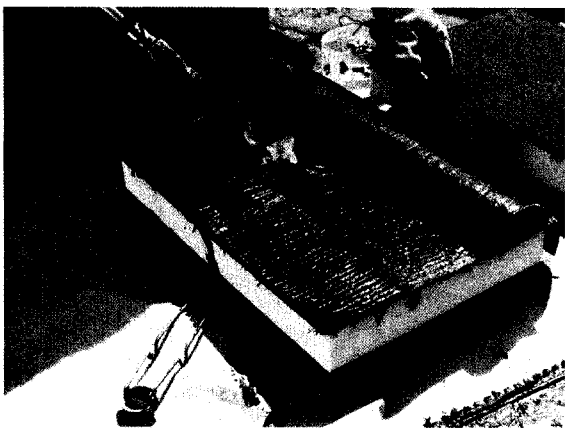

Figure 3.2i: Torching of base sheet to cap sheet

Decks

Although there are many types of decks used in roofing, two types of decking are most common – steel and concrete. And the details of these two types of decks are as follows.

Steel

Fluted steel decks were used for specimens constructed on steel decking and were prepared several days prior to the day of construction. Painted or galvanized steel deck with 33 ksi strength and 0.75 mm nominal thickness was used. Since steel decking is manufactured to American specifications, the center to center distance between adjacent flutes (male or female) was 6 inches (150 mm) A skill saw was used to cut 20' (6.10 m) sections of fluted steel decks into smaller sections. These smaller sections would then be cut to the proper size using a band saw. Figure 3.3 illustrates the important dimensions on steel decks, as well a differentiation between male and female flutes.

Concrete

Concrete decks were constructed at NRC facilities several days prior to the date of specimen construction. 40 MPa concrete was selected and reinforced with steel wire mesh to provide tensile reinforcement. The concrete was made from Portland cement with medium sized aggregates. It should be noted that the strength characteristics of the slabs were irrelevant for the purposes of this study as no concrete deck failed. The decks were created to simulate the concrete surface to characterize the adhesive bond joint between the vapour barrier and concrete deck. The dimensions of the slabs were 300 x 450 x 25 mm (l x w x t) Figure 3.4a illustrates the forms used to make the decks, Figure 3.4b & c illustrate steps in the slab construction process and figure 3.4d illustrates the final slab immediately after curing and removal from the form.

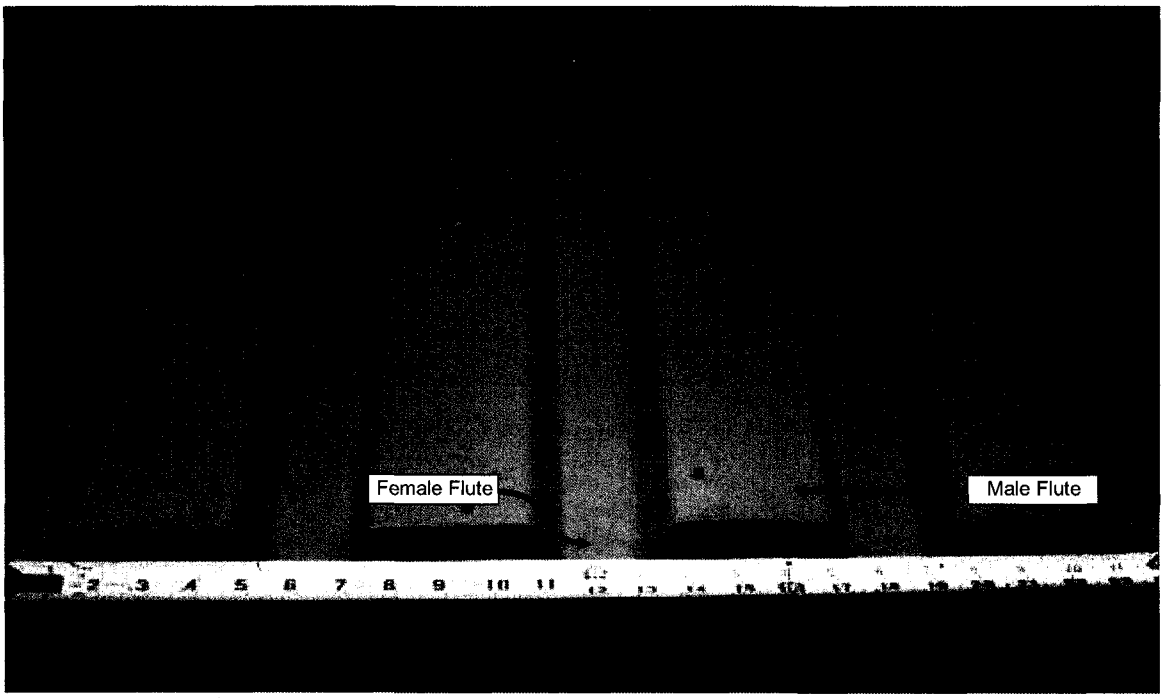

Figure 3.3: Steel decks illustrating male and female flutes and their relevant dimensions

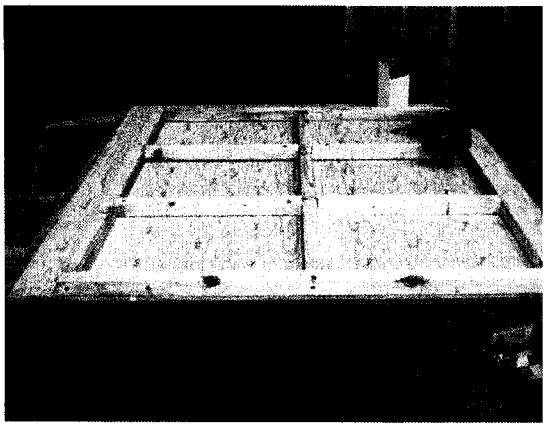

Figure 3.4a: Concrete formwork constructed to produce slabs

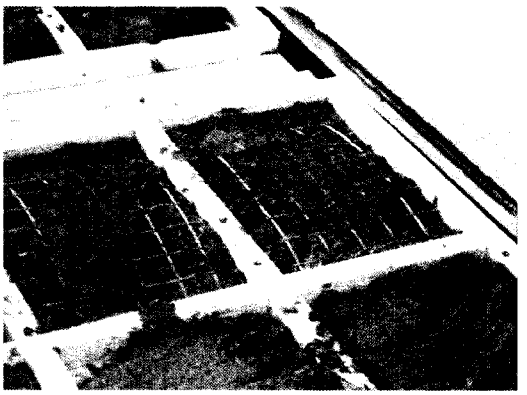

Figure 3.4b: Concrete formwork showing tensile reinforcement

Figure 3.4c: Concrete forms before tamping and troweling

Figure 3.4d: Concrete slabs, final product

Vapour Barrier

Two types of vapour barrier were encountered by the present study. One was a self adhering vapour barrier which consisted of a polyethylene side and a side with a pressure sensitive adhesive on the opposite side. These vapour barriers are more commonly referred to as "peel & stick" membranes. The other type of vapour barrier encountered was a construction paper, or kraft paper vapour barrier. It consisted of two pieces of construction paper that had been factory-laminated together and then was adhered to the decking with a separate adhesive.

Insulation

For all pullout tests that were performed, the insulating material was a 50 mm thick paper faced or acrylic faced polyisocyanurate. In field applications, paper faced insulation is usually the norm. Like steel decking, insulation was cut several days prior to the day of construction. 4' x 4' (1.22 m x 1.22 m) sheets of insulation were cut on a table saw at NRC facilities to their appropriate specimen sizes.

Cover Board

Two types of coverboard materials are typically encountered in field applications. The first is an asphalt core board. It is manufactured in sheets that measure 4' x 5' (1.22 x 1.52 m) It is approximately 5 mm thick and typically the asphalt core board were cut to size with a utility knife on the day of construction. Asphalt core board has bituminous materials impregnated in it, so that with the application of heat the bituminous materials becomes molten and can be torched to secure the base sheet. Another type of coverboard material is fiberboard. Fiberboard consists of densely packed wood fibers and comes in sheets that are 2' x 4' (0.61 x 1.22 mm) Although substantially thicker (12 mm) and less dense

than the asphalt core board, the fiberboard was effortlessly cut to size on the day of construction with a utility knife.

Base & Cap Sheet

Both base and cap sheet come in rolls that were 990 mm wide. On one of the sides of these rolls was a 75mm "refuse" which is used in field applications to overlap adjacent rolls to create a water tight seal. In most cases of specimen construction, this refuse was trimmed and removed. The cap sheet was a common material used by all sources and the differences on a source by source basis were negligible. However there were slight difference between the base sheets employed and it depended on methodology (see Section 3.2.2 – Adhering & Torching for further details) When the base sheet was adhered to the coverboard, a base sheet with a higher surface porosity was applied. Higher porosity was achieved by the application of a base sheet that had surface impregnated grains of sand on the coverboard to base sheet adhering surface. When the base sheet was torched to the coverboard, both sides of the base sheet were smooth with a bituminous material that would melt with the application of heat.

3.2.2 Differences in Specimen Construction Protocol

Since the specimen protocol of four companies was studied there were obvious differences in construction methodologies. The reasons behind these differences are far ranging and beyond the scope of this thesis report, however it is important to note that they do exist. Outlined below are some of the differences in methodologies that were employed by different sources.

Full and Partial Adhesion

One of the biggest differences in protocol between the industrial partners was the difference in the application of adhesive. Some of the industrial partners preferred to fully adhere all layers of construction materials with a layer of adhesive of uniform thickness; this is referred to as full adhesion. Conversely, some of the industrial partners preferred to adhere the construction materials with strategically placed beads of adhesive; this is referred to as partial adhesion. The difference between beading and full adhesion is most relevant between the vapour barrier and the insulation and the coverboard and the insulation.

When partial adhesion is applied, it is extremely difficult to quantify the width, breadth and thickness of beads of adhesive, especially once a layer of construction materials has been laid down on top of the adhesive. It is also an unfair comparison to compare the performance of partially-adhered specimens with fully-adhered specimens because of the significant difference in adhesive contact areas between the two. This difference in protocol was taken into account when analyzing the results. As defined in the scope of this report, the purpose of testing was to determine the range of loading over which failure occurred when the specimens were subjected to a pullout test. These differences will help to quantify what the end result of these methodologies will yield in pullout strength.

Adhering and Torching

As alluded to in Section 3.2.1, there is more than one option for the application of the base and cap sheet membranes. These two layers can either be adhered to one and other with adhesives (cold application) or these two membranes can be torched to one and other. (hot application) A detailed review of the results of location of failures planes (Chapters 5 & 6) showed a low incidence of pullout failure in between these two components. Due to its lack of importance with respect to pullout failure, specimen construction protocol of

these two membranes was left to the industrial partners to decide – and this part of specimen construction was not reported.

3.3 Experimental Variables

As outlined in chapter 1, the project-based nature of this experimental investigation required that a test method be developed as part of the deliverables once the investigation had been completed. Thus, experiments were required to be undertaken to discover two types of information about experimental variables. The first type of variable is a test parameter. This is examined because understanding the nature and influence of this variable on the results of the pullout testing will be stipulated in the test method. An example of this type of variable would be the pullout rate. The second type of variable examined is a specimen variable. This is a variable that will affect the pullout strength of the test but had no bearing on how the test is performed. This is examined because different specimen-unique variable parameters will have different resulting pullout strengths. An example of this type of variable would be the materials that constitute the specimen. The following two sections will provide an overview of the test variables and then provide an overview of variables relevant to applications of the test method.

3.3.1 Test Variables

Pullout Rate

Over the course of experimentation, it was of importance to know the optimum deflection rate for conducting pullout tests. Originally experiments were conducted at 6.35 mm/min. However additional tests were run at 1.27, 2.54 and 12.7 mm/min in order to characterize the different behaviour observed at these test speeds. Each source constructed 4 identical samples of specimens,

constructed with the same materials following the same construction protocol to determine the optimum pullout rate for pullout testing.

Specimen Size

It was of interest to find out what would happen to the behaviour of the specimens during a pullout test once the size no longer remained at the standard of 300 x 450 mm. All sources built control specimens that were this size and in addition to these, additional specimens of 300 x 900 were constructed. These would be useful when compared to the smaller specimens. (300 x 450 mm)

Attachment Conditions

An additional variable of interest was determining the effect a different specimen attachment condition would have on the pullout resistance of AARS specimens. It is difficult to replicate the attachment condition of specimens in the field and the attachment condition described in section 4.2.1 is simply an approximation to those observed in the field. Therefore a deviation of the attachment condition of section 4.2.1 was experimented to provide a comparison and to see if there was some identifiable pattern between specimens tested with these two different conditions. Source workmanship was removed as a possible variable and client companies were instructed to produce identical specimens. Half of these specimens were tested with attachment strips on each one of the four female flutes. This was assumed to be the "best-possible" case scenario and could provide a benchmark in testing from earlier experimentation. The other half of the specimens were tested with attachment strips on only the outer two flutes. These two conditions (two and four flutes attached) are illustrated in Figure 3.5a and 3.5b respectively.

Figure 3.5a: Specimen with outer two flutes attached

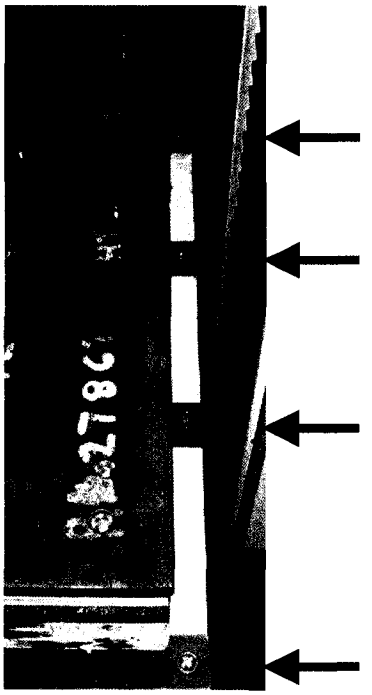

Figure 3.5b: Specimen with all four flutes attached

3.3.2 Specimen Variables

Materials

One of the key variables examined was testing the effect of different roofing materials. Each industrial partner constructed 4 different samples of 6 specimens each to test the effect of materials in the AARS roofing specimens. One of the materials that was evaluated was the performance of different types of polyisocyanurate insulation facer. The materials that were tested were an Acrylic Facer (AF) and a Paper Facer (PF). Another material that was being evaluated was the cover board. The two cover boards that were tested were an asphalt core board (ACB) and a fiberboard (FB). By combining the effects of each different combination of insulation facer and coverboard the result was 4 different samples. This resulted in 96 experiments that were conducted to test the effect of material combinations.

Different Adhesion Patterns

An additional 4 different samples were created for each of two sources with the same 4 material combinations outlined in a preceding section with adhesive applied only on the two outer male flutes between the steel deck and the vapour barrier. In the first 96 tests, adhesive was applied between the steel deck and the vapour barrier on all three male flutes of the 300 x 450 mm specimens. The traditional method for adhering deck to vapour barriers is illustrated in figure 3.6a – this will be referred to as "Type A" adhesion. An alternative method for adhering the deck to the vapour barrier is illustrated in figure 3.6b – this will be referred to as "Type B adhesion". Sources 3 & 4 were chosen to undertake this investigation because they did not use self-adhering vapour barriers which do not permit flexibility in the placement of vapour barrier adhesive as shown in Figure 3.6.

Figure 3.6a: Specimen construction – "Type A" adhesion

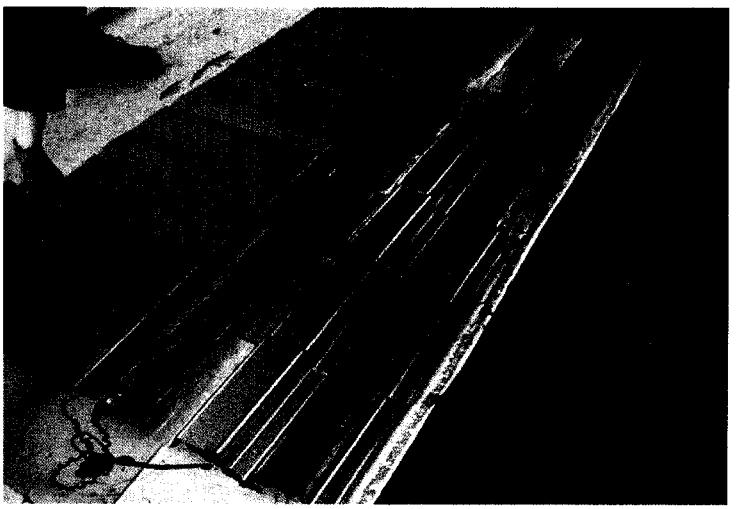

Figure 3.6b: Specimen construction – "Type B" adhesion

Figure 3.6a: Cross sectional view – "Type A" adhesion

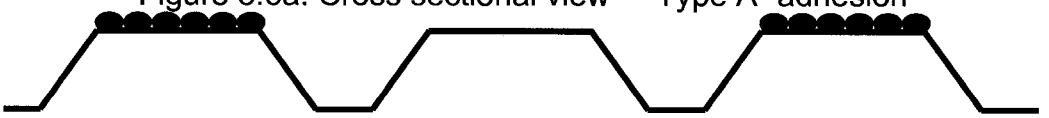

Figure 3.6b: Cross sectional view – "Type B" adhesion

Deck

Another variable of interest that was explored was the effect of different decking. Reinforced concrete slabs 450 x 300 mm and 900 x 300 mm were fabricated at the NRC for this purpose as discussed in section 3.2.1. In order to accommodate the proper boundary conditions, concrete specimens were flanged. Thus all roofing construction materials that were adhered to the deck measured 400 x 300 mm.

3.4 Experimental Apparatus

The experimental apparatus used for the present study included the following components:

- 4502 Series Instron Frame
- Stress Plate
- Stress Plate Mounting Platform
- Specimen Mounting Platform
- Attachment Strips for
    - Steel Deck
    - Concrete Deck

In the following sections each component is described in greater detail.

3.4.1 4502 Series Instron Frame

The testing equipment used in this experimental investigation was a 4502 series Instron Frame. The main hardware components of the Instron illustrated in Figure 3.7 frame include:

- Frame
- Crosshead
- Load Cell
- Plate Flanged Housings
- DAQ

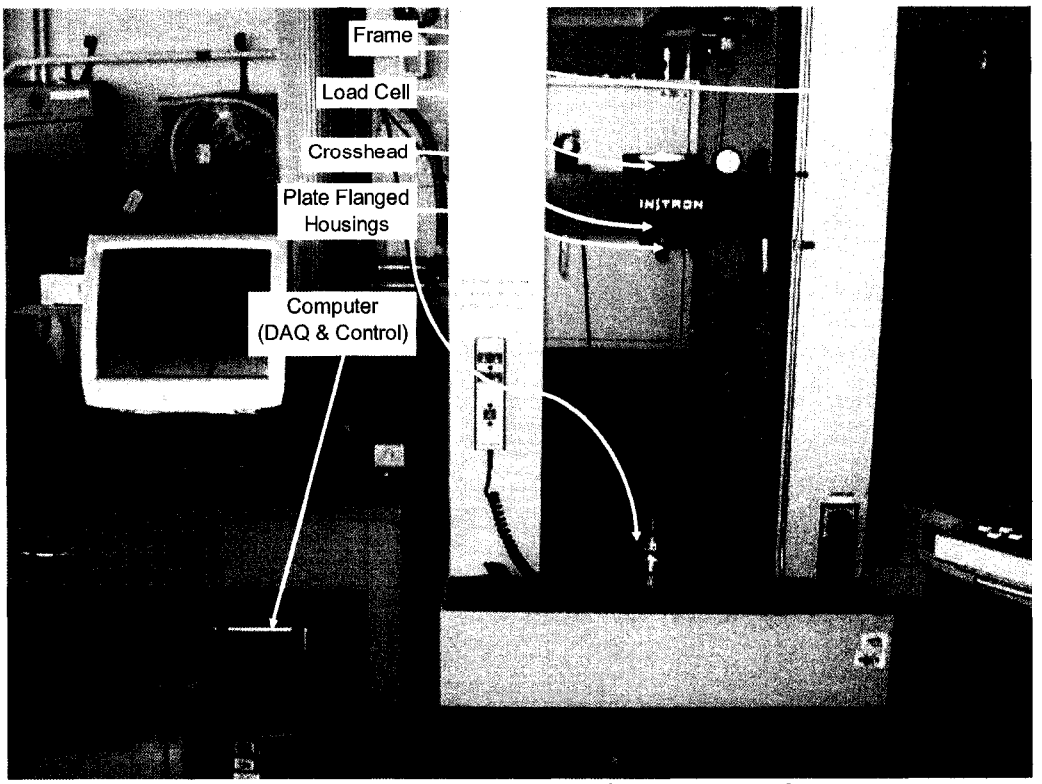

Figure 3.7: Key components of the Instron frame

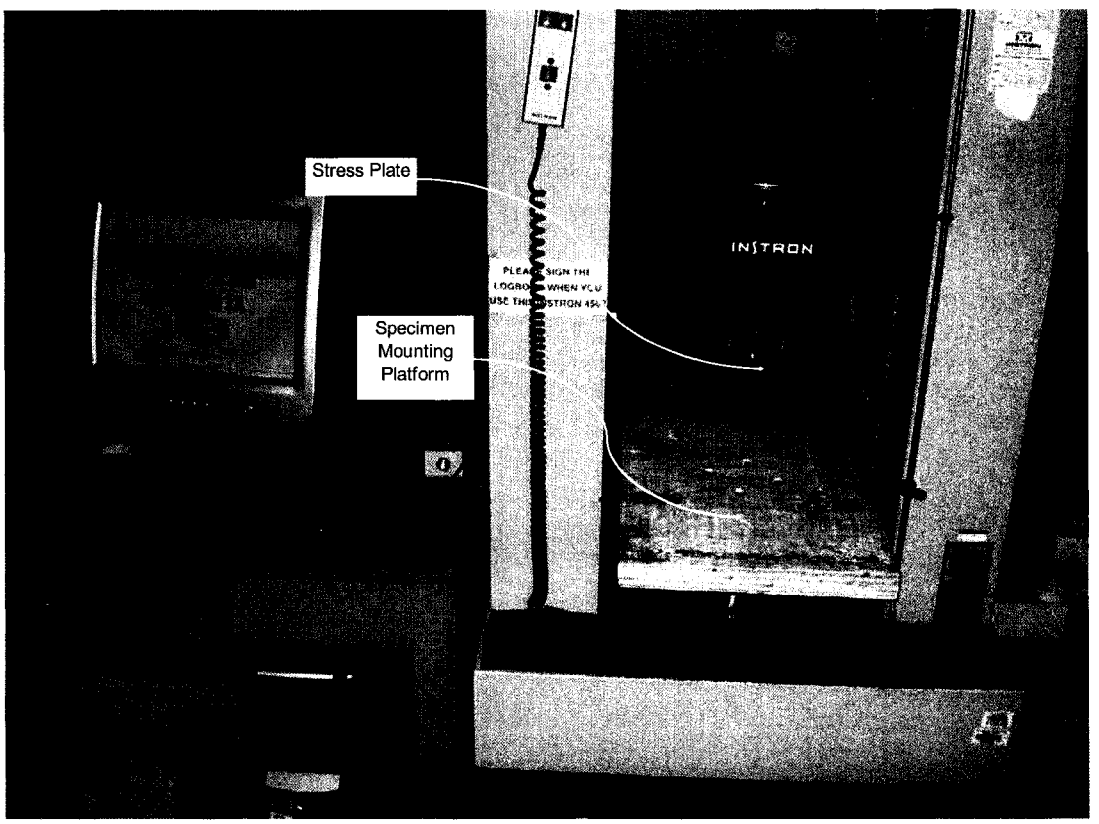

Figure 3.8: Key components of the Instron frame with AARS pullout apparatus installed

An Instron frame is used for performing a wide array of mechanical tests including tensile, compressive, shear, torsion and bending tests. Similar to the AARS testing, tests of this nature are usually conducted to determine unknown mechanical properties of materials. The frame is controlled remotely by PC through the Bluehill software pack and manually controlled with a pendant. This software allows a user to define the input parameters like pullout or stress application rate, end of test parameters and raw data sampling rate. The software also allows users to input specimen parameters and to publish customizable reports which can show an overview of experimental results, graphs and user-defined comments. These functions are further explained in Chapter 4.

The frame refers to the vertical members that hold the track and guide the crosshead. They permit the smooth transmission of loads from actuation directly to the test specimens. The crosshead is a linear translating platform that the load cell sits on. Its design permits the smooth and even transmission of loads directly to the test specimens. The load cell is the hardware that electronically measures loads and then transmits a conditioned signal back to the PC for memory storage and future data manipulation. The top & bottom plate-flanged housings function as fixed anchors to attach to Instron machine components.

The plate-flanged housings consist of both a male and female component. The female components illustrated in Figure 3.7 attach to a mating male component on both the stress plate, and the mounting platform.

The top plate-flanged housing is attached directly to the load cell and moves at the same rate and in the same direction as the crosshead. As discussed in Chapter 2, many of the adhesive pullout tests required a fixed member and a translating member. This is accomplished in a similar fashion through the use of the bottom and top plate-flanged housings. The Instron test frame and all its components used for the AARS pullout testing are shown in figure 3.8 and consists of the following components, described in sections 3.4.2 to 3.4.5.

3.4.2 Stress Plate

The stress plate is a rigid steel plate that is attached directly to the male component of the top plate-flanged housing as shown in a plan view of Figure 3.9. The purpose of the stress plate is to transfer loads from a point source, like the loads generated by an Instron Machine, over the full test area of the AARS specimens. The dimensions of the stress plate are 300 x 450 x 9.5 mm. Although tests were conducted on specimens of lengths that exceeded 450 mm the same stress plate was used and centered on the stress plate mounting platform (see section 3.4.3). As shown in Figure 3.9, the plate has holes drilled and countersunk to accommodate ¼" #8 or # 10 Robertson-Head woodscrews. There are a total of fourteen holes drilled in this plate for attachment to the stress plate mounting platform. The attachment holes labeled in green (6) were used for both concrete and steel deck specimens. The attachment holes labeled in yellow (4) are for concrete deck specimens only. And the red holes (4) are for steel deck specimens only. The attachment holes are necessary because they facilitate the temporary attachment of the stress plate to the stress plate mounting platform and allow for quick and easy attachment and removal.

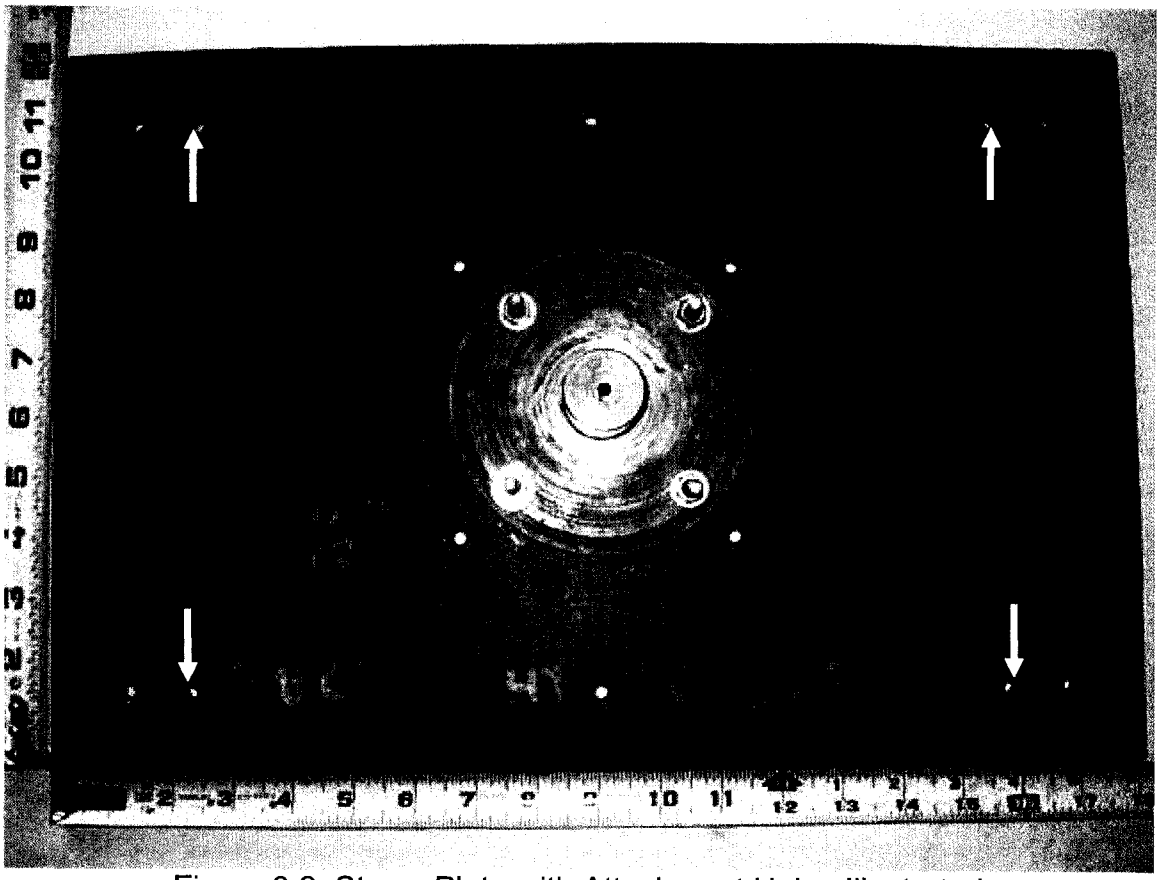

Figure 3.9: Stress Plate with Attachment Holes Illustrated

3.4.3 Stress Plate Mounting Platform

In order to conduct a pullout test on an AARS specimen, a stiff and rigid surface is required to transfer the applied loads from the Instron Machine to the test specimens. The cap sheet on the top surface of the roofing specimens is obviously not the ideal surface to work off of due to its flexibility and lack of rigidity. In order to overcome this lack of rigidity, an 18.75 mm thick piece of 300 x 450 mm or 300 x 900 mm plywood was superimposed overtop of the roofing specimen. The plan dimensions of the plywood depended on the size of the specimen that was being tested. This plywood sheet was glued to the top of the roofing specimen with a high-strength two-part polyurethane and epoxy adhesive mix. This adhesive, which is more commonly referred to as Millennium adhesive creates a joint that is much stronger than any other bond existing in the roofing specimen so that when a pullout test is conducted other layers of adhered materials will fail before the glued plane does. Figure 3.10 illustrates the process of adhering a plywood member to the cap sheet of an AARS roofing specimen and creating the stress plate mounting platform.

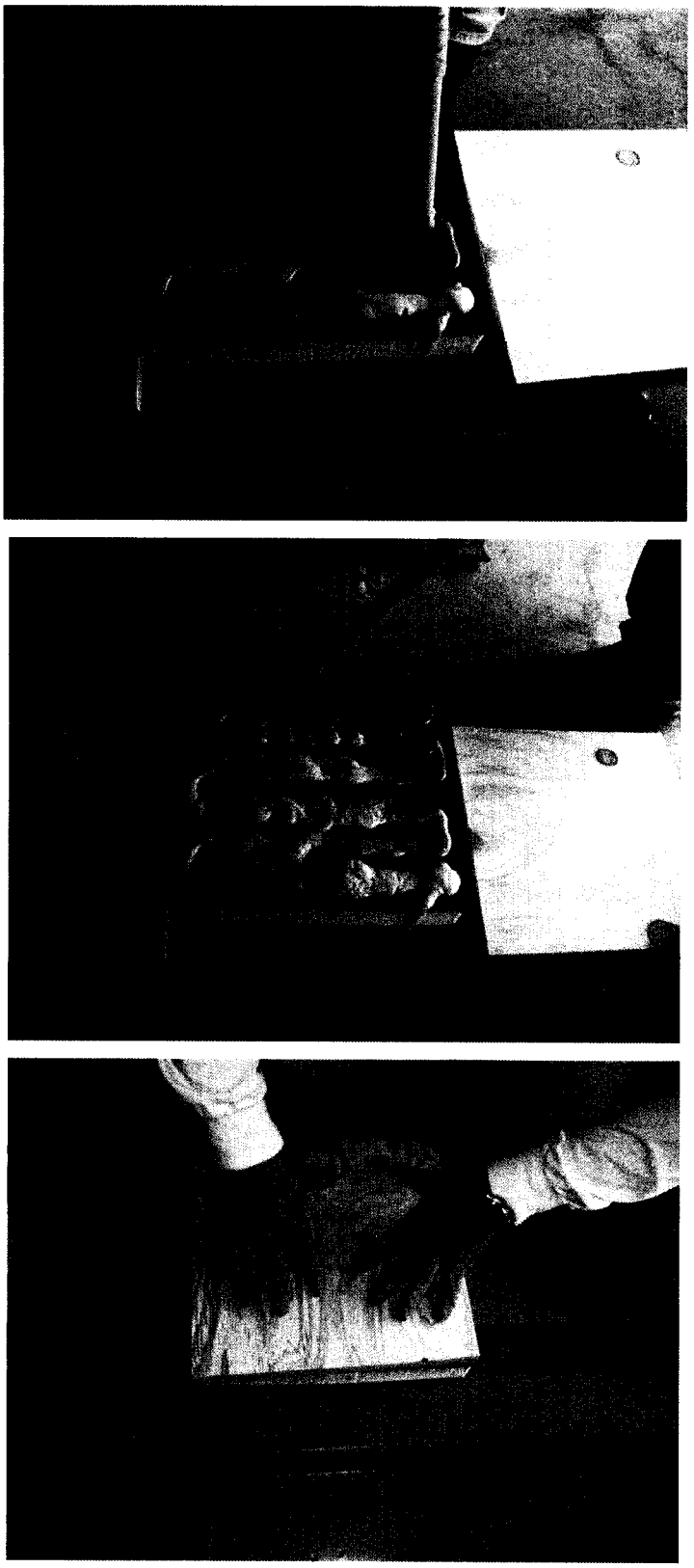

Figure 3.10: Plywood Adhering– Attaching Stress Plate Mounting Platform

3.4.4 Specimen Mounting Platform

The specimen mounting platform is illustrated in Figure 3.11a and it is a platform that consists of two pieces of mechanically attached 18.75 mm plywood. The specimen mounting platform creates a stiff working platform on which all the tests can be performed. The specimen mounting platform is fixed to the base of the Instron machine by connecting the male end of the plate flanged housing to the female end of the housing as illustrated in Figure 3.11b.

As emulated from the literature study of Chapter 2, the platform acts as the immovable and rigid base on which to perform all pullout tests. The platform consists of two pieces of 18.75 mm plywood, mechanically attached to one and other with wood screws to create a stiff working platform on which all the tests can be performed.

Two different sized platforms were required for testing. To accommodate the 300 x 450 mm specimens, a platform that was 375 x 500 mm was constructed. In addition to this, another platform that measured 375 x 1000 mm was built to accommodate the more slender specimens that measured 350 x 900 mm. Both platforms had holes drilled along the perimeter to accommodate ¼" bolts. These holes were strategically drilled in the approximate locations of where the female flutes of the roofing specimens would be when the specimen was centered relative to the crosshead and load cell. The location of the mounting holes for a 375 x 500 mm specimen mounting platform(used for testing specimens that were 300 x 450 mm) is shown in Figure 3.11a.

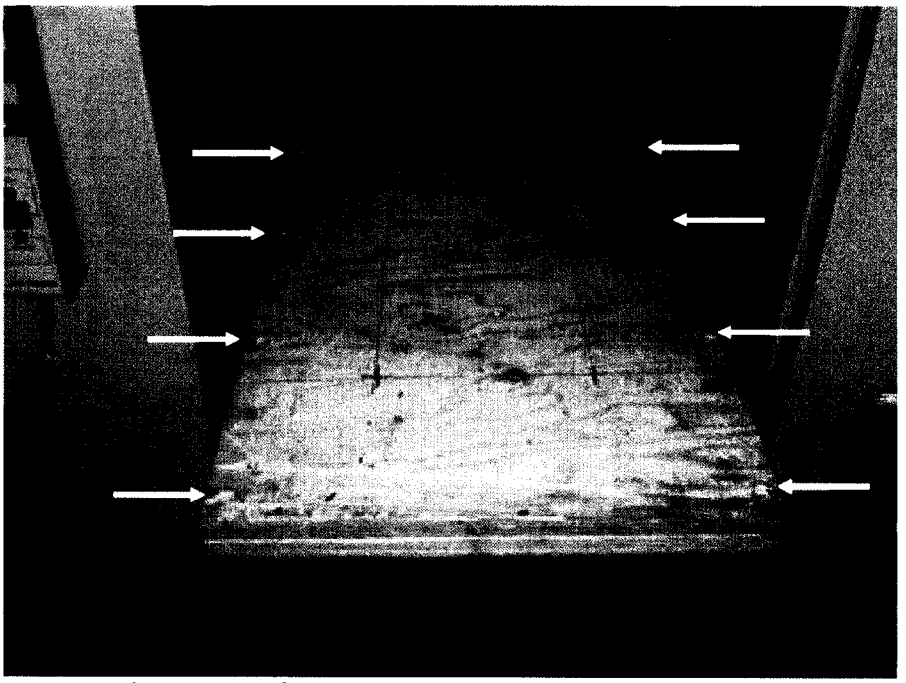

Figure 3.11a: Location of mounting holes on specimen mounting platform

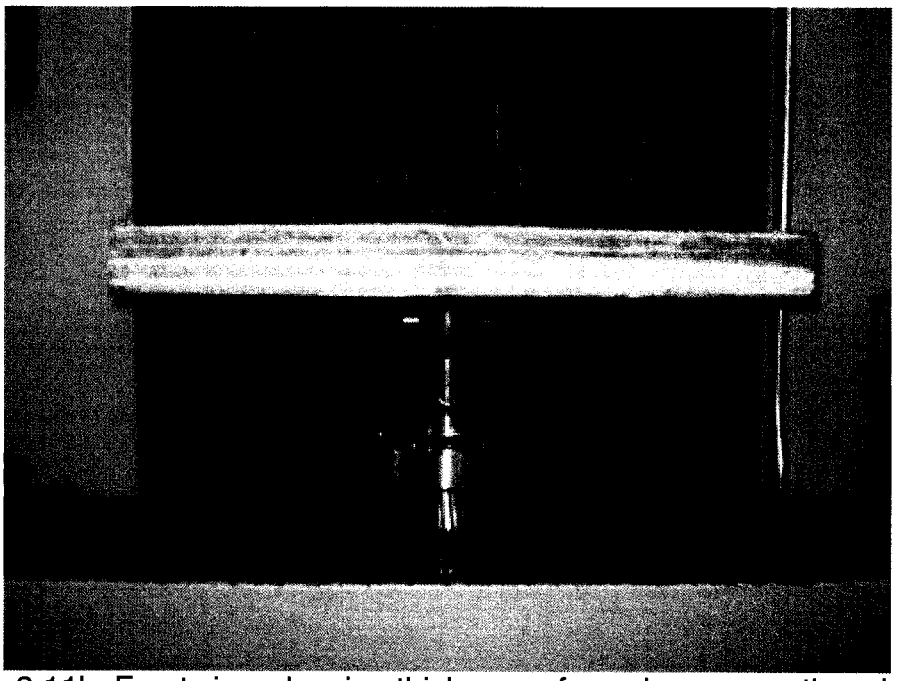

Figure 3.11b: Front view showing thickness of specimen mounting platform

3.4.5 Specimen Attachment Strips

AARS specimens were constructed using concrete and steel decks. Since these decks have different profiles and physical properties, different mechanisms were required to securely attach the specimens to the platform and create the fixed-end condition. These mechanisms are described in the proceeding sections.

Steel Deck Attachment Strips

The steel deck attachment strips were used to secure roofing specimens while tests were being undertaken. The attachment stripes measured 375 x 25 x 10 mm and were fabricated with a coarse grade of construction steel. These strips were significantly over-designed for the purposes of the experiment. This thickness was chosen to ensure that steel deck deflections would be minimized.

Like the platform, the strips had holes drilled at their outermost edges so that they would align with the holes on the specimen mounting platform. The design of the attachment system capitalized on the fluted geometry of the deck. The attachment stripes were slid into the female flutes parallel to the 300mm dimension of the specimens. When the holes from the strips and platform were aligned ¼" hex-head bolts were torqued to mating nuts to fixture the specimen in place. On 300 x 450 mm specimens, there were four female flutes that required fastening; thus 8 pairs of nuts and bolts were required. For the slender 300 x 900 mm specimens, an additional 3 strips and 6 pairs of nuts and bolts were required to fasten down the specimens on all flutes. Figure 3.12 illustrates the steel deck attachment strips.

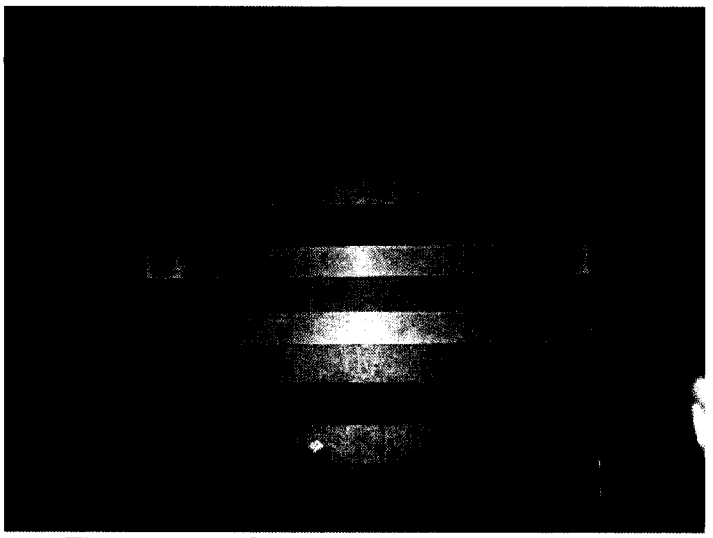

Figure 3.12: Steel deck attachment strips

Figure 3.13a: Concrete deck attachment strips

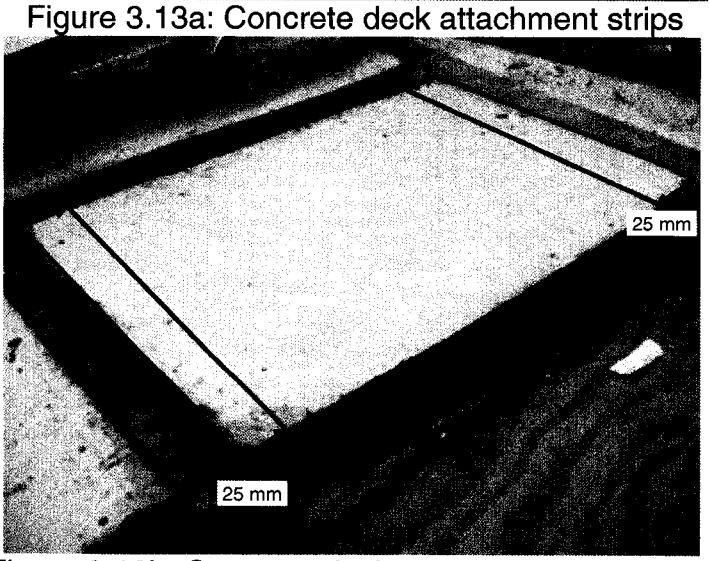

Figure 3.13b: Concrete deck – attachment locations

Concrete Deck Attachment Strips

For the 300 x 450 mm concrete deck specimens, attachment strips illustrated in Figure 3.13a were used. Concrete deck specimens were flanged in design in that all the materials above the deck - the vapour barrier, insulation, cover board, base sheet and cap sheet were cut to the size of 300 x 400 mm. When the roofing materials were centered on the deck, this left a 25 mm flange on either side of the specimen. This concept is illustrated in Figure 3.13b. The concrete attachment strips capitulated on this design and clamped on this flange and underneath the platform to rigidly fix concrete specimens in place. They consisted of a pair of matching attachment strips with 25 mm holes bored out at either end. A piece of threaded rod was run through the holes and four nuts were placed on the ends of each pair of threaded rod to hold the attachment strips in place. The bottom strip that was clamped underneath the platform had a nut spot-welded in place to the bottom of the strip. The top nut was free to rotate and placed on top of the attachment strip and tightened down prior to the test to ensure that the deck met the fix-end condition.

Chapter 4: Experimental Protocol & Data Interpretation

4.1 Introduction

This chapter will explain the application of the test. It will provide an overview of how a test was set up and explain the physical significance of numerical calculations and classification of observations.

Section 4.2 outlines the experimental protocol for completion of a pullout test. This section provides a step-by-step layout to complete an AARS pullout test.

In section 4.3, the classification of quantitative and qualitative observations has been provided. This section explains how the data was reported and provides an explanation of where the numerical values used for evaluating AARS came from. In addition, this section introduces a key concept referred to as "failure planes". This section provides an overview of the categorization of failures and what constituted the failure planes discussed in this report.

4.2 Experimental Procedure

This section outlines the procedure that was followed for conducting laboratory pullout tests on specimens built with steel deck. This protocol was observed, regardless of specimen size, or test speed. There are two main objectives that need to be accomplished in order to assure that a test specimen is set up properly. The specimen needs to be installed properly in the Instron Frame; this will be addressed in Section 4.2.1. The Instron Machine needs to be set up properly with the correct variables; this will be addressed in Section 4.2.2.

4.2.1 Specimen Setup

Step 1:

The male end of the plate flanged housing on the specimen mounting platform is attached to its mating female component inside the Instron frame. The two are then rigidly connected by a pin connection. With the specimen mounting platform properly attached, the stress plate was placed on top of the specimen mounting platform. The crosshead was then jogged so that the male end of the plate flanged housing, which was connected to the stress plate, slid into the female component on the crosshead and the two were pin-connected. An empty frame without a specimen inside is shown in Figure 4.1a and this figure shows the proper setup of the specimen mounting platform and stress plate.

Step 2:

Place the attachment strips in the female flutes of the specimen and place the specimen on the mounting platform. A visual inspection was conducted to ensure there was alignment between the stress plate mounting platform and the stress plate and to ensure that the female flutes were aligned with the holes on the specimen mounting platform (Figure 4.1b)

Step 3:

Once the specimen was properly aligned, ¼" bolts and nuts fastened the attachment strips to the mounting platform – ensuring that the specimen was rigidly fixed to the platform. (Figure 4.1c) With the bottom attachment condition satisfied, the next step that needed to be completed was the attachment of the stress plate to the stress plate mounting platform. The Instron machine was jogged downwards until the stress plate was sitting on top of the specimen. Then the pin was removed from the top plate-flanged housing. This released the stress plate and left it sitting directly on top of the specimen. (Figure 4.1d)

Step 4:

The Instron machine was jogged upwards so that the stress plate could be attached to the stress plate mounting platform. This required the use of a cordless drill to fasten down the 10 #10 1" Robertson head wood screws to the

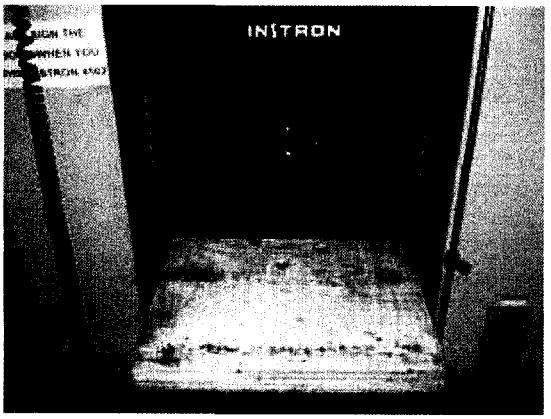

Figure 4.1a: Attachment of stress plate & platform

Figure 4.1b: Installation of specimen in frame & alignment check

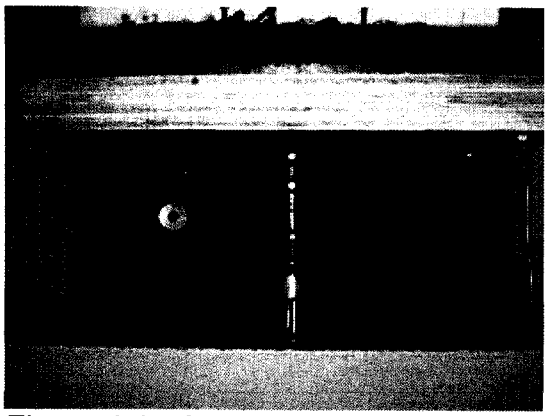

Figure 4.1c: Installation of attachment strips & securing specimen

Figure 4.1d: Detachment of female component of plate flanged housing

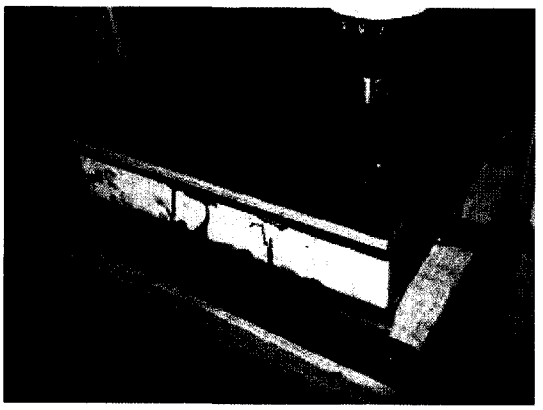

Figure 4.1e: Attaching stress plate to stress plate mounting platform

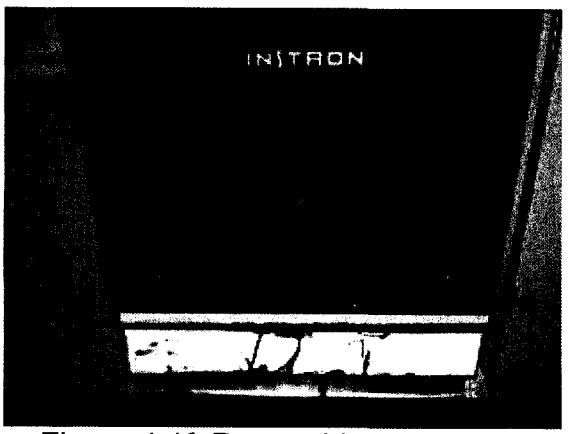

Figure 4.1f: Reattaching male and female components of stress plate housing

stress plate to the stress plate mounting platform plane (Figure 4.1e). Once the stress plate was secured to the specimen, the Instron machine was jogged back down to its original position before the stress plate was removed. The pin was then replaced in the top plate-flanged housing, re-attaching the specimen to the crosshead and the load cell. (Figure 4.1f) At this point the specimen was ready for testing and the Instron Machine required set up.

4.2.2 Instron Machine Setup

After installation of the specimen in the frame, it was necessary to setup the software package to ensure the correct setup of the input parameters. The software package used for controlling the laboratory pullout tests is called Bluehill Series IX. This software is opened and the appropriate method is selected. The method is a program that allows the specific test variables to be inputted into a program. Only four different methods were required to be set up to run the tests outlined in this thesis report – these four different methods were virtually identical in all aspects except they had different pullout rates. These methods were developed prior to testing and the methods were called upon when necessary. Some of the features of the Bluehill software package have been outlined below:

- Pullout Rate/ Rate of Loading
    - Bluehill Series IX permits the specification of how the tensile tests will be performed. This can be specified as a fixed (constant) extension or loading rate. It can also be specified as a ramp for non-constant loading conditions. Due to the nature of the tests being conducted, a fixed pullout rate was specified. An original method was written for tests to be conducted with a fixed extension rate of 6.35 mm/min. Other tests of 1.25 mm/min, 2.54 mm/min and 12.70 mm/min were copies of the original method, with the only difference being the substituted new pullout rate.

- Sampling Rate
    - The rate at which output variables are sampled can be adjusted in order to maximize data resolution or minimize computer memory usage.
- Tabular Display
    - As tests are performed, each new data point that is added is placed in a table, allowing for quick comparisons between specimens within a given sample set while testing is being undertaken.
- Statistical Analysis
    - As tests are performed, built in software analysis can perform statistical analysis on the data sample. This analysis can include the maximum, minimum, mean value and standard deviation of a given variable within the sample. A built-in software package can perform complex calculations by specifying key variables. Calculations shown in this investigation were performed independently following the guidelines of section 4.3.2.
- Graphic Display
    - As each test is performed, a time history of that test is added to the Instron plot area, adjacent to the tabular display. This permits users to observe the phenomenon of what happens to specimens over the course of time during a pullout experiment.
- End of Test Condition
    - The specification of this variable was required because it was a specification of the conditions necessary for completion of the test. There were two end of test conditions, one was performed automatically, the other manually. A 90% reduction of the "live load", the load directly on the cell, from the peak load was specified for all tests. This was automatically performed as a check by the Instron software. The user could manually stop the test once the extension had reached 25 mm.
- Output format

- Every time an Instron test is performed, the raw data is exported to an external (non-Instron) file. Users can customize the format and type of this output file. This data file was imported into Excel and the data manipulated to perform calculations carried out in this report.

- Comments
  - Users can input comments about the test, like phenomenon about a sample or specimen that makes it unique.

After performing each pullout test, the gauge length was reset. For AARS pullout testing, the gauge length would correspond to the thickness of the specimen. Since there were inherent differences in thickness of the materials and adhesives, differences in thickness that an Instron Machine would measure, the gauge length was reset after each specimen. This was also performed to ensure that load-extension plots would begin at zero.

One further operation needed to be performed intermittently during the running of pullout tests - the load cell had to be calibrated and balanced. Typically this was performed each time a new sample was started. (Every 6-8 specimens) Calibration was performed with the stress plate attached to the load cell but without the stress plate fastened to the stress plate mounting platform. This was done so that the weight of the stress plate was not accounted for in the load measurements taken by the load cell.

4.3 Failure Plane Classification & Data Analysis

Part of the test procedure was to accurately and fully report all observations. The following sections will evaluate the performance of a pullout test by providing guidelines for the classification of the observed phenomenon and explanations on the physical significance of empirical values.

4.3.1 Failure Planes Classification

After completion of experimentation, failures were categorized based upon the location at which the failure occurred. All experiments were categorized based on the criteria outlined below. In some cases during tensile loading, failure initiated in one component and propagated to another. Thus at the end of the tensile loading the specimen failed due to a sequential series of events. The events that lead to failure were not universally recorded throughout experimentation, and thus the major component that resulted in overall catastrophic failure was selected as the failure plane. By using this standardized categorization it will help to determine trends between samples and to correlate the numerical data with the observed phenomenon.

There are five planes where adhesive is applied, as shown in Figure 3.1, and failure can occur at any one of those locations. No special significance was given to an adhesive failure between specific components - all adhesive failures were grouped together, regardless of whether the adhesive failure was between the vapour barrier and the insulation or the adhesive failure was between the insulation and the coverboard. Three component failures that were never encountered were with the steel deck (or concrete deck, where applicable) and failures between the external waterproofing membranes – the base and cap sheet. However failures were encountered in the vapour barrier. Two types of failures were encountered with the insulation – a facer delamination and a facer rupture. Failures were also observed in the coverboard. In the following sections, a definition of what constituted each failure is provided along with illustrations of these failures – both actual photos of the failures, and artistic depictions of the failures as well. Under some pullout testing combinations of failures were observed; under this scenario the failure plane spanning the larger surface area of the specimen was selected.

Adhesive Failure

Adhesive failures were encountered frequently in almost all sources. Rarely was adhesive failure observed in specimens that were fully-adhered. Instead adhesive failure was indicative that the specimen had been partially adhered. Adhesive failures occurred under one of two circumstances. The first occurrence of adhesive failure was material separation. This occurred when one layer of construction materials separated from an adjacent layer of construction materials with the adhesive still fully bonded to one of the construction materials. The second occurrence was within the adhesive. This occurred when the adhesive yielded with the adhesive still partially bonded to the adjacent layers of construction materials. Adhesive failures were typically failures that occurred when pullout resistance is low and were indicative of specimens that performed poorly under pullout testing. Adhesive failures have been illustrated in Figure 4.2.

Vapour Barrier Delamination

Vapour barrier delamination occurred when the two sheets of kraft paper that are laminated together to form the vapour barrier become unglued. Please note that the kraft paper is pre-laminated and this failure is due to a manufactured adhesive failure and is a failure unrelated to specimen construction. Due to the materials used by the different sources who participated in this study, vapour barrier delamination was a failure observed exclusively by Sources 3 & 4. Sources 1 & 2 used peel and stick vapour barriers where this failure plane was not observed. Figure 4.3 illustrates typical vapour barrier delaminations.

Facer Delamination

Facer delamination was observed by all sources during testing. Facer delamination occurred when failure occurred in the polyisocyanurate immediately adjacent to the paper-based or acrylic-based facer. Typically this was a planar failure – meaning that the entire plane separated inside the insulation adjacent to

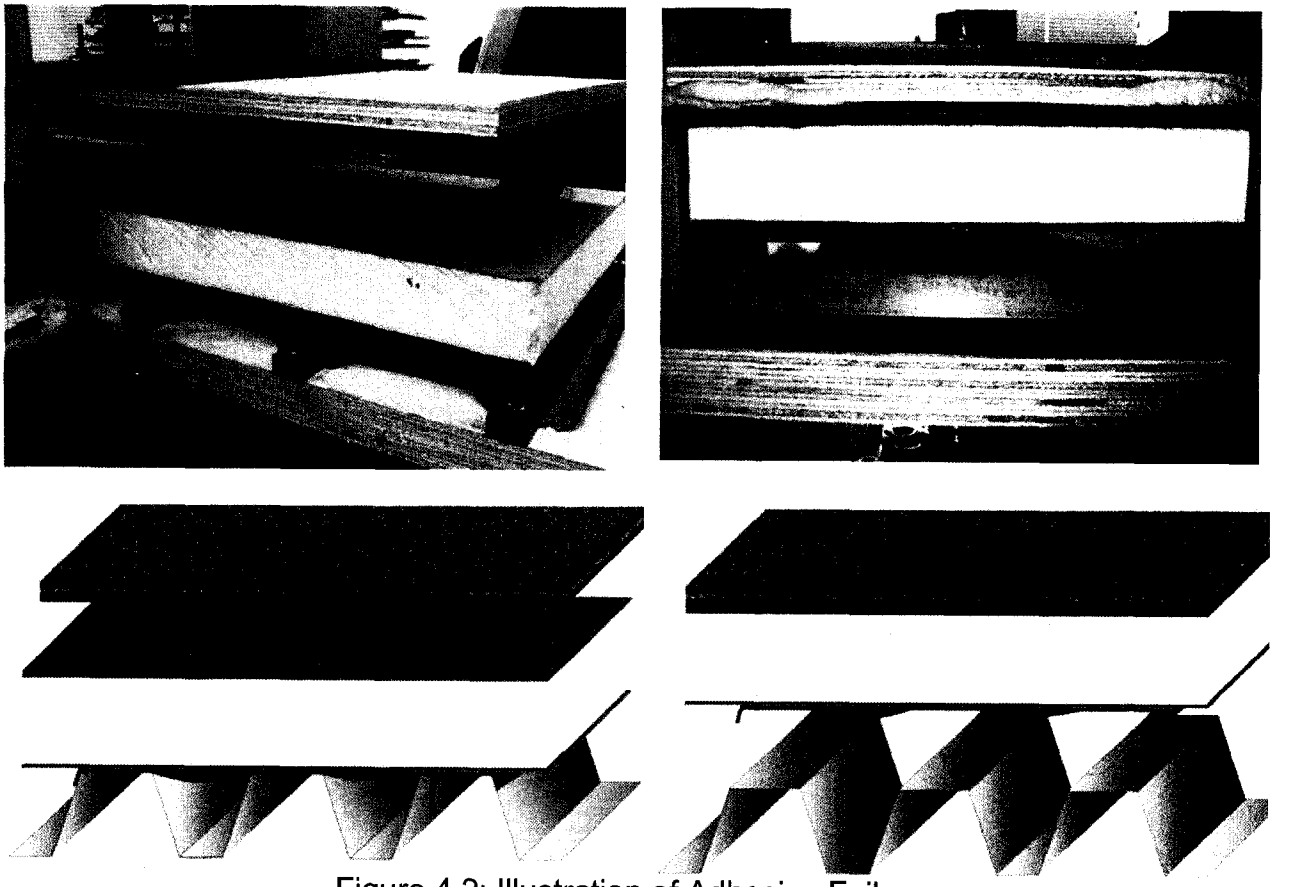

Figure 4.2: Illustration of Adhesive Failure

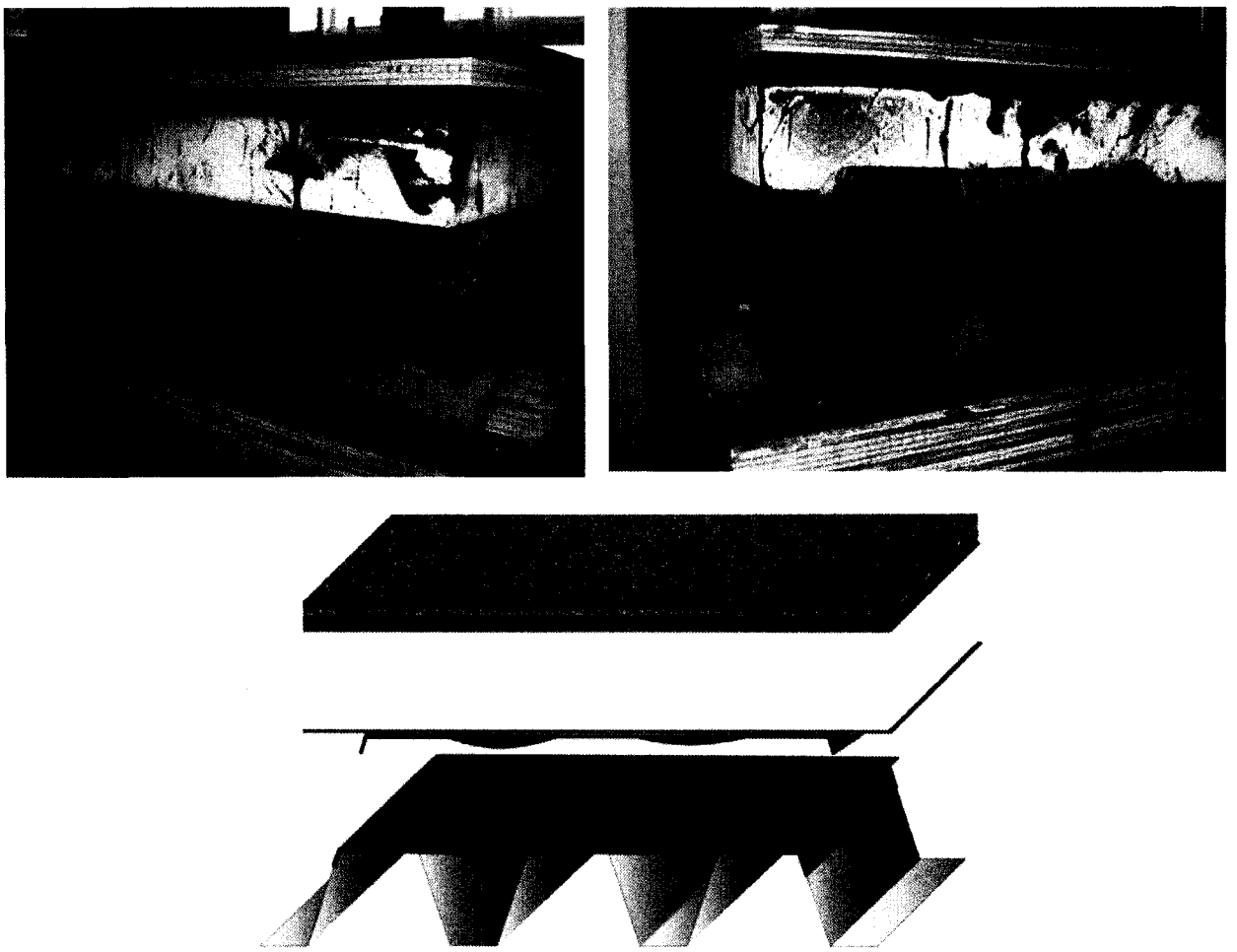

Figure 4.3: Illustration of Vapour Barrier Delamination

insulation. Failures in the insulation foam also constituted facer delaminations. Based on observations in the lab, foam failures were propagated due to the foam delaminating from the facer. Figure 4.4 illustrates typical facer delaminations. At the conclusion of experimentation it was determined that a facer delamination was a positive observation – indicating that if a given specimen failed in this plane, the specimen had been properly constructed.

Facer Rupture

Facer rupture was observed by all sources during testing. It was a failure that occurred in the facer and partially into the insulating materials. It was a slightly more ductile failure than the facer delamination and typically resulted in tearing of the facer. The difference in between a facer delamination and facer rupture is the location in initial failure. Failure for facer ruptures starts in the facer, while failure for the facer delaminations starts in the foam adjacent to the facer.

Based upon observations, the facer rupture is another failure plane that is indicative of a properly constructed specimen – this would be the second most desirable failure plane after facer delamination. Figure 4.5 illustrates typical facer ruptures.

Coverboard Failure

Coverboard failures occur when the coverboard loses cohesion adjacent to the beads of adhesive or the full-coat of adhesive. Fiberboard is a particularly weak material in tension and this failure plane was exclusive to fiberboard. The ductility of cohesive coverboard failures are comparable to adhesive failures. Figure 4.6a illustrates a typical cohesive coverboard failure with partial adhesion while figure 4.6b illustrates a typical cohesive coverboard failure with full adhesion.

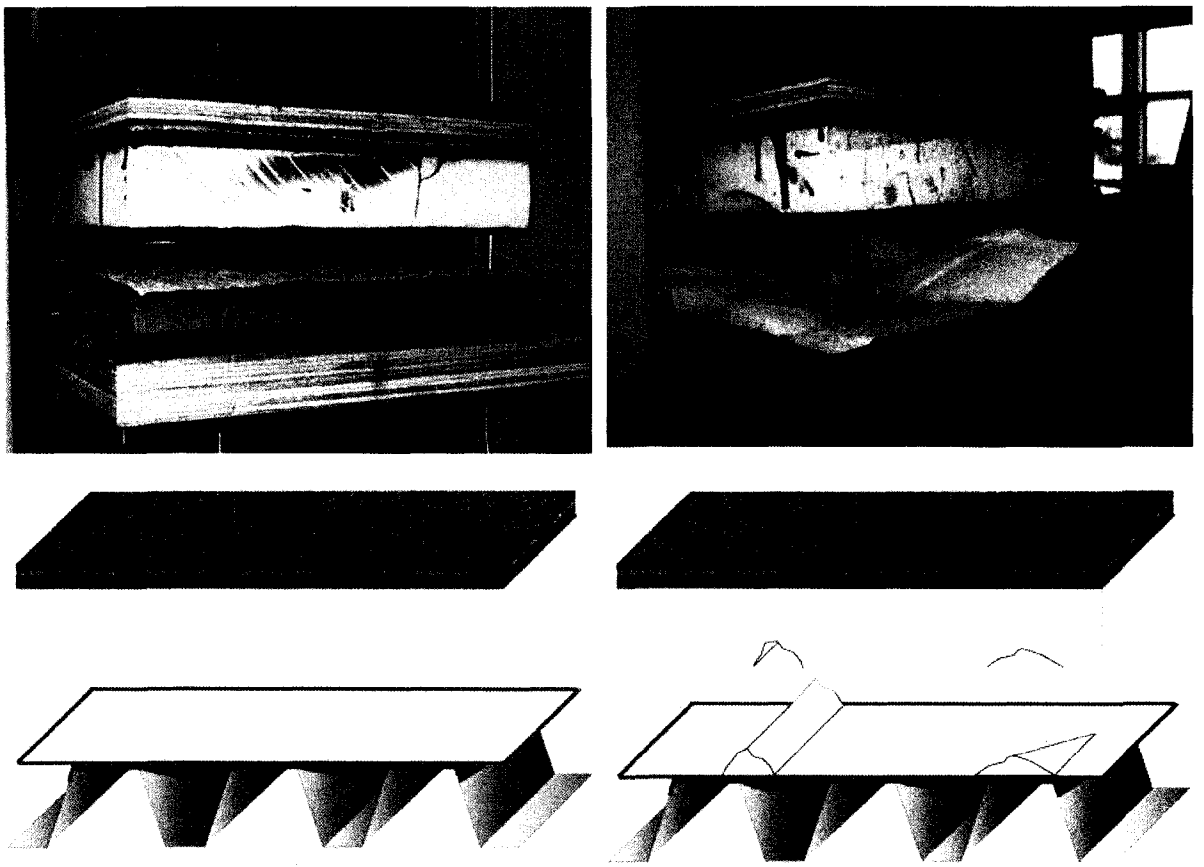

Figure 4.4: Illustration of Facer Delamination

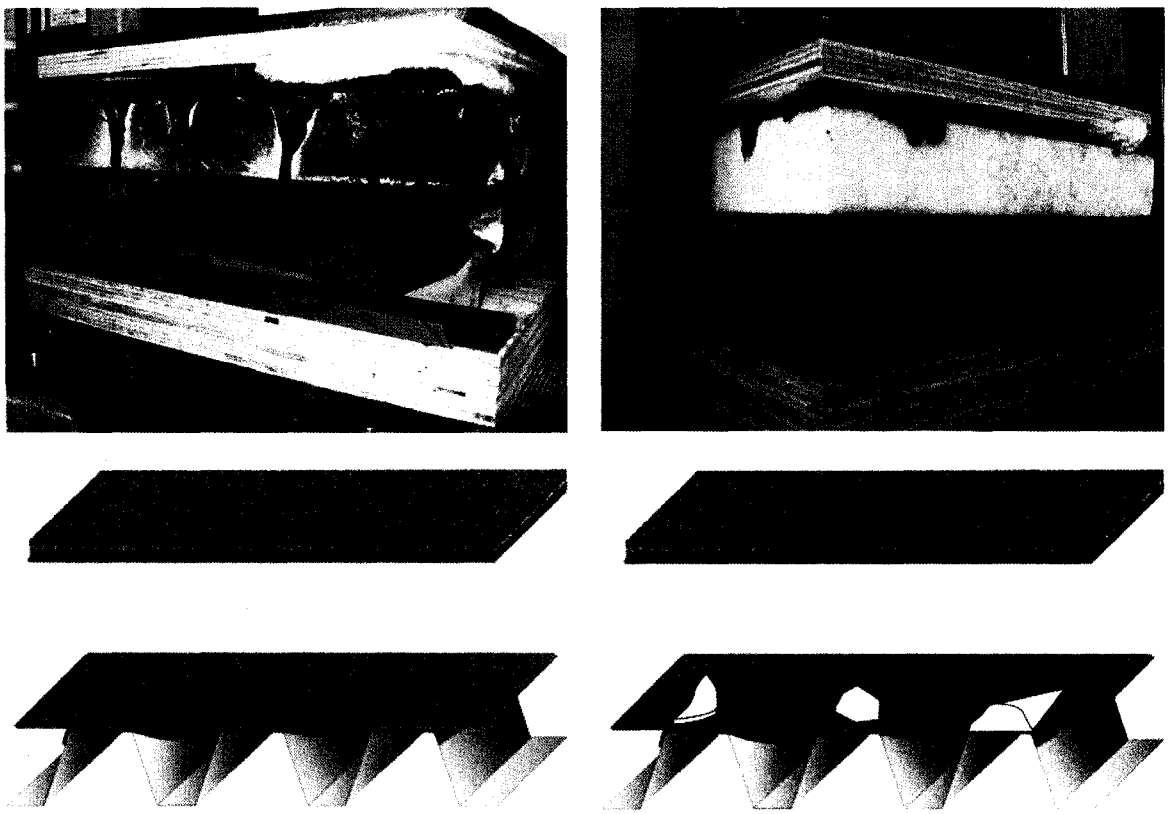

Figure 4.5: Illustration of Facer Rupture

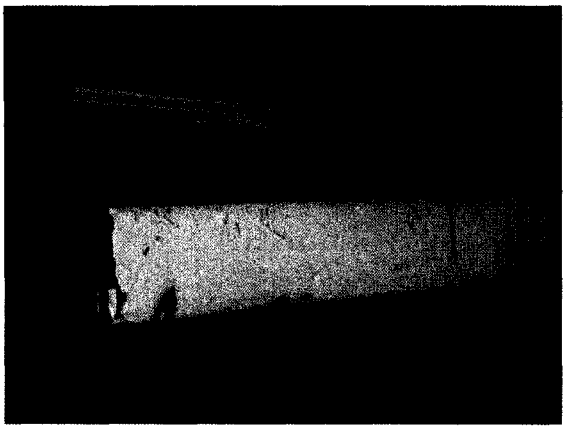

Figure 4.6a: Coverboard Failure with partial adhesion

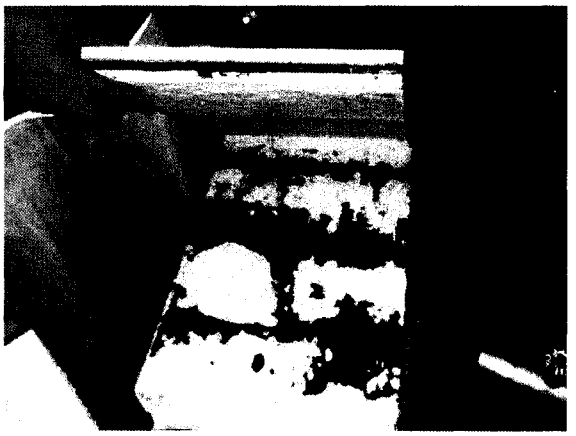

Figure 4.6b: Coverboard Failure with full adhesion

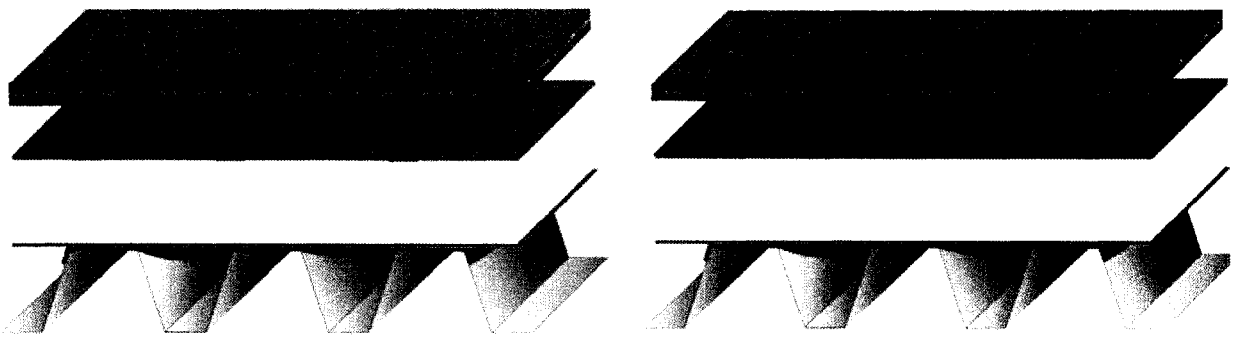

Figure 4.6: Coverboard Failure

4.3.2 Data Analysis

All pullout tests that were conducted had an associated raw data file where the Instron machine logged the load and the deflection at a fixed sampling rate as discussed in Section 4.2.2. These raw data files were exported into graphing software (Microsoft Excel) to produce graphs that permitted visual inspections and comparisons of different tests. Figure 4.7a & b illustrate two separate specimens from the same source constructed from different materials. Figure 4.7a illustrates the expected behaviour from what would typically be characterized as a successive failure. This means that multiple failures, commonly in the same plane, caused overall failure of the specimen. The failure plane would be the plane in which failure was first observed. A failure plane that exhibited such behaviour was the facer delamination. Notice in figure 4.7a, that two major failures occur before specimen failure is observed. These are the defining characteristics of successive failure. Figure 4.7b illustrates the expected behaviour from a catastrophic failure. This means that there was one singular failure (Failure 1 in figure 4.7b) that propagated to lead to a catastrophic failure which led to overall failure of the specimen. A failure of this nature typically was a coverboard failure. As noted in figure 4.7, specimen failure is synonymous with the end of test conditions described in section 4.2.2.

One of the most generic measurables is the global maximum of the dependent variable. This was referred to as the peak load and was used heavily as a barometer of pullout performance. This was the same measurement used for determining pullout resistance from the literature study of Chapter 2. This is a very simple and robust measurement and gives a fairly general idea of relative performance.

Another useful measurement is the deflection at peak load. This is a measurement of the independent variable when the dependent variable is at a global maximum.

Typically, ideal behaviour would consist of both a high peak load and a high deflection at peak load. Based on the definition of mechanical work, this

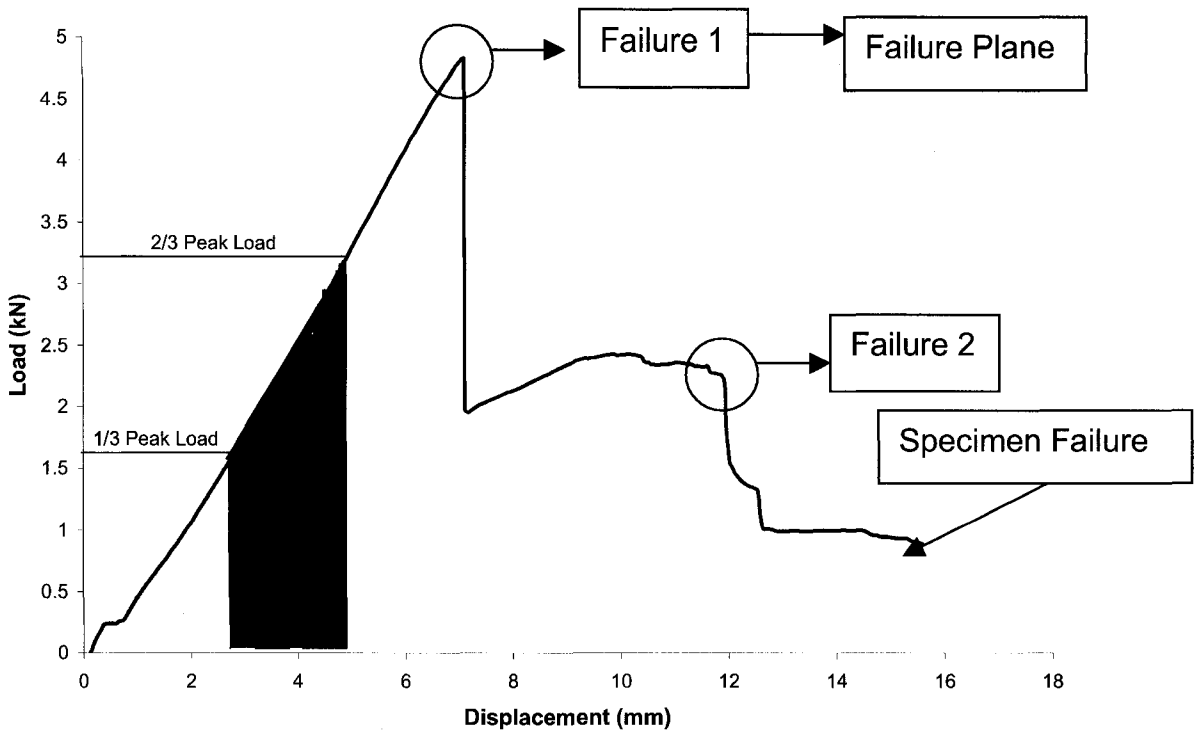

Figure 4.7a: Load-Deflection Response for a successive failure illustrating numerical integration bounds for elastic energy calculations

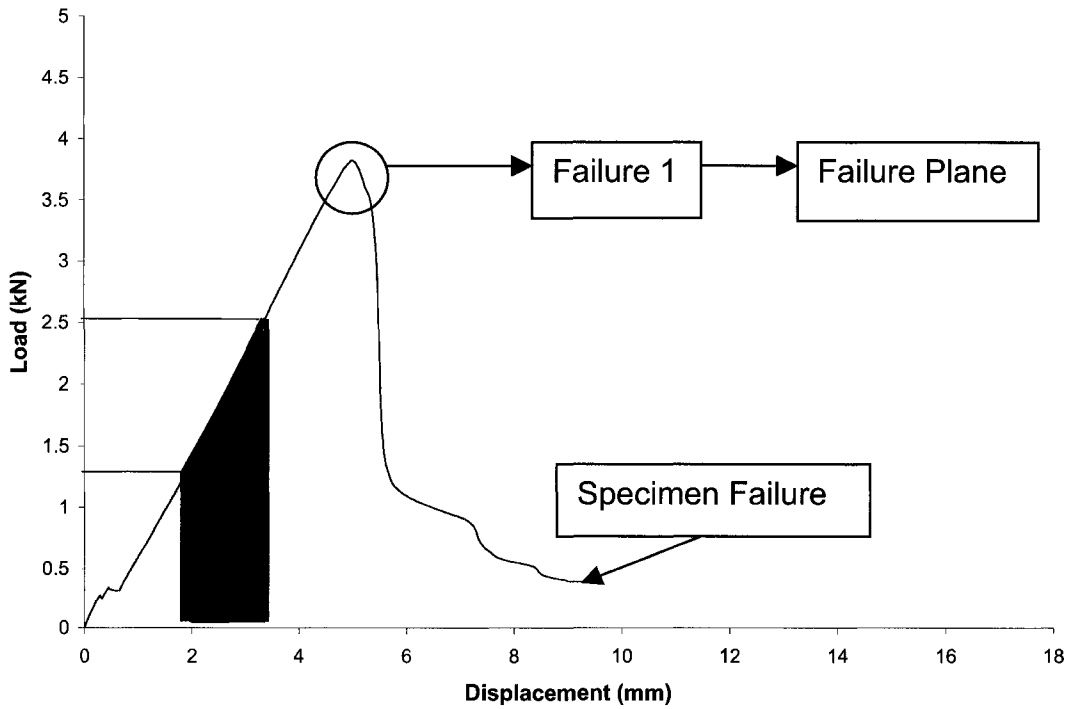

Figure 4.7b: Load-Deflection Response for a catastrophic failure illustrating numerical integration bounds for elastic energy calculations

means that a large amount of energy would have to be put into the specimen before failure occurred. This is determined by summing the area under the curve. First a definition must be provided of what constitutes elastic behaviour in AARS, before providing the methodology to determine the area under the curve.

For the sake of this investigation, elasticity was defined as the portion of the curve between one third of the peak load and two thirds of the peak load. One third and two thirds of the peak load were systematically chosen because over the course of the first few millimeters of deflection, slack was removed from the specimen and this resulted in unpredictable behaviour, hence these measurements were removed from the area under the curve calculations. In the final 1/3 of the test (from 2/3 to the peak load) the slope evolved from linear to non-linear. Based on these observations, the portion of the curve between these two bounds was numerically integrated. The numerical integration that was chosen is explained by the following equation:

$$\int_{1/3PL}^{2/3PL} F(x) = \Delta x[(f(x_1)+f(x_2))/2+(f(x_2)+(f(x_3))/2+....+(f(x_{n-1})+f(x_n))/2]$$

Where,

- $\int_{1/3PL}^{2/3PL} F(x)$ is the area under the curve from 1/3 of the peak load to 2/3 of the peak load.
- $f(x_n)$ is a data point measurement indexed by starting at the load measurement at 1/3 of the peak load.
- Δx is the rectangle thickness. Since all numerical integration was performed on specimens tested at 6.35mm/min and the data was sampled 10 times/second, this would correspond to a constant rectangle thickness of approximately 0.0106 mm.

This is essentially numerical integration using the mid-point rule. Although the methodology was not perfect it provided an adequate and robust estimate of how loading would build based on a fixed pullout rate, under the consistent boundary conditions applied. With reference to this investigation, elastic energy calculations were used for determining the pullout resistance of applications of the test method (Chapter 6).

4.4 Concluding Remarks

This section provided an overview of the constituents of AARS specimens. It also provided the apparatus and the procedure for conducting an AARS pullout test. This section laid out the objectives of the study with respect to experimentation and experimental variables and provided the guidelines for evaluation of both observations and numerical measurements. In the following chapters the proposed test method was followed.

Chapter 5: Parameter Specification for the Development of a Test Method

5.1 Introduction

As mentioned in earlier discussions, the unique nature of AARS assemblies requires unique evaluation methods, the product of which is this study. There are methods for evaluating the wind uplift performance of other types of assemblies at full-scale (CSA A123.21-04), however existing test methods are inappropriate for AARS. The unique nature of AARS requires a unique test and in this chapter the key parametric variables isolated in chapter 2 will be assessed and then specified.

In the absence of a proper understanding of the nature of how failure is initiated and propagated, the development of a standardized test requires careful experimentation to assess the nature of important variables that are relevant in determining the pullout response. These variables must be sensitive to mechanisms that lead to failure. The mechanisms that drive failure in AARS are two-fold; they are:

- Shear Forces
- Tensile Forces

The specific details of how these two forces interact and lead to failure is not entirely understood, however it is known from a mechanics of materials standpoint that one failure can precipitate another and vice versa. Wu, (2008) established a test method for quantifying and categorizing the shearing and peeling behaviour of small-scale AARS roofing specimens. This chapter will present the results that were carried out to specify the key variables that were singled out for determining the important test-related variables for determining the pullout strength of small-scale AARS roofing assemblies.

To achieve adequate pullout performance it is necessary to locate the likely planes of failure, and the loading at which failure occurs. These are the two keys parameters by which evaluation of small-scale AARS assemblies will be performed. Consistent behaviour between sources will be necessary to ensure a repeatable test procedure. Without consistency, it will be difficult to predict behaviour in the field, which is the overall purpose of this study. Sections 5.2 & 5.3 present the results of experiments that were performed to assess the pullout rate. Sections 5.4 & 5.5 present the results of experiments that were performed to specify the specimen size. Finally sections 5.6 & 5.7 will present the results of experiments conducted to determine the effects of different deck attachment conditions.

5.2 Pullout Rate Specification – Comparative Analysis

The pullout rate was one of the key parameters that needed to be specified for the development of a pullout test. The pullout rate is defined as the rate at which deflections were imposed on the stress plate mounting platform of the specimens. This section summarizes the data from 128 experiments that were conducted in order to determine the appropriate rate at which pullout tests should be conducted on AARS specimens. In Figure 5.1, a flowchart of all the experimental variables has been provided in determining the appropriate pullout rate.

As shown in figure 5.1, all sources constructed specimens to a size of 300 x 450 mm on steel deck, with 50 mm polyisocyanurate insulation, and asphalt core board. 8 Specimens were constructed from each source for each sample - corresponding to a total of 128 specimens. Based on the results of these experiments, the data would indicate which speed is most appropriate for conducting pullout tests.

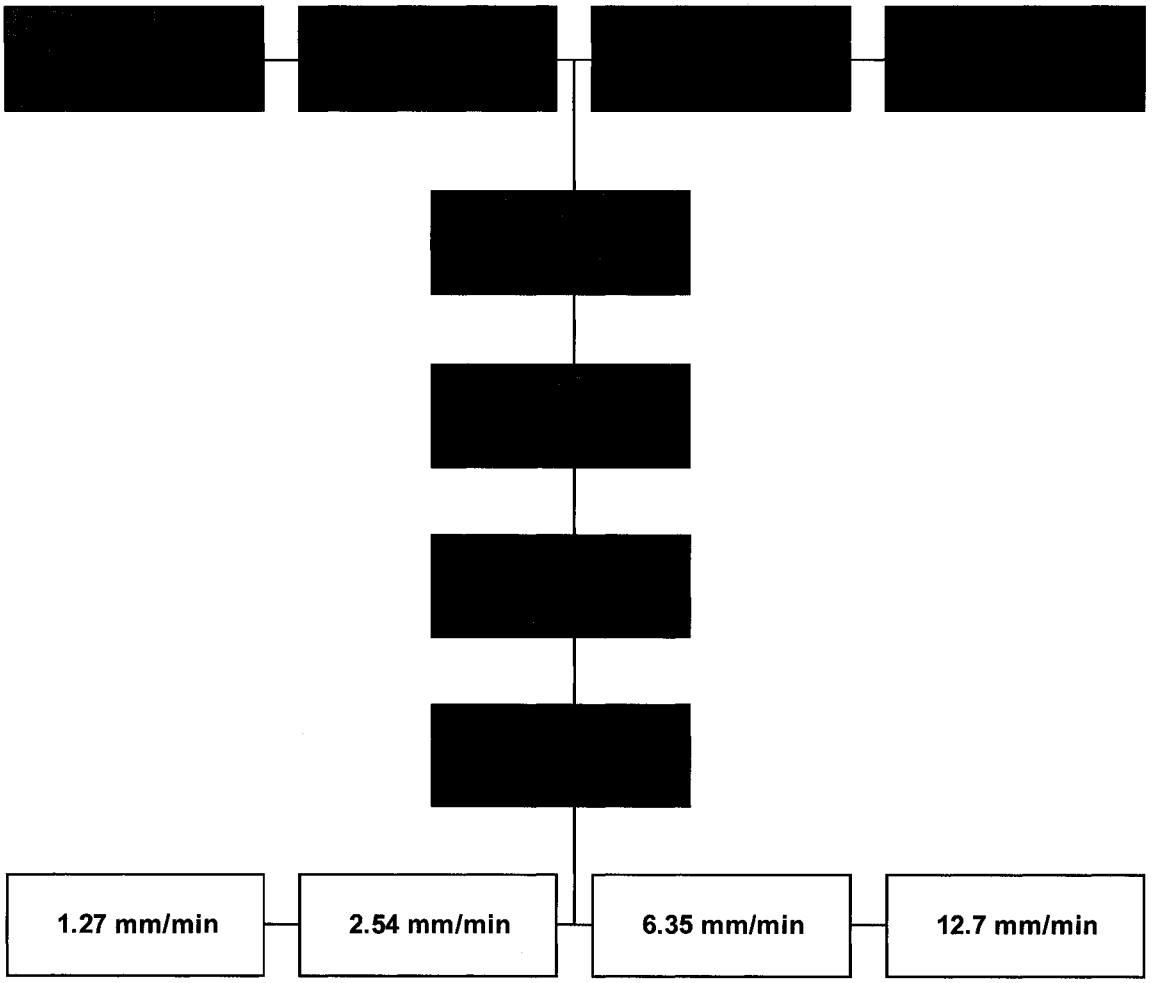

Figure 5.1: Test matrix for pullout rate determination

A typical response to the pullout tests is shown in Figures 5.2 for tests conducted for the sample with a pullout rate of 2.54 mm/min for Source 4. The curves in Figure 5.2 are characterized by two sections. The first section consists of a mostly linear region where loading builds until failure occurs. The behaviour in this region of the curve is the region that the present study is most interested in characterizing. However, linearity is not observed in the regions immediately at the start of the test and prior to failure. As discussed in section 4.3.2, this is due to the removal of slack in the system (start of test) and the evolution of linear elastic behaviour to non-linear plastic deformation (prior to failure). After failure the response varies significantly – typically the failure plane will dictate the post-failure specimen response and the resulting shape of the curve.

In Figure 5.3, a bar graph illustrates the peak load attained from each specimen illustrated in Figure 5.2. Note that even with the inclusion of specimens 4 & 8, the testing exhibits repeatable behaviour and that the data falls within a reliably predictable range, with a sample average peak load of 3.45kN. The raw data illustrated in Figures 5.2 & 5.3 are relevant but it does not depict the entire message all by itself. The relative results – meaning the results with respect to similar experimentation – are what are most important in determining the appropriate pullout rate.

Figure 5.4 exhibits how the peak load measurements change over the range of the four applied pullout rates of 1.27, 2.54, 6.35, 12.7 mm/min and with respect to the 4 different sources. Therefore figure 5.4 plots the results from 16 samples. Each data point represents the sample average peak load measurement from one sample of eight specimens. Additionally, two generalized curves have been plotted; one characterizing the pullout behaviour of fully adhered samples (Sources 1 & 4) and another characterizing partially-adhered samples (Sources 2 & 3). These generalized curves have been generated by averaging the results from experiments conducted at the same pullout rate for Sources 1 & 4, and averaging the results from experiments conducted at the same pullout rate for Sources 2 & 3. Henceforth these curves will be referred to

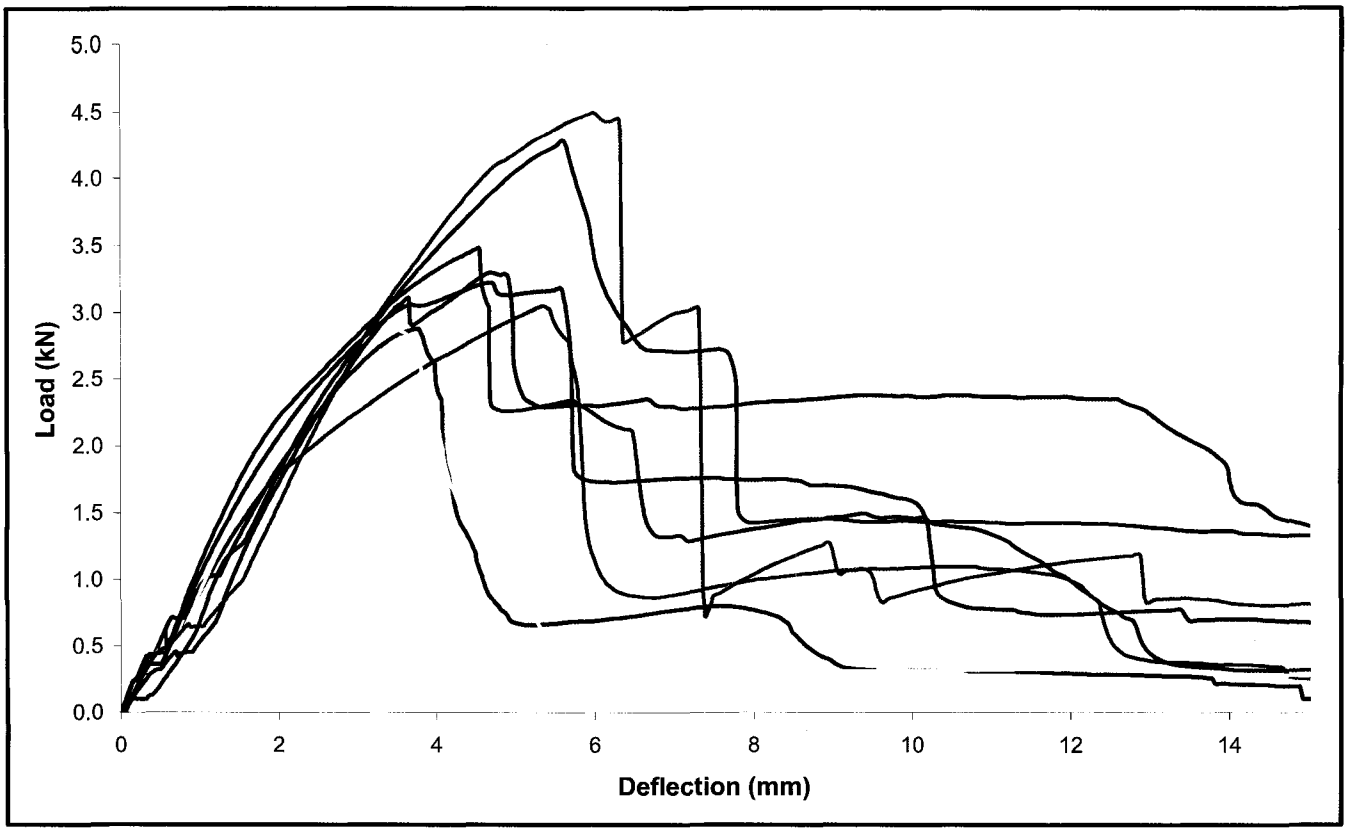

Figure 5.2: Typical load-deflection response for a pullout rate of 2.54mm/min

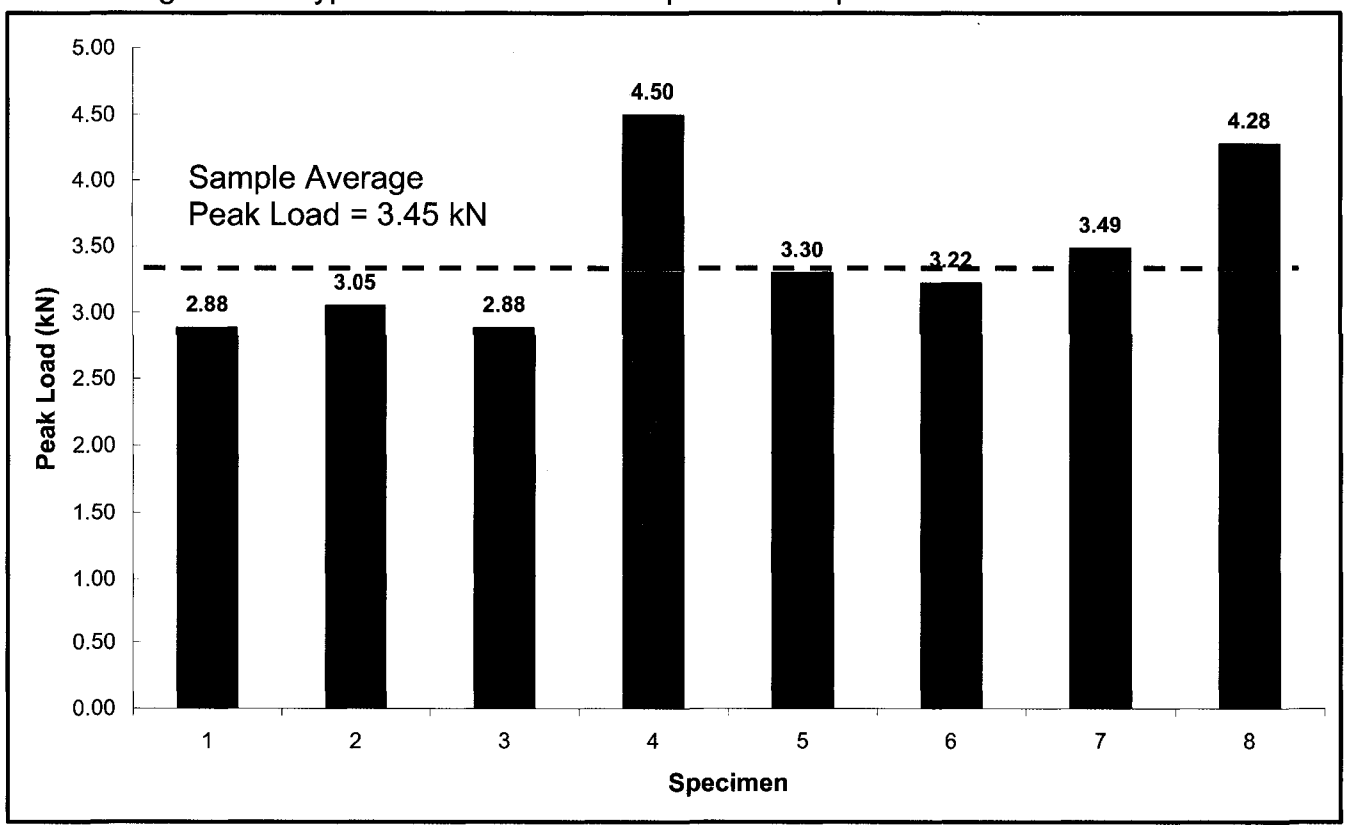

Figure 5.3: Peak load data extracted from load-deflection response of figure 5.2

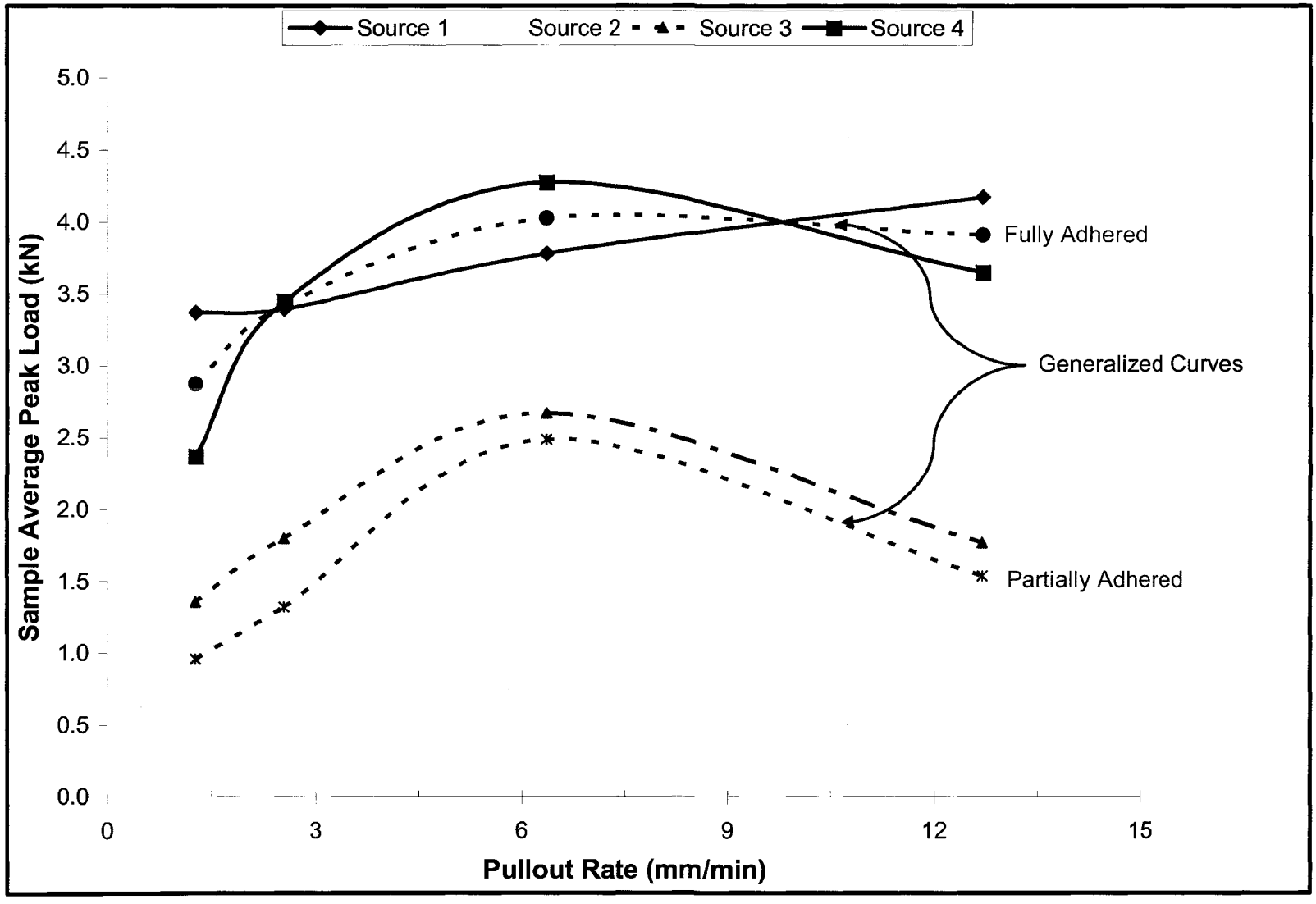

Figure 5.4: Sample average peak load for pullout rates of 1.27-12.7mm/min with generalized curves for full and partial adhesion

as the generalized curves for pullout rate for full and partial adhesion.

Figure 5.4 exhibits a definitive overall trend – pullout performance improves gradually from 1.27 to 2.54 to 6.35 mm/min and then descends when the speed is increased to 12.7 mm/min. Source 1 exhibits similar behaviour, however instead of decreasing from 6.35 mm/min to 12.7 mm/min the pullout performance actually improves when the pullout rate is increased, however this is an exception. The shapes of the generalized curves confirm this observation; they are a maximum at 6.35 mm/min and the performance decreases when the speed is either increased or decreased from this rate. Since the purpose of this study is to specify a pullout rate it would appear that the pullout rate of 6.35mm/min is optimum based on the argument presented above. The test speed that is selected for the test method should be the one which displays the highest performance because in future tests it will be much easier to identify specimens that don't conform to the results exhibited by past experiments.

Figure 5.5 presents the normalized results of Figure 5.4. The normalization data comes from the generalized curves. For example, the 1.27 mm/min data point for Source 2 (≈ 0.6) is the quotient of the sample average, as illustrated in Figure 5.4, divided by the generalized value for partially-adhered specimens for the 1.27mm/min condition. Each data point in Figure 5.5 is populated in a similar fashion. In this figure, the numerical values are important, but what is paramount for the purposes of this study is finding consistent behaviour across sources. The curves in figure 5.5 illustrate convergence around the pullout rate of 6.35 mm/min. (ie: The vertical gap between sources for the pullout rate of 6.35mm/min is a minimum when compared to other pullout rates) For the purposes of this study this is significant because it represents a pullout rate where performance is least dependent on the effect of source and all sources are at a maximum when the pullout rate is 6.35 mm/min.

As discussed in Chapter 4, repetitions of experiments were performed in order to provide statistical significance to this experimentation. Another measurement of interest is the amount of "potential" error or deviation within

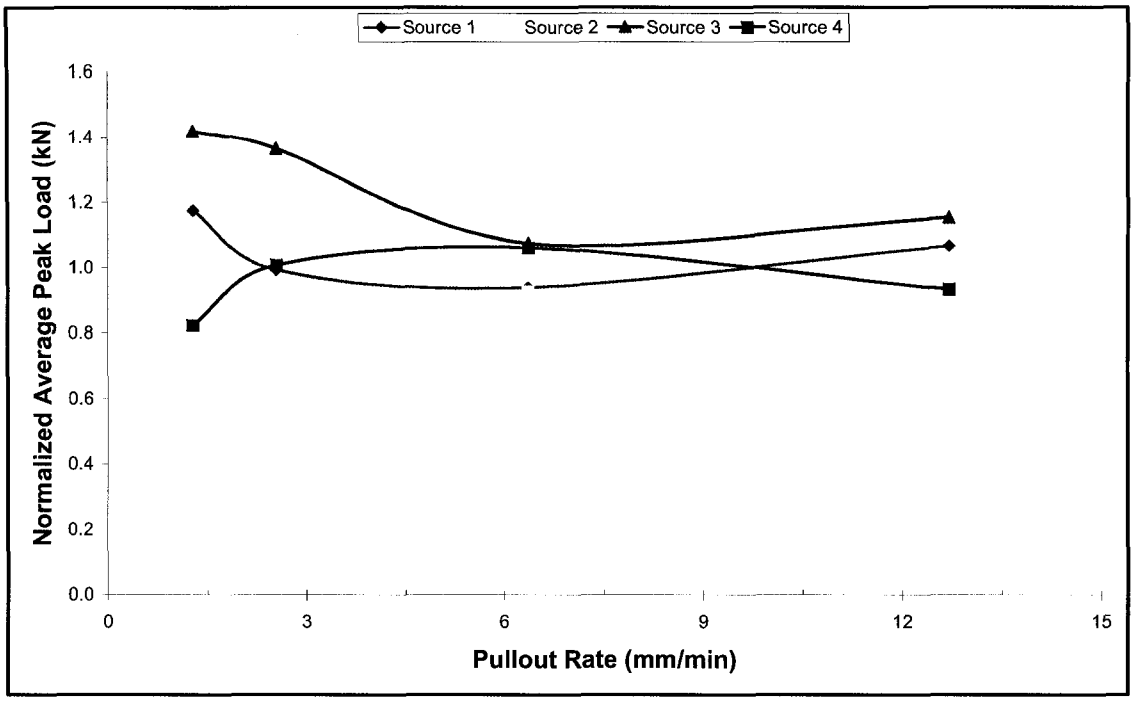

Figure 5.5: Normalized sample average peak load for pullout rates of 1.27-12.7 mm/min

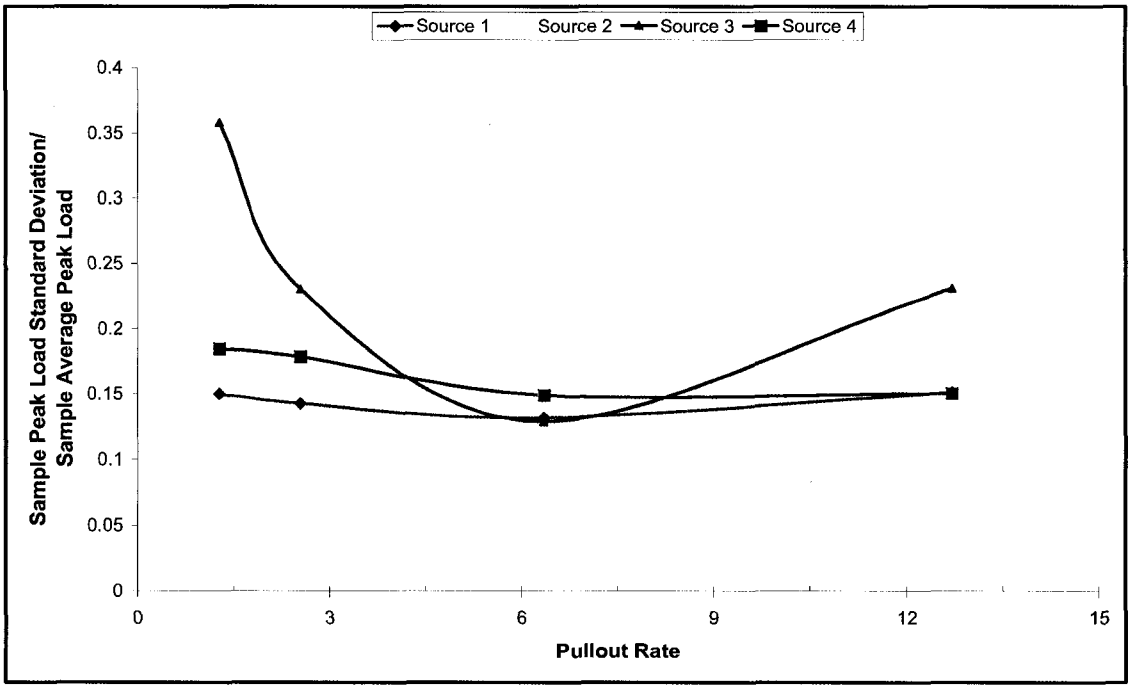

Figure 5.6: Normalized sample standard deviation of peak load for pullout rates of 1.27-12.7mm/min

these data sets. As a result, in addition to the sample average, the sample standard deviation was also calculated.

When the sample peak load standard deviation was divided by the sample peak load average and the relative deviation was calculated, a noticeable trend emerges as shown in Figure 5.6.

Despite the slightly anomalous behaviour exhibited by Source 1, there appears to be a trend in Figure 5.6 that shows that the relative deviation for the 6.35 mm/min condition is a minimum when compared to the other speeds, even though the absolute deviation is not necessarily a minimum for 6.35 mm/min. This indicates that the 6.35 mm/min pullout rate yields the results with the least amount of deviation as a function of the measurement.

Empirical analysis of experimental data yields a conclusion that the 6.35 mm/min condition is the optimum for conducting pullout experimentation. This analysis will have to be cross-referenced with failure plane analysis to corroborate qualitative and quantitative results.

5.3 Pullout Rate Specification – Failure Plane Analysis

After performing comparative analysis, it was necessary to categorize the failures as per the specifications outlined in section 4.3.1. All failures were categorized based on the criteria provided in this section and classified appropriately. Figure 5.7 illustrates the breakdown of failure planes. The x-axis shows the different pullout rates that were being evaluated, with the y-axis illustrating the percentage of occurrences of a given failure plane with respect to the total number of experiments conducted at a given pullout rate. The total number of occurrences of a given failure plane have been provided inside the figure. As an example 19 adhesive failures were observed from all Sources tested at 1.27 mm/min and correspond to approximately 60% of all failures at this pullout rate. Failure planes have been categorized from least desirable to most desirable from the bottom to top. (ie Adhesive Failure < VB Delamination < Facer Rupture < Facer Delamination)

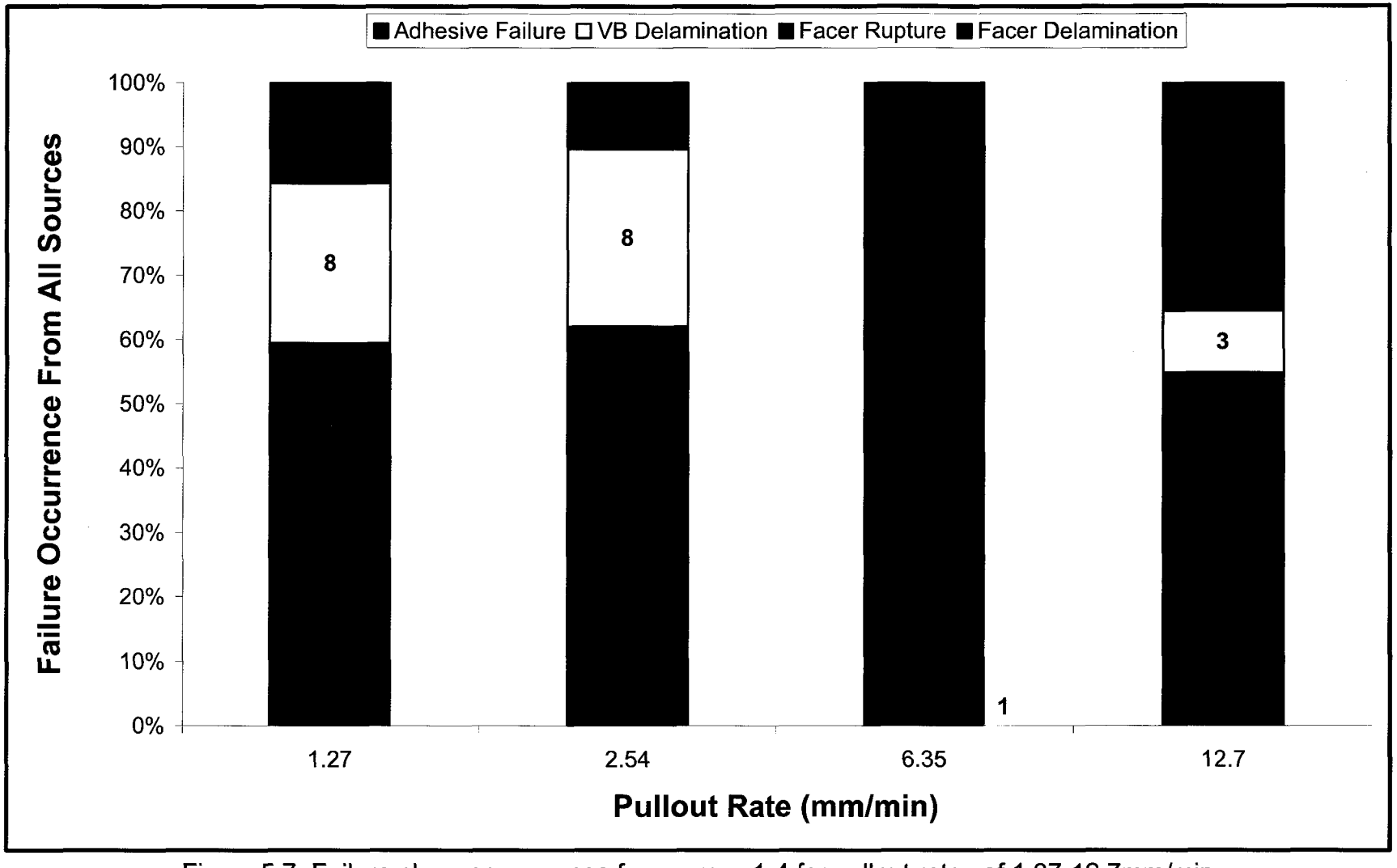

Figure 5.7: Failure plane occurrences for sources 1-4 for pullout rates of 1.27-12.7mm/min

There are several conclusions that can be drawn based on the information presented in figure 5.7. The 6.35 mm/min pullout rate exhibits more consistency with respect to the failure plane than any other speed. If the failure plane is consistent, this indicates that the failure load and the numerical results should be consistent. With the slight exception of Source 1 (1 observation of adhesive failure) For the 6.35 mm/min condition, all failures were on the facer. No other speed was able to demonstrate such consistency at a similar scale. Another generic observation appears to be that failures on the facer - rupture or delamination appear to be the failures that attain the highest peak load prior to failure. In some cases, as in Source 2, the only occurrences of facer failure in any form occur at 6.35 mm/min.

In figures 5.8 to 5.11 illustrations of the most predominant failure plane from the speeds of 1.37, 2.54, 6.35, and 12.7 mm/min have been provided as per the breakdown of Table 5.1. Please note that for the adhesive failures observed in Table 5.1, the exact plane in which failure occurred has been provided for clearer identification and cross-reference with figures 5.8 – 5.11.

Take special note how there are an increasing number of failures on the facer as the speed increases towards 6.35 mm/min and a decreasing number of failure on the facer as the speed continues towards 12.7 mm/min.
This is an observation that is independent of source, although the results are more telling for some sources. This trend exhibits an important point regarding the failure planes of AARS specimens. The increasing trend towards the occurrence of facer failures – delaminations or rupture – indicates that an ideal speed has been determined and only serves to confirm the findings that were concluded in section 5.2.

Pullout Rate	Source 1		Source 2		Source 3		Source 4	
(mm/min)	Failure Plane	Occurrence	Failure Plane	Occurrence	Failure Plane	Occurrence	Failure Plane	Occurrence
1.27	Adhesive (SD-VB)	5	Adhesive (SD-VB)	5	Adhesive (ISO-CB)	4	VB Delamination	8
	Facer Rupture	3	Adhesive VB-ISO	2	Adhesive (SD-VB)	2		
			Adhesive (ISO-CB)	1	Facer Delamination	2		
2.54	Adhesive (SD-VB)	5	Adhesive (SD-VB)	7	Adhesive (ISO-CB)	3	VB Delamination	8
	Facer Rupture	2	Adhesive (VB-ISO)	1	Adhesive (SD-VB)	2		
					Delam	1		
6.35	Facer Delamination	7	Facer Rupture	6	Facer Rupture	6	Facer Delamination	6
	Adhesive (SD-VB)	1						
12.7	Facer Rupture	4	Adhesive (ISO-CB)	5	Adhesive (ISO-CB)	3	Facer Delamination	5
	Adhesive (SD-VB)	2	Adhesive (VB-ISO)	2	Adhesive (VB-ISO)	3	VB Delamination	3
	Facer Delamination	1	Adhesive (SD-VB)	1	Adhesive (SD-VB)	1		
					Facer Delamination	1		

Table 5.1: Failure plane occurrences for sources 1-3 for pullout rates of 1.27-12.7mm/min

Adhesive failure between steel deck and vapour barrier (Source 2)

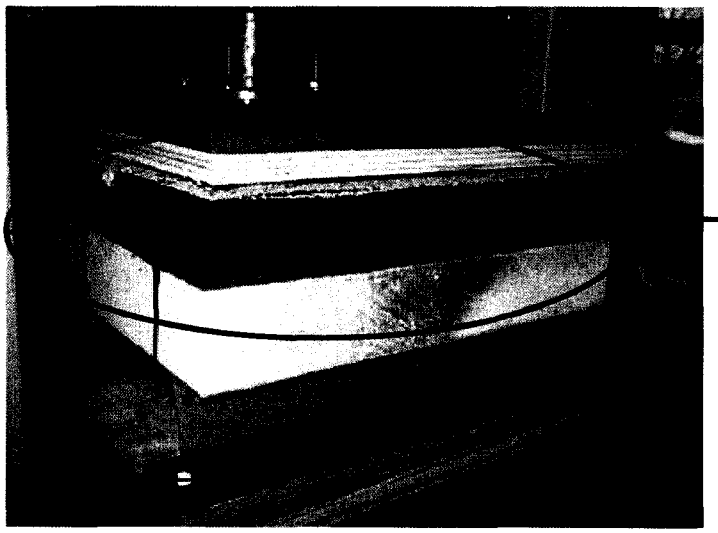

Adhesive failure between insulation and coverboard (Source 3)

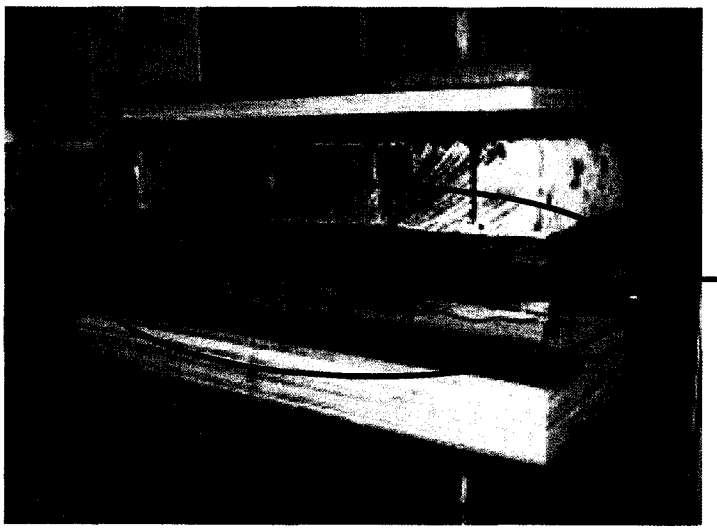

Vapour barrier delamination (Source 4)

Figure 5.8: Illustrations of typical failure planes for a pullout rate of 1.27mm/min

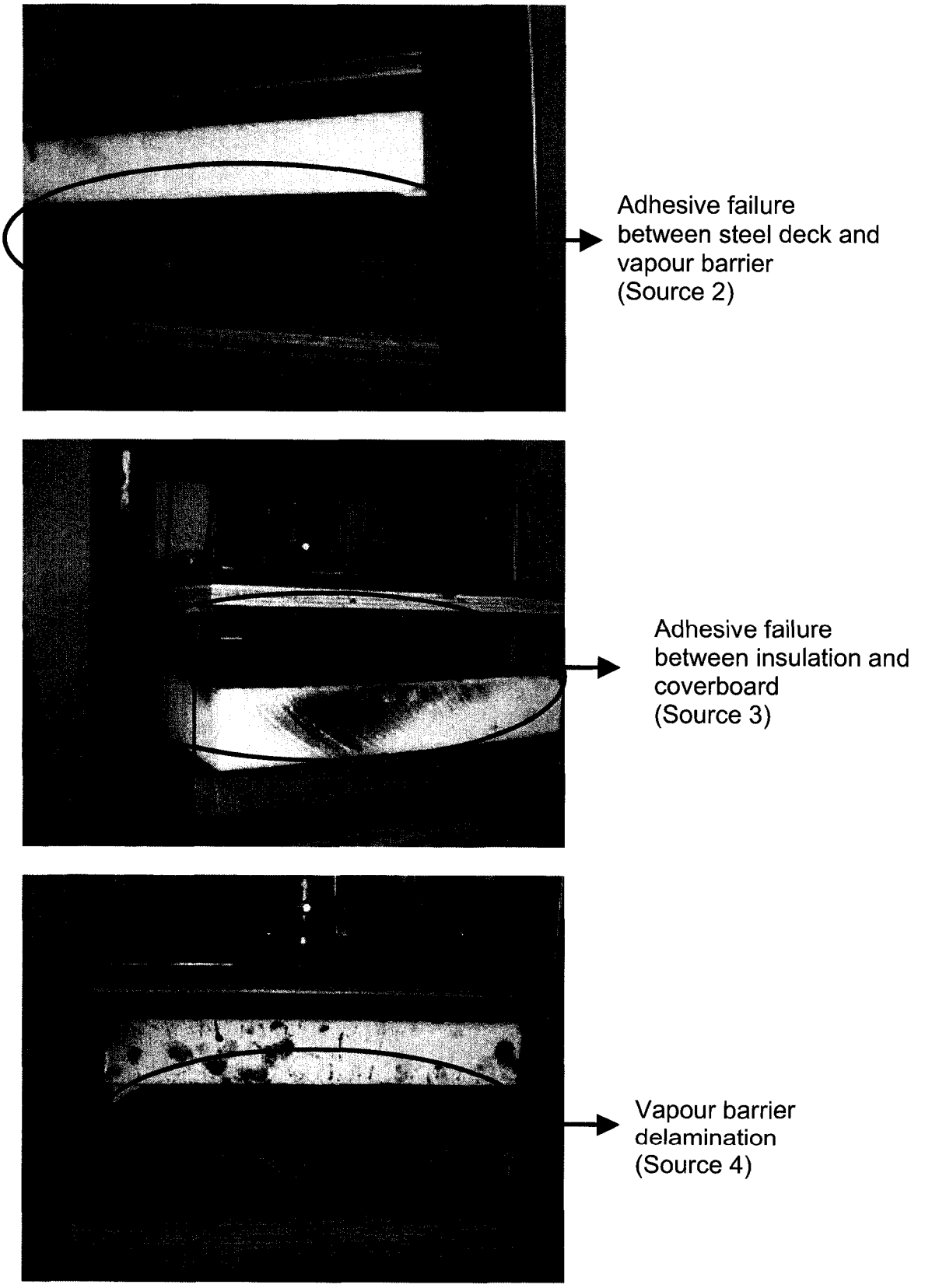

Figure 5.9: Illustrations of typical failure planes for a pullout rate of 2.54mm/min

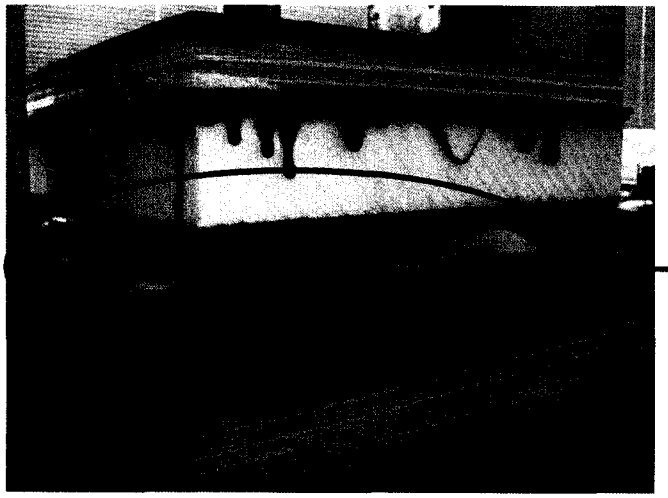

Facer delamination
(Source 1)

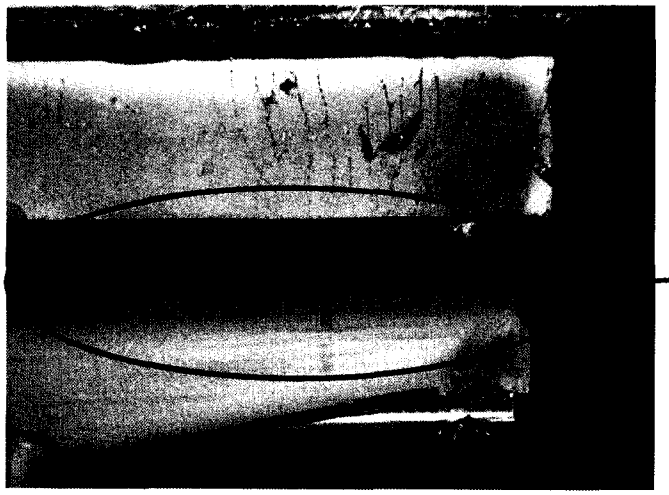

Facer rupture
(Source 2)

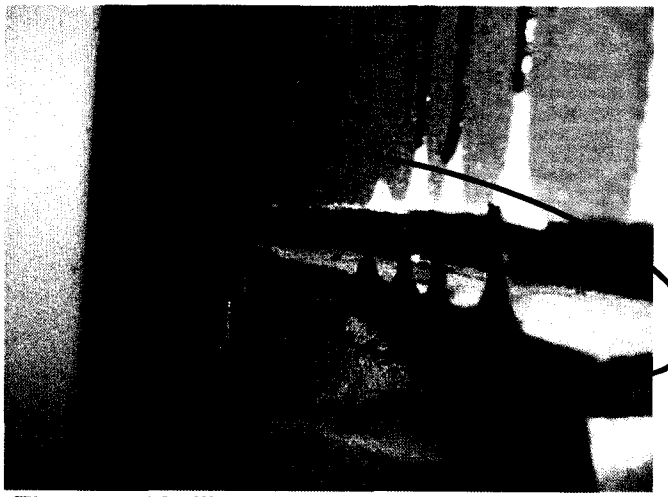

Facer delamination
(Source 4)

Figure 5.10: Illustrations of typical failure planes for a pullout rate of 6.35mm/min

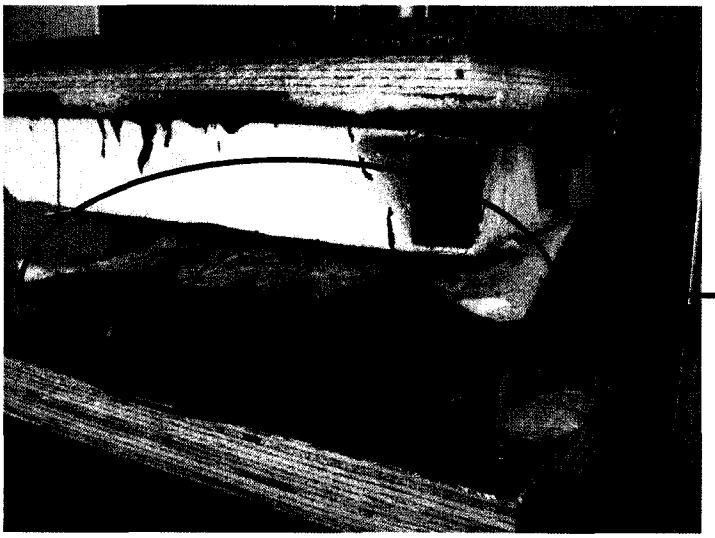

Facer rupture
(Source 1)

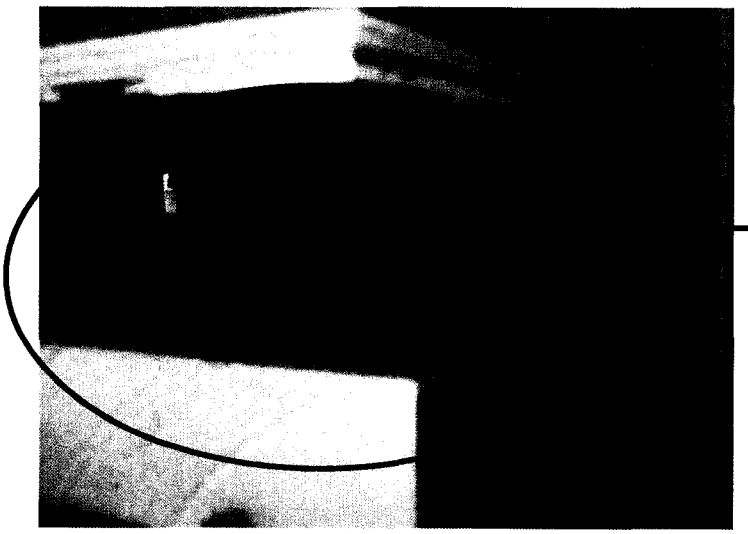

Adhesive failure
between insulation
and coverboard
(Source 2)

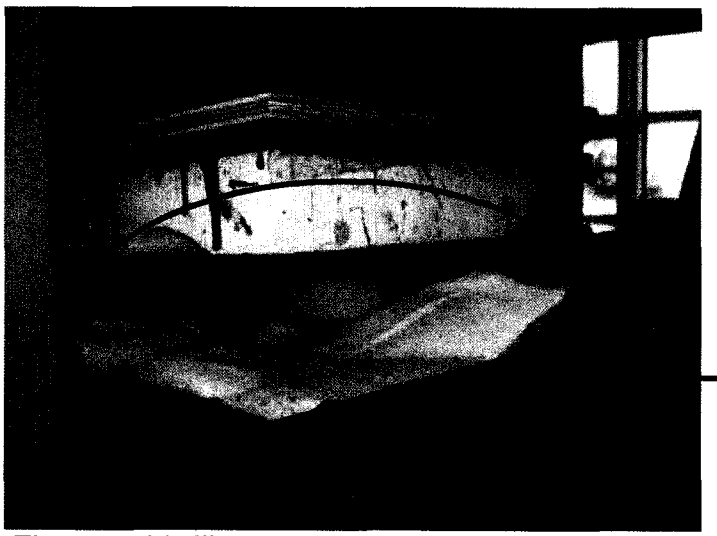

Facer
delamination
(Source 4)

Figure 5.11: Illustrations of typical failure planes for a pullout rate of 12.7mm/min

5.4 Specimen Size Specification – Comparative Analysis

Another variable of paramount importance when developing the test method is the specimen size. This would be the ideal size at which tests should be conducted. The size has to be large enough to ensure that sufficient contact area is provided and that the results would provide an indicative value of the pullout strength of the roof at full-scale. However some compromise has to be reached; the size could not be excessively large – so large that any implementation of the test would be rendered impractical for the purpose of instituting the lessons learned in this study, to field applications. The final size would be a compromise between these two opposing factors. During this analysis a basic assumption was invoked. Two sizes of specimens were tested in this section however the same stress plate was used during pullout testing as illustrated in Figure 5.12. Inherently there will be different stress paths taken in the completion of pullout testing and most notably a stress concentration on the larger specimen around the perimeter of the stress plate as it transfers loads from the stress plate to the stress plate mounting platform. For the purposes of this study, the effect of this stress concentration is assumed. In other words, it is assumed that stress transfer from the steel stress plate to the plywood stress plate mounting platform is uniform irrespective of specimen size and will have a minimal effect on pullout performance.

Another factor that had to be considered is the dimensions of the deck. Standard steel roof decking, is manufactured to imperial specifications. Figure 3.3 illustrates this phenomenon. The center to center distance of adjacent female flutes is 6" (150 mm) and it is an important factor that must be put into consideration because any arbitrary selection of dimensions perpendicular to the flutes of the steel decking could lead to eccentric loading – and turn the pullout test into a combined evaluation of both pulling and peeling. Due to the nature of the test and the materials that are used in AARS it will be completely impossible to devise a test method where the exclusive driving-force to failure will be direct tension. Combined failure is something that can only be minimized and it cannot be avoided all together. The combined failure will result in increased data scatter.

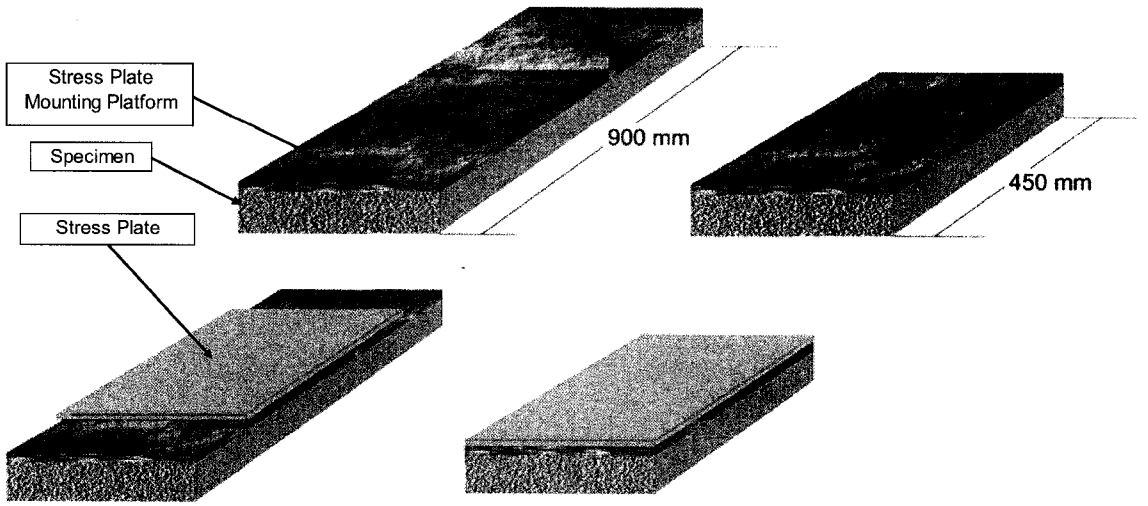

Figure 5.12: Stress Plate & Stress Plate Mounting Platform Setup for 300 x 900 mm and 300 x 450 mm Specimens

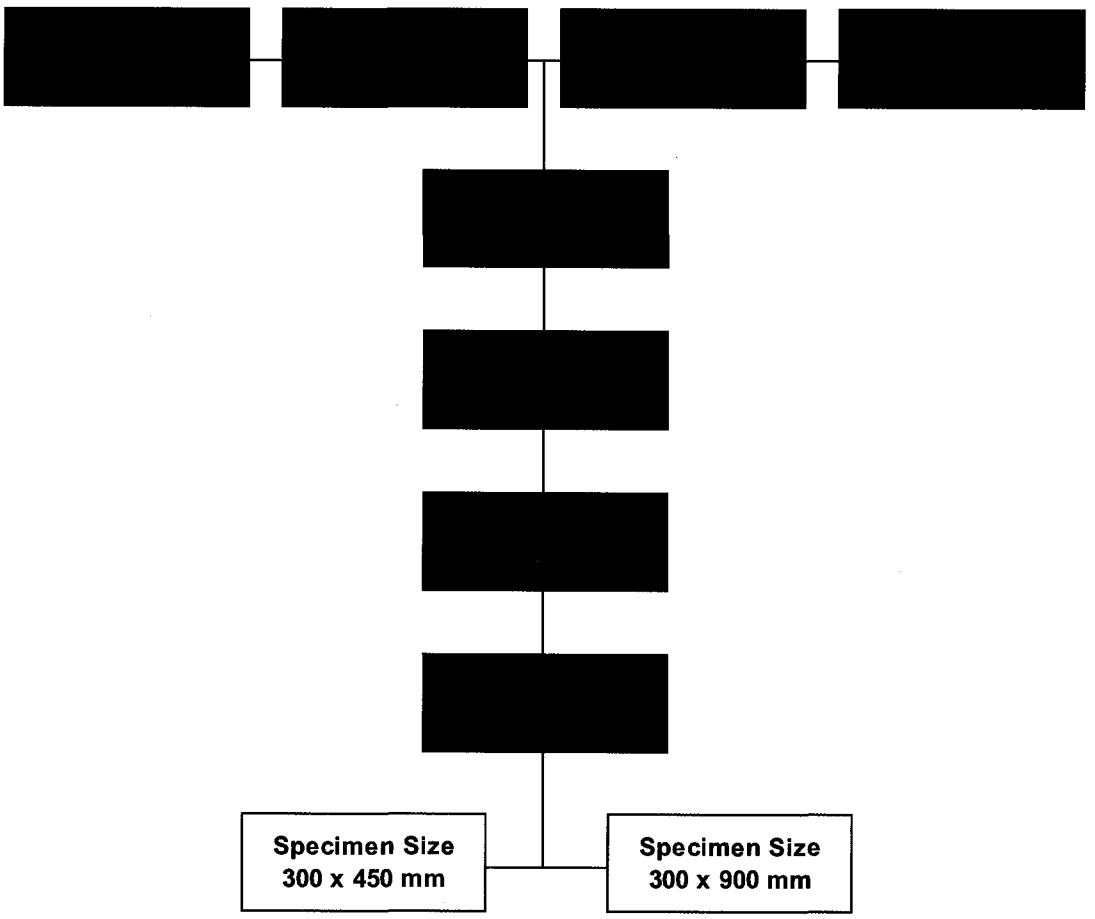

Figure 5.13: Test matrix for specimen size determination

and a larger degree of scatter convolutes any of the lessons learned from this study.

Based on the arguments provided above, the sizes of 300mm x 450 mm and 300mm x 900 mm were selected. The size of 300mm x 300mm realistically could have been selected based on the key dimensions illustrated in Figure 3.3. However, some sources typically do not apply adhesive to all flutes of the deck as a cost and labour savings measure. Alternatively, they apply adhesive on every other flute. This would exclude the specimen size of 300mm x 300mm and it is why 300mm x 450mm was selected. 300mm x 900mm was then selected as a comparative value to 300mm x 450mm. If it was deemed that the results from 300mm x 450mm were inadequate, then experiments could be compared with something that is twice as slender.

Figure 5.13 illustrates the key variables that were selected in determining the appropriate test specimen size. As per the guidelines of figure 5.13, all specimens were constructed on steel deck, with 50 mm polyisocyanurate insulation, and asphalt core board.

As outlined in section 3.2.2, there were different specimen construction methodologies employed by different sources. Specifically, sources 1 and 4 applied all construction materials via full-adhesion, while sources 2 and 3 applied all construction materials via beads of adhesive. Similar to section 5.2, sources that employed different methodologies will not be compared to one and other because the results indicate that these two different construction methodologies play a significant enough role in the failure of the specimens – particularly when the size of the specimens are different.

Single specimen pullout responses of both fully and partially adhered specimens for both 300 x 900 mm & 300 x 450 mm specimens have been illustrated in Figure 5.14. These responses have been selected based on their proximity to the overall size and methodology average. For example, the sample average peak load for partial adhesion for a specimen size of 300 x 450 mm is 2.50 kN. The pullout response that has been illustrated is for a specimen from

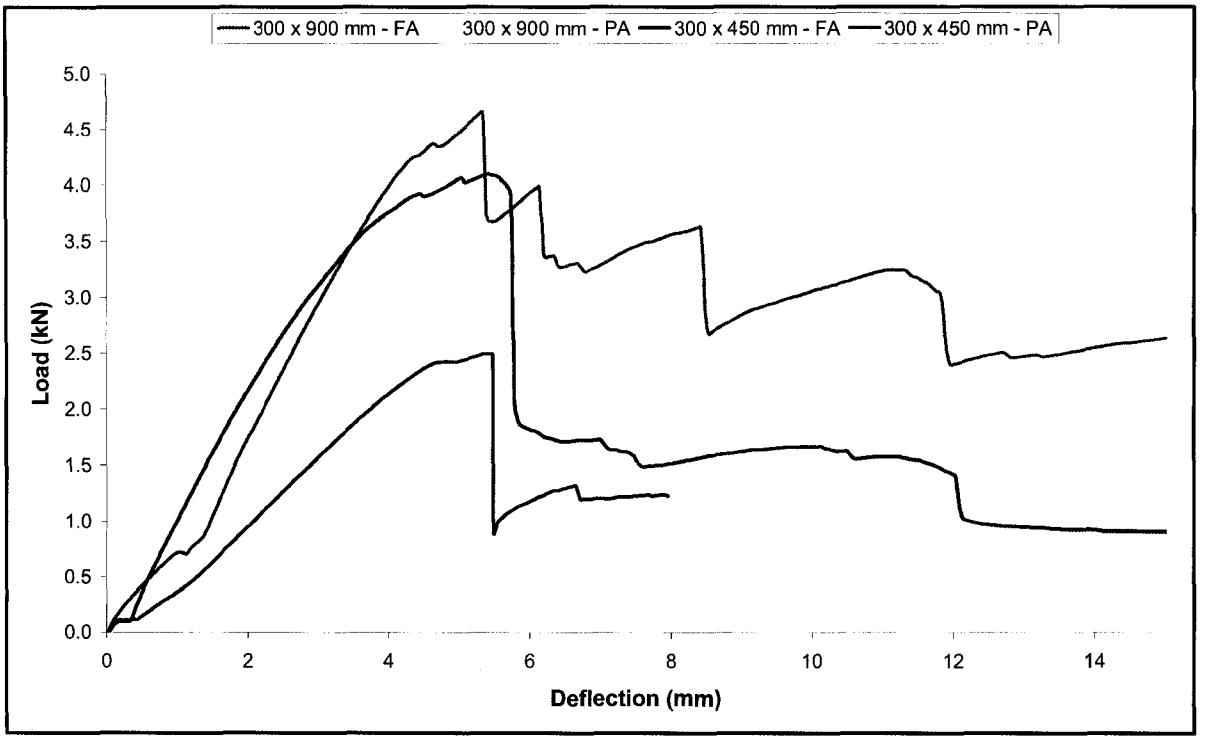

Figure 5.14: Load deflection response of fully & partially adhered specimens of size 300 x 900 mm & 300 x 450 mm

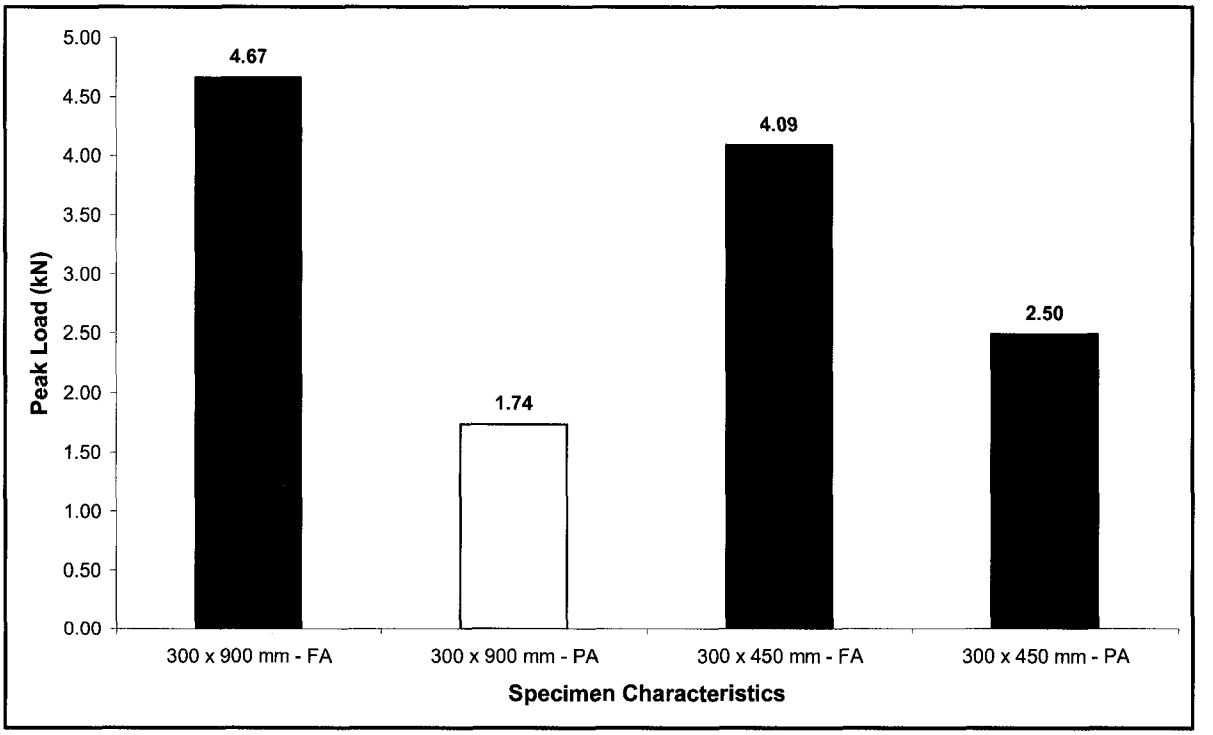

Figure 5.15: Peak load data extracted from load-deflection response of figure 5.13

Source 3 that failed at 2.50 kN. This curve is representative of all specimens of this size (300 x 450 mm) and of this construction methodology. (partial adhesion)

Figure 5.15 illustrates the peak load extracted from the pullout responses of Figure 5.14. With respect to Figure 5.14, take special note that the slopes of the curves in the elastic region are similar when comparing specimens with similar construction methodologies. This confirms a logical point – that the specimen size does not significantly affect the load-deflection characteristics of AARS specimens.

Some basic observations are made from the results presented in Figure 5.15. It would appear that the pullout response is more sensitive to construction methodology than it is to specimen size. This conclusion is drawn based on the closer proximity of the results from full adhesion (4.67 & 4.09 kN) and partial adhesion (1.74 & 2.50 kN) rather than proximity based upon size for 300 x 900 mm specimens (4.67 & 1.74 kN) and 300 x 450 mm (4.09 & 2.50 kN)

Figure 5.16 was then constructed to provide a baseline comparison between the two different specimen sizes by accounting for differences in construction methodology. Figure 5.16 illustrates the sample average peak load of 300 x 450 mm & 300 x 900 mm specimens for Sources 1 & 4 (fully-adhered) and Source 2 & 3 (partially-adhered).

From Figure 5.16, 300 x 900 mm specimens from all Sources typically fail in the expected range of 1.14 kN – 4.72 kN, while 300 x 450 mm specimens from all Sources typically fail in the range of 2.30 kN – 4.27 kN. Although it would be beneficial to use the 300 x 900 mm because it has a higher peak load threshold when compared to 300 x 450 mm specimens (4.72 kN vs. 4.27 kN) – the range of the data acquired through experimentation is simply too large, particularly based on the results found for 300 x 450 mm specimens. Based on initial observations, it would appear that 300 x 450 mm is a more appropriate size based on the smaller and more refined range of peak load results attained.

The results from figure 5.16 depict two contradictory statements. When full adhesion is applied the larger specimens fail at higher loads. When partial adhesion is applied the smaller specimens fail at higher loads. Logically, the

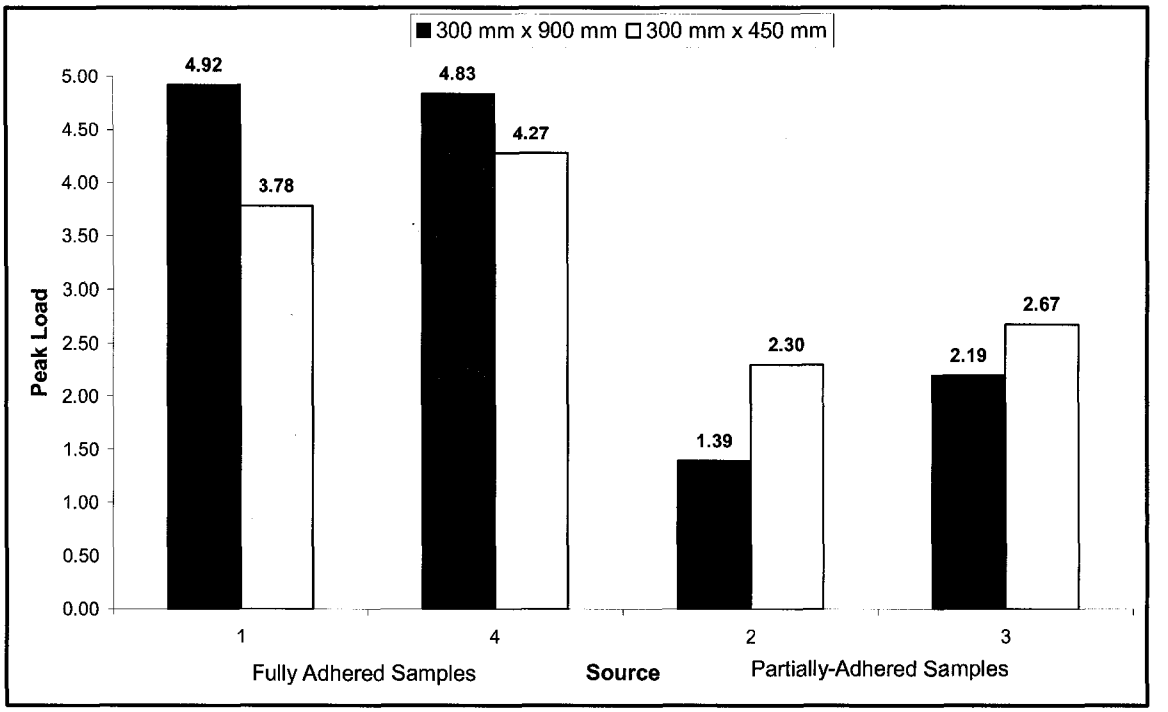

Figure 5.16: Peak load pullout performance comparison of fully-adhered specimens & partially adhered specimens

assumption should be made that a larger specimen will fail at higher loads because there is a larger adhesive contact area. A larger contact area would indicate that more work would be required to stretch and destroy the adhesive bonding, or cause cohesive material failure adjacent to the adhesive bonds. However this is not necessarily the case because partial adhesion does not maximize contact area. In order to adequately explain this phenomenon, a possible explanation of the failure mechanism is required and will be provided in the following section when the failure planes are discussed.

The second objective of this section was to determine the relationship between the pullout performances of the two different sizes. Based on the data collected, no direct relationship was found between the pullout performance and the different sizes of specimens. It is probable that there is a relationship between pullout performance of 300 x 900 mm specimens and 300 x 450 mm specimens but determining this relationship will require the characteristic dimensions of the beads of adhesive (length, width, and thickness of all beads as well as center-to-center spacing of adjacent beads and the relative location of beads with respect to different layers of components.) However metrology equipment cannot be found that can measure all these parameters to a significantly high enough level of precision in order to confidently draw a conclusion. This was also outside the scope of what the industrial partners deemed relevant to their application.

The results of Figure 5.16 provide a concise trend, however these results provide mixed conclusions – no single conclusion blankets all Sources and explains the phenomenon that is observed. It is necessary to examine the data from another angle. Figure 5.17 accomplishes this by plotting the deflection at peak load performance against the different size specimens with the different adhesion methodologies.

Figure 5.17 illustrates the deflection at peak load from all Sources for the 300 x 450 mm & 300 x 900 mm specimens. What appears to be evident is that

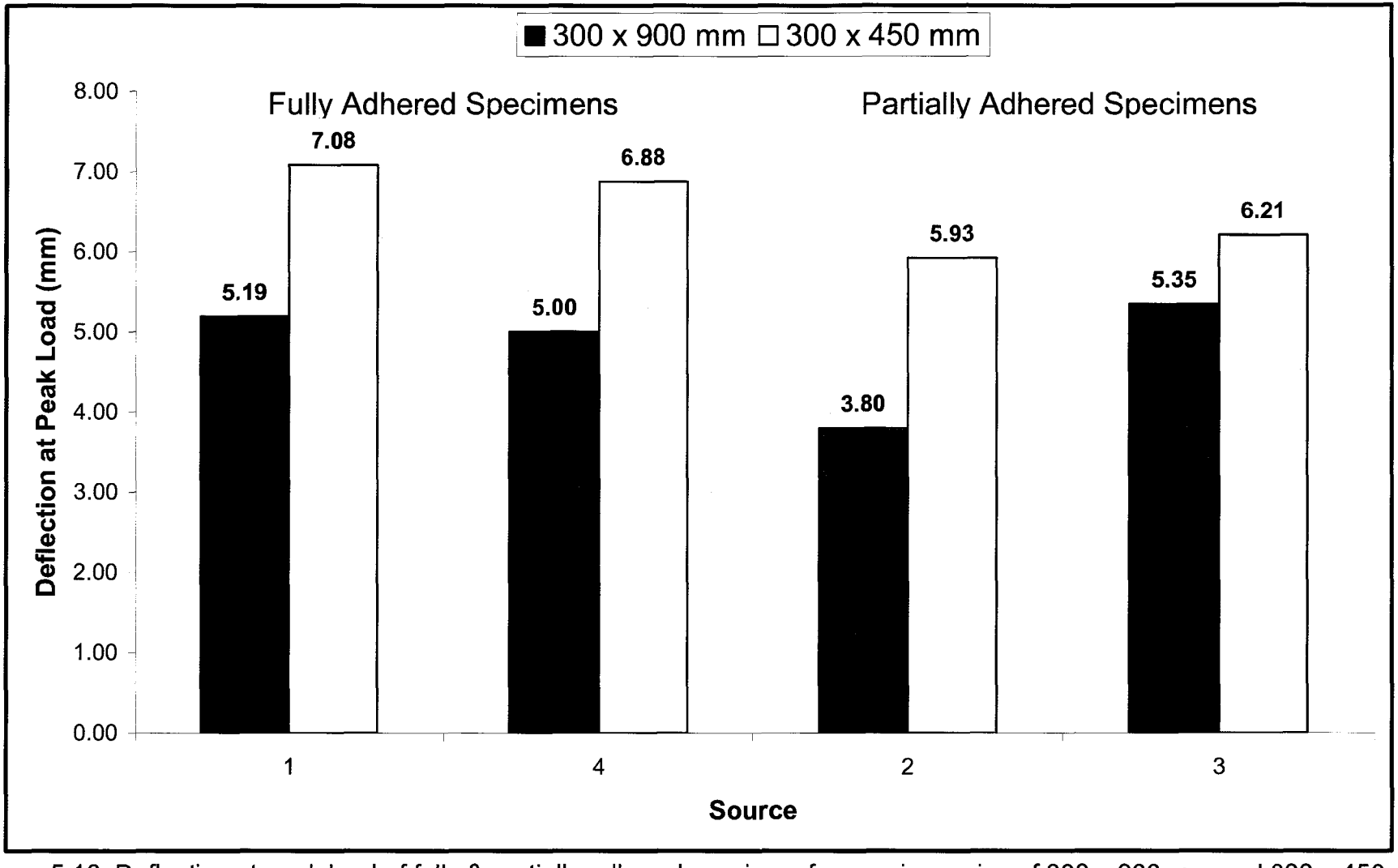

Figure 5.16: Deflection at peak load of fully & partially adhered specimen for specimen size of 300 x 900 mm and 300 x 450 mm

for the conditions provided in figure 5.13, 300 x 450 mm specimens will fail when the deflection is on the order of 6.5 +/- 0.5 mm, regardless of source. This is an important observation, because this is a very finite range. When the specimen size is 300 x 450 mm, the amount of deflection that can incur prior to failure is significantly less. With a deflection at peak load that does not exceed much more than 5 mm, the 300 x 900 mm specimens exhibit far less deformability especially when compared to 300 x 450 mm specimens. This means that these specimens are less malleable and probably more likely to exhibit successive failure. A possible line of reasoning explaining this phenomenon behind the observed behaviour will be provided in the following section.

Before selecting 300 x 450 mm as the appropriate size outright, it will be necessary to expand on the observations from above and perform a failure plane investigation to determine which size of specimens exhibited the most consistent failure plane location.

5.5 Specimen Size Specification – Failure Plane Analysis

After analyzing the empirical data, it was necessary to categorize the failures as per the specifications outlined in section 4.3.1. Figure 5.18 illustrates the breakdown of failure planes with a fixed specimen size and construction methodology. A breakdown of source-by-source failure planes is shown in Table 5.2.

It would appear that for full adhesion, failure planes do not change when the specimen sizes change from 300 x 900 mm to 300 mm x 450 mm. The failure plane of a 300 x 900 mm specimen that has been fully adhered (Source 1 & 4) does not change with the change in specimen size. This is a logical conclusion – since all experimental parameters are similar between these two the expectation should be that the failure plane should be in the same location except at a higher level of loading. Empirical analysis and the results of Figure 5.18 confirm these conclusions.

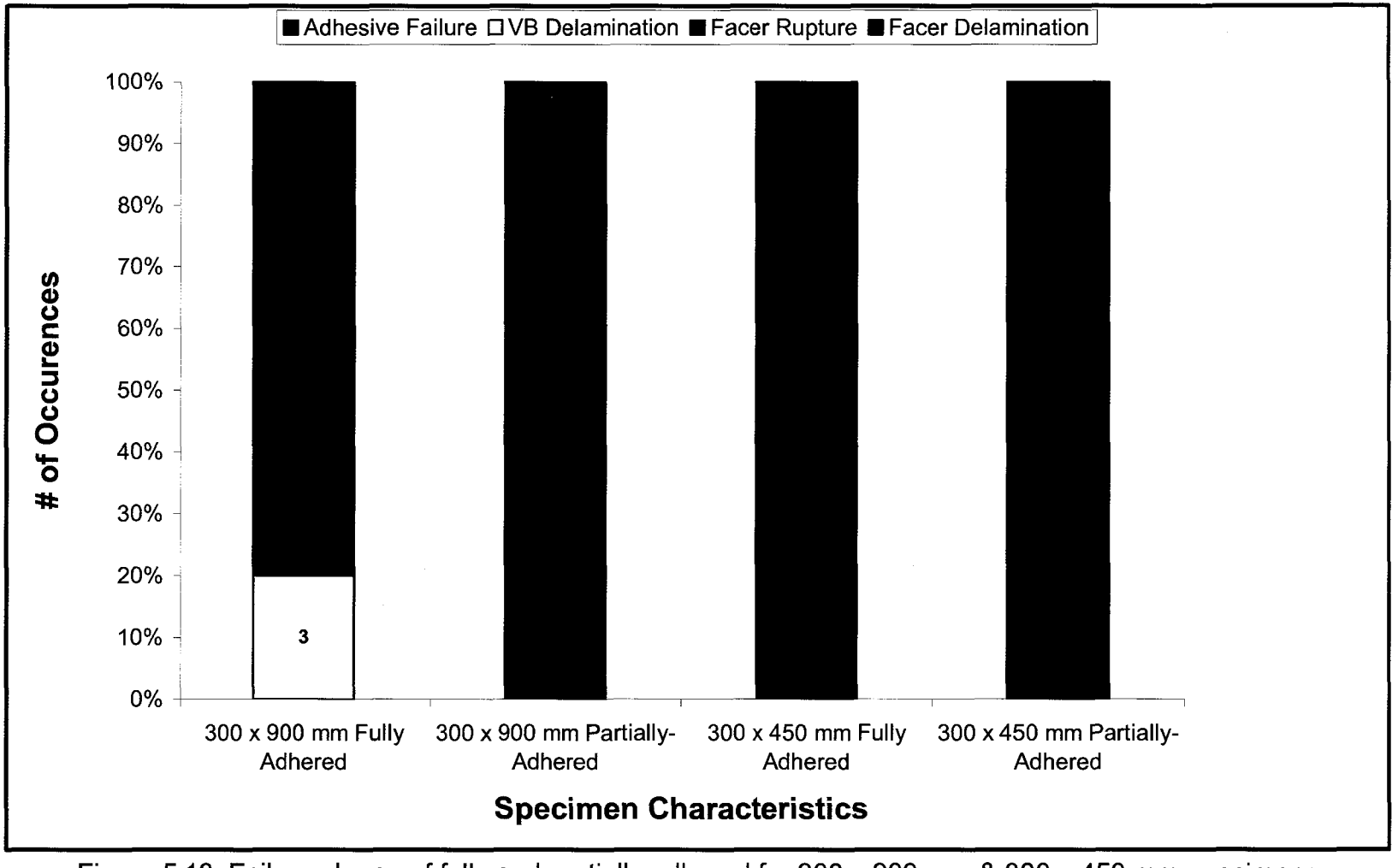

Figure 5.18: Failure planes of fully and partially adhered for 300 x 900 mm & 300 x 450 mm specimens

Specimen Size (mm x mm)	Source 1		Source 2		Source 3		Source 4	
	Failure Plane	Freq	Failure Plane	Freq	Failure Plane	Freq	Failure Plane	Freq
300 x 900	Facer Rupture	4	Adhesive Failure	8	Adhesive Failure	7	Facer Delamination	5
	Facer Delamination	3			Facer Delamination	1	VB Delamination	3
300 x 450	Facer Delamination	7	Facer Rupture	6	Facer Rupture	6	Facer Delamination	6
	Adhesive Failure	1						

Table 5.2: Frequency table of failure planes for sources 1-4 of different size specimens

However, the failure plane of a 300 x 900 mm specimen that has been partially adhered (Source 2 & 3) will change significantly in both location and nature in comparison to the failure plane of a 300 x 450 mm specimen. A significant reason for this is due to the specimen construction – the more slender specimens (300 x 900 mm) were constructed with slightly larger center to center distances between adjacent beads of adhesive.

In order to most effectively carry out this analysis, it would have been wise to maintain identical center to center distances between adjacent beads of adhesive for both the 300 x 900 mm specimens and 300 x 450 mm specimens. However, this variable was inadequately controlled and can account for the differences in observed phenomenon between specimens that were 300 x 900 mm and specimens that were 300 x 450 mm for all specimens constructed with partial adhesion. Observations that prove this hypothesis are presented in Figure 5.18. 300 x 900 mm specimens that were constructed with partial adhesion failed adhesively in between the insulation and the coverboard. The failures of 300 x 450 mm specimens that were constructed with partial adhesion were facer ruptures. The same type of deck was used to construct these samples (300 x 900 – PA & 300 x 450 – PA) as explained in Figure 5.13. This means that there must have been constant spacing between beads of adhesive between the vapour barrier and insulation. However, the same remark cannot be made about the spacing between adjacent beads of adhesive in between the insulation and the coverboard. The change in failure plane shown in Figure 5.18 between the two different sized specimens with partial adhesion must account for the changes in failure planes as well as the empirical differences between these two samples. (300 x 900 – PA & 300 x 450 – PA) If the same spacing between adjacent beads of adhesive had been applied to both the 300 x 450 mm and 300 x 900 mm specimens the expectation would have been reflected with a constant failure plane location – adhesively between the insulation and the coverboard if the 300 x 900 mm adhesive spacing had been used, or as a facer rupture if the 300 x 450 mm adhesive spacing had been used.

However, regardless of specimen size, when a pullout test was conducted a stress path was created through the specimen. This stress path was fairly uniform over the surface area of the specimen for specimens constructed with full adhesion. But with specimens constructed with partial adhesion, the beads of adhesive act as stress concentrations because these are the only routes through which loading can be transferred through adjacent layers of components.

Figure 5.19 has been generated to help conceptualize this phenomenon. Figure 5.19 illustrates a simplified version of AARS. In this figure only the deck, insulation, coverboard and weatherproofing membrane have been included. The spacing of the adhesive in between the deck and insulation has been labeled D_1, the spacing between the insulation and the coverboard has been labeled D_2 and the spacing between the coverboard and waterproofing membrane as D_3. Changing the distance D_1, D_2, or D_3 will result in a different pullout response due to load eccentricity. With different distances of D_1, D_2, and D_3 for 300 x 450 mm and 300 x 900 mm additional variability has been unintentionally introduced into the analysis.

Images of the actual failures from this testing have been provided in Figures 5.20 - 5.23 to provide additional insight into these failures. The central argument from this section is that there is a change in the failure mechanism that occurs, provided that partial adhesion is applied, when the specimen size changes from 300 x 900 mm to 300 x 450. But when developing evaluation criteria, a distinction cannot be made between construction protocol. Pullout guidelines have to be independent of the process by which the specimens were constructed. Results show that the 300 x 900 mm specimens are far more sensitive to construction protocol, than 300 x 450 mm specimen. This reasserts the point that the specimen size should be 300 x 450 mm.

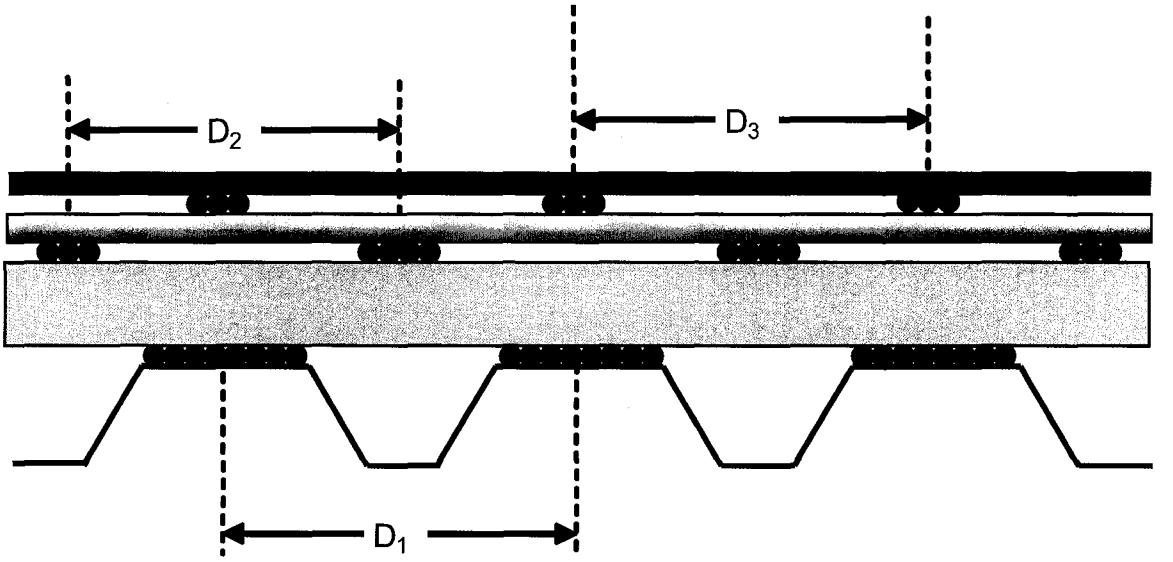

Figure 5.19: Stress Transfer in an AARS Specimen

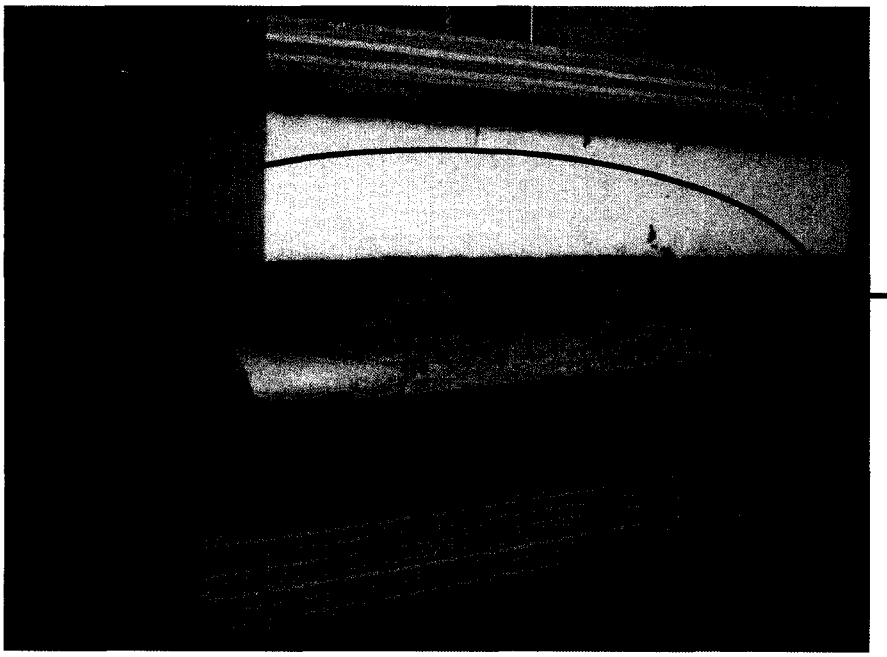

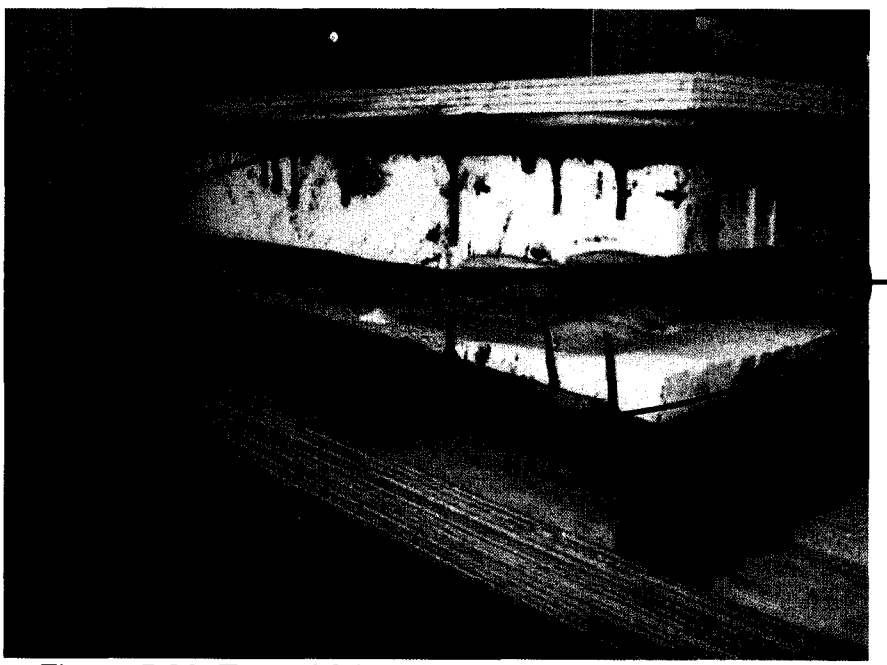

Figure 5.20: Typical failure planes of 300 x 900 mm fully-adhered specimens

Adhesive Failure between Insulation & Coverboard (Source 2)

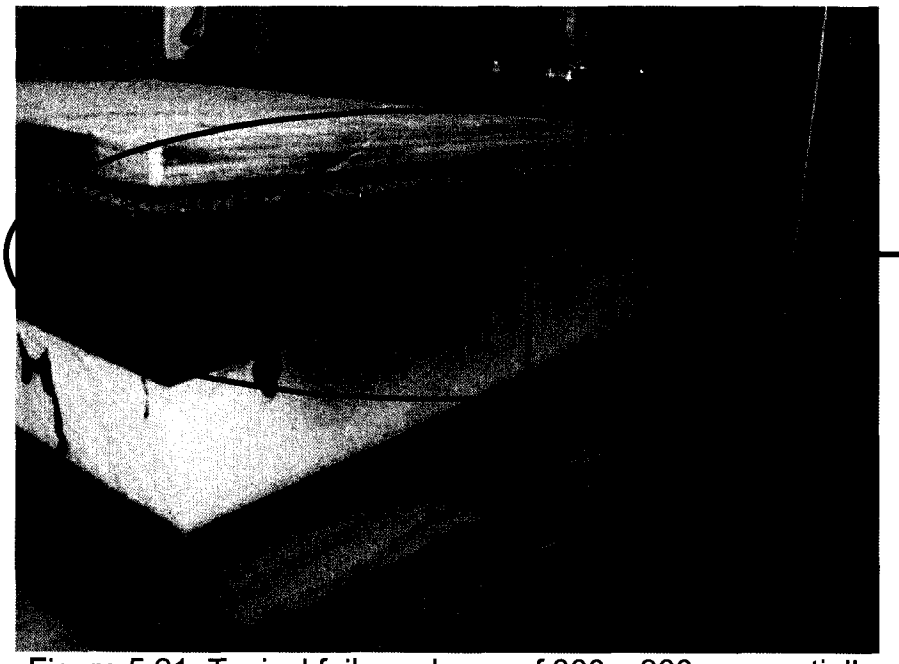

Adhesive Failure between Insulation & Coverboard (Source 3)

Figure 5.21: Typical failure planes of 300 x 900 mm partially-adhered specimens

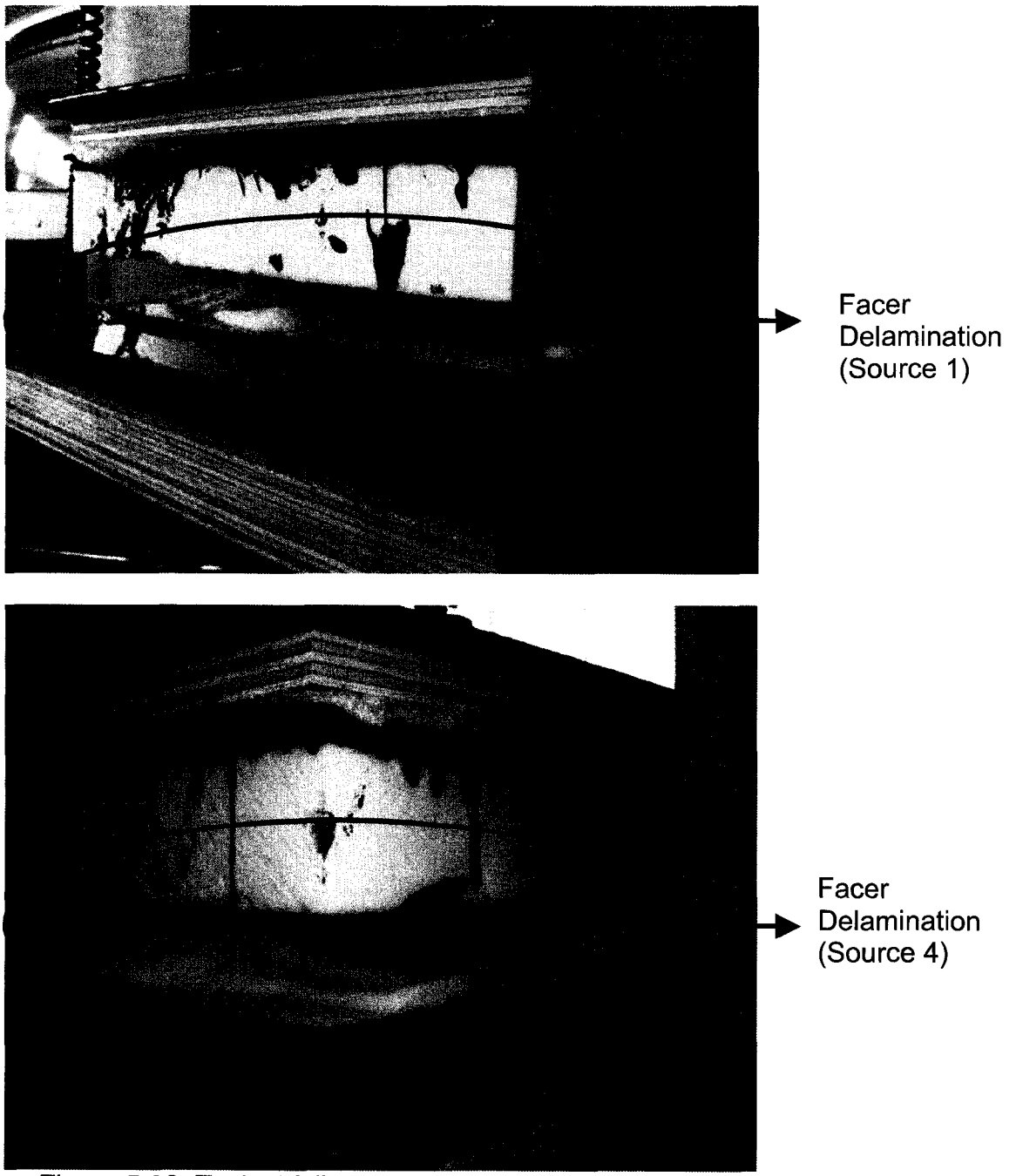

Figure 5.22: Typical failure planes of 300 x 450 mm fully-adhered specimens

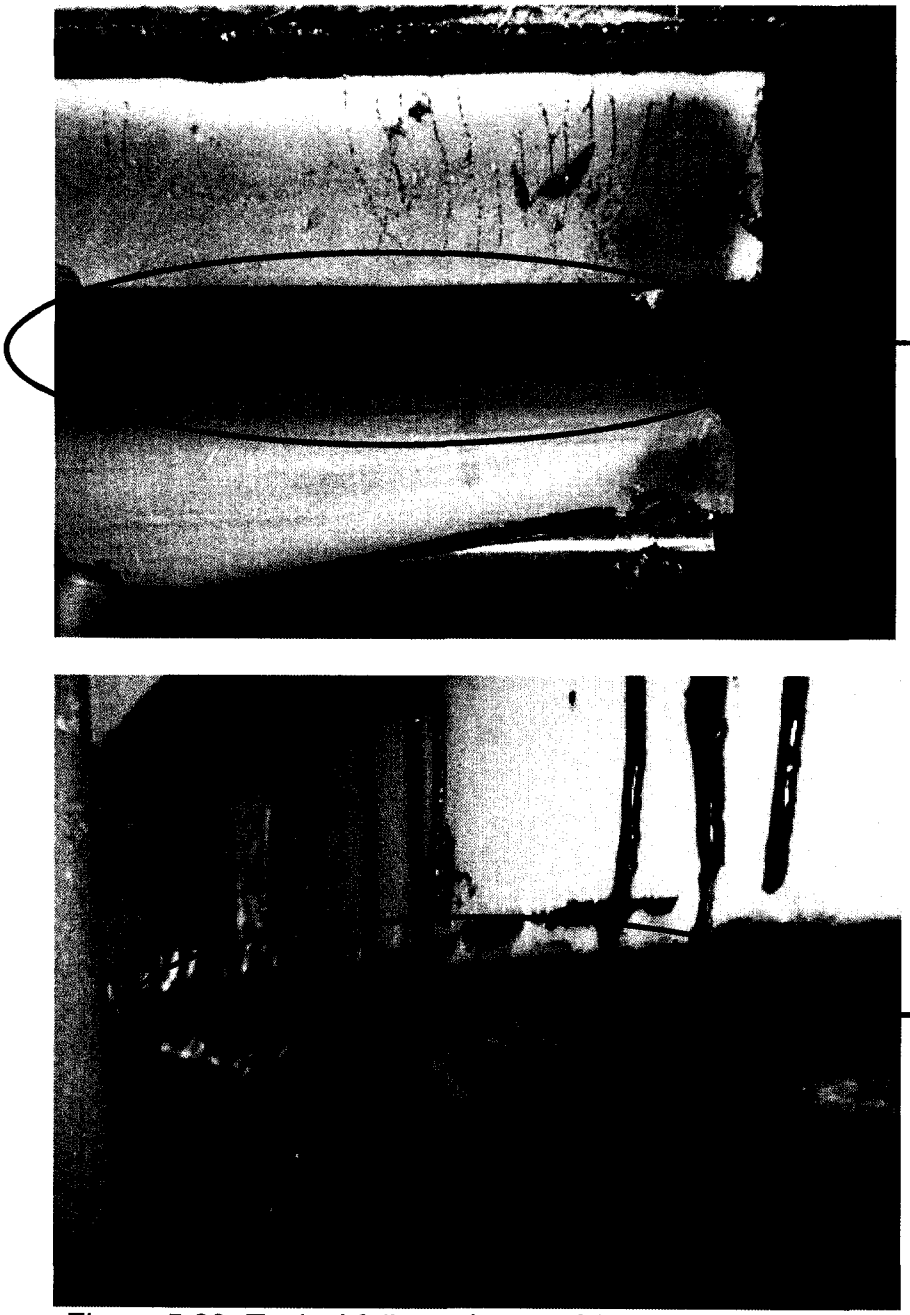

Figure 5.23: Typical failure planes of 300 x 450 mm partially-adhered specimens

5.6 Attachment Condition Verification – Comparative Analysis

As outlined in section 4.2.1, the experimental protocol stipulated that every flute of the steel deck required attachment to the specimen mounting platform. If the protocol is critically analyzed, this attachment condition is not entirely reflective of what would be observed in actual roofing applications. The part of the roof that most closely reflects this fixed behaviour is the part of the roof above the structural (steel) joists. Figure 5.23 illustrates the underbelly of typical steel roof joists observed in commercial and industrial application. The red lines in this figure correspond to the female flutes that form part of the test area, based on the findings of the previous sections, and the "X"s mark the spot of where the specimen would be fixed from deflection. The attachment condition illustrated in Figure 5.23 is not emulated in this study because accomplishing the attachment condition of Figure 5.23 is difficult to achieve with numerous repetitions. The difference in between the lab tested attachment condition and the field attachment is that in reality a significantly greater amount of deflection can occur in the field condition than under laboratory testing conditions.

As such, the third parameter that required verification prior to the development of a pullout test method was to change the attachment condition to one which permits greater levels of deflection and then determining if changing this condition introduced a significant difference in the pullout response. Alternatively, tests should be performed to see if the specimens tested with four flutes attached could be used as a bench mark for cross referencing. Since the test facilities could not accommodate a test arrangement reflective of Figure 5.24, it would be more prudent to simply change the attachment condition to something that resembled Figure 5.24 and then compare these new results to the results obtained with the four flute attachment condition and to take note of any major differences.

The new attachment condition that was chosen was one in which the outer two flutes of the 300 x 450 mm were fastened, with the inner two flutes free to

Figure 5.24: Structural roof components

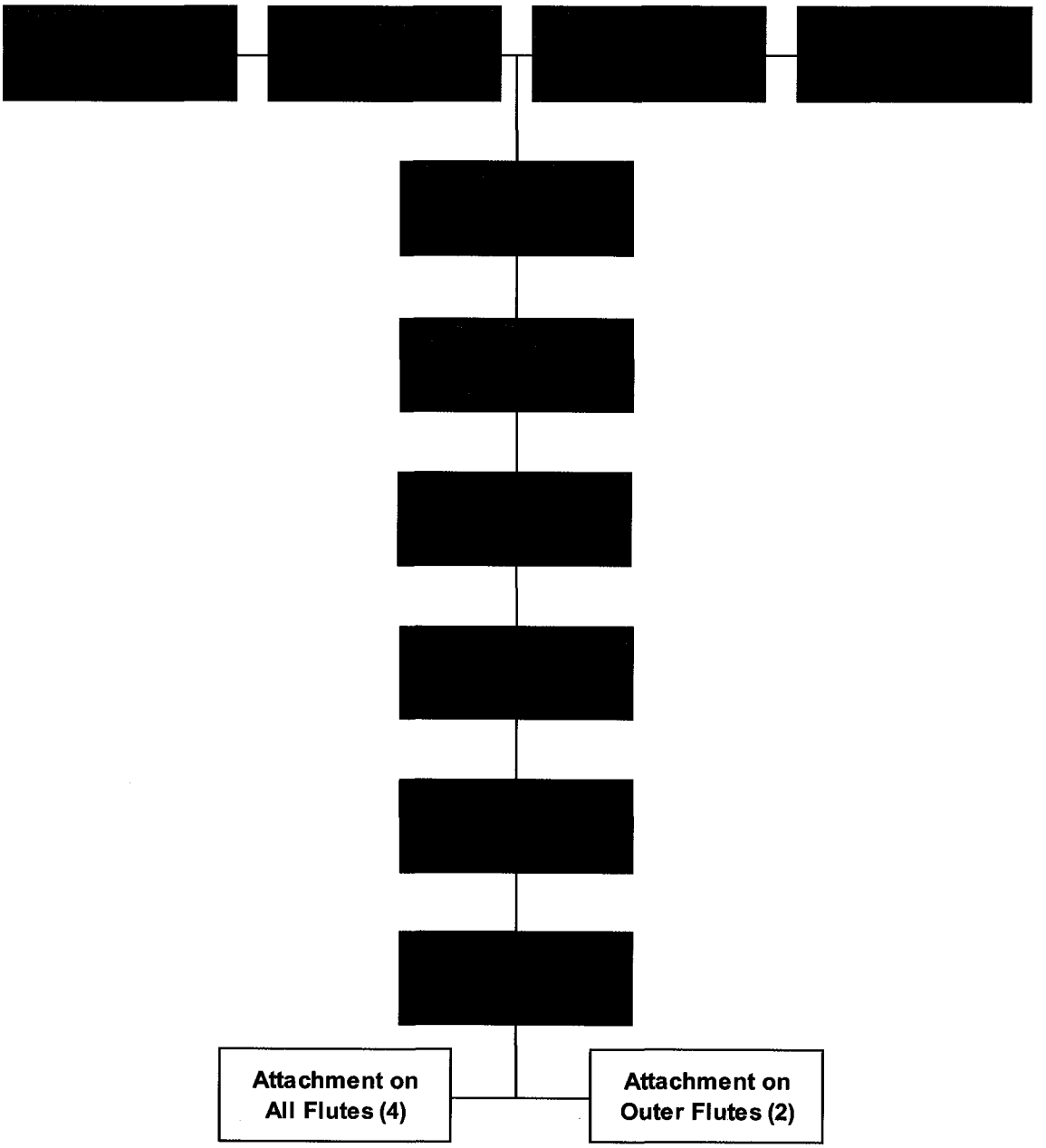

Figure 5.25: Test matrix for attachment condition determination

deflect. Figure 3.5a and 3.5b illustrate both the two flute attachment condition and the four flute attachment condition respectively.

Figure 5.25 illustrates an overview of the key variables that were selected in the development of these test parameters. Of special note, all pullout tests that were conducted in this section were performed on specimens where all construction materials were fully-adhered. This was chosen to remove the element of full vs partial adhering and was chosen to avoid the excessive peeling forces that would have been subjected to the beads of adhesive, had partial adhering been applied.

Figure 5.26 illustrates the typical pullout response of 4 specimens that were 300 x 450 mm, tested at 6.35 mm/min, with asphalt core board and paper insulation facer with pullout tests conducted on these specimens with four flutes and two flutes attached.

Other than the obvious differences in magnitude in pullout results between the two attachment conditions, which is most clearly illustrated in figure 5.26, there is another subtle difference between these two. The shapes of the curves differ significantly. Specimens fastened with four flutes typically take the shape of curves like those found in figures 5.2 and 5.14. The load typically builds until an ultimate state is reached, then successive failures occur and the specimen loses any additional load carrying capacity. However for specimens tested with two flutes, specimens never really attain an ultimate state, they maintain a high level of loading throughout the course of testing and fail catastrophically with a high deflection at peak load.

An explanation for this is that due to the experimental setup for specimens being tested with only two flutes attached, there is a high stress concentration on the bottom face of the insulation due to the high relative ductility of the steel deck (with respect to other construction materials). When the deck deflects upwards, it transfers these stress concentrations to the insulation and vapour barrier. As the deflection continues to increase, these stress concentrations manifest themselves as peeling forces that start at the outer edge of the specimen and propagate inwards (along the 450mm dimension) towards the middle of the

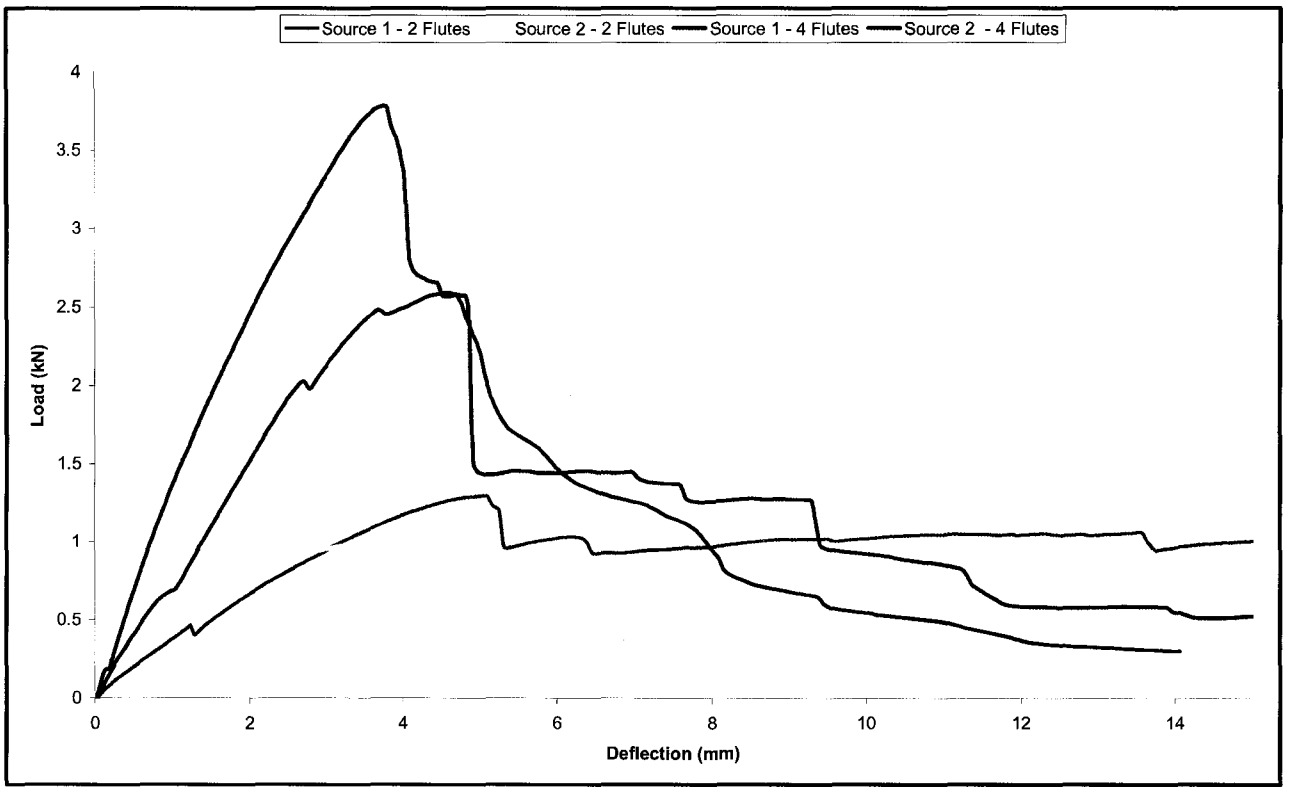

Figure 5.26: Typical load-deflection response of specimens attached with 4 flutes & 2 flutes for Sources 1 and 2

specimen. However, when the specimens are attached on all four flutes, the deck is not as free to deflect – and the stress concentrations are either not present or do not cause the onset of failure until much later on in the pullout test.

When comparing the numerical results, an encouraging sign of attachment condition repeatability is observed in Figure 5.27. In Figure 5.27, the eight sample peak load measurements have been extracted and compared for the two conditions that are being examined. An encouraging result that presents itself in Figure 5.27 is the ordering of the sources. The highest peak loads generated for four flutes were from Sources 1 & 3, and these also correspond to the two highest Sources when two flutes are instituted. This is not the case for Sources 2 & 4.

If the peak loads are directly compared to one and other on a source-by-source basis, figure 5.28 is generated where the peak load of the 2 flute attachment condition has been divided by the peak load of the 4 flute attachment condition on a source-by-source basis.

Figure 5.28 illustrates credible proof that there is some relationship between the peak loads generated between the four flute and the two flute attachment condition. The empirical results indicate that pullout tests conducted with a specimen attached on 2 flutes attains only 35 % of the peak load that a specimen attached on all four flutes. This is a strong relationship and is illustrated for 3 out of 4 sources, with the fourth source demonstrating similar behaviour, however only attains 25% of a peak load that a specimen attached on four flutes could attain. A failure plane analysis however will help determine the level with which the location of failure is being maintained.

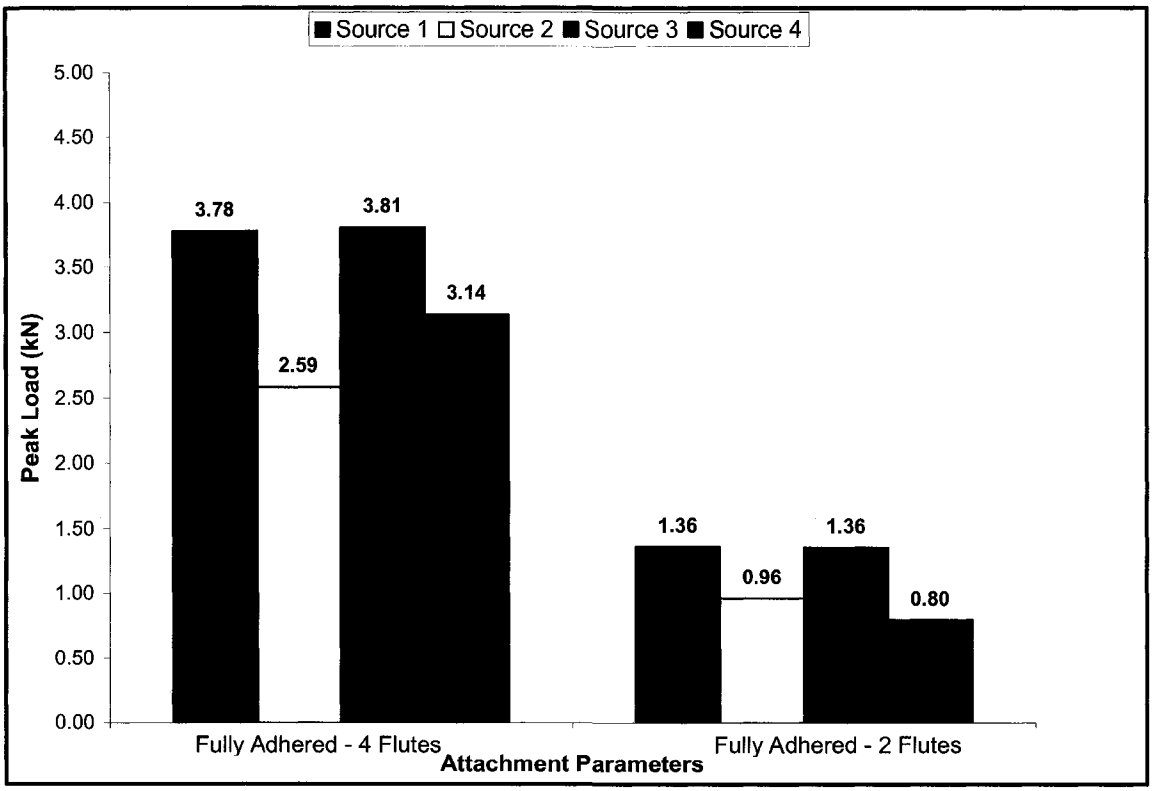

Figure 5.27: Peak load comparison of specimens with 4 flute & 2 flute attachment condition

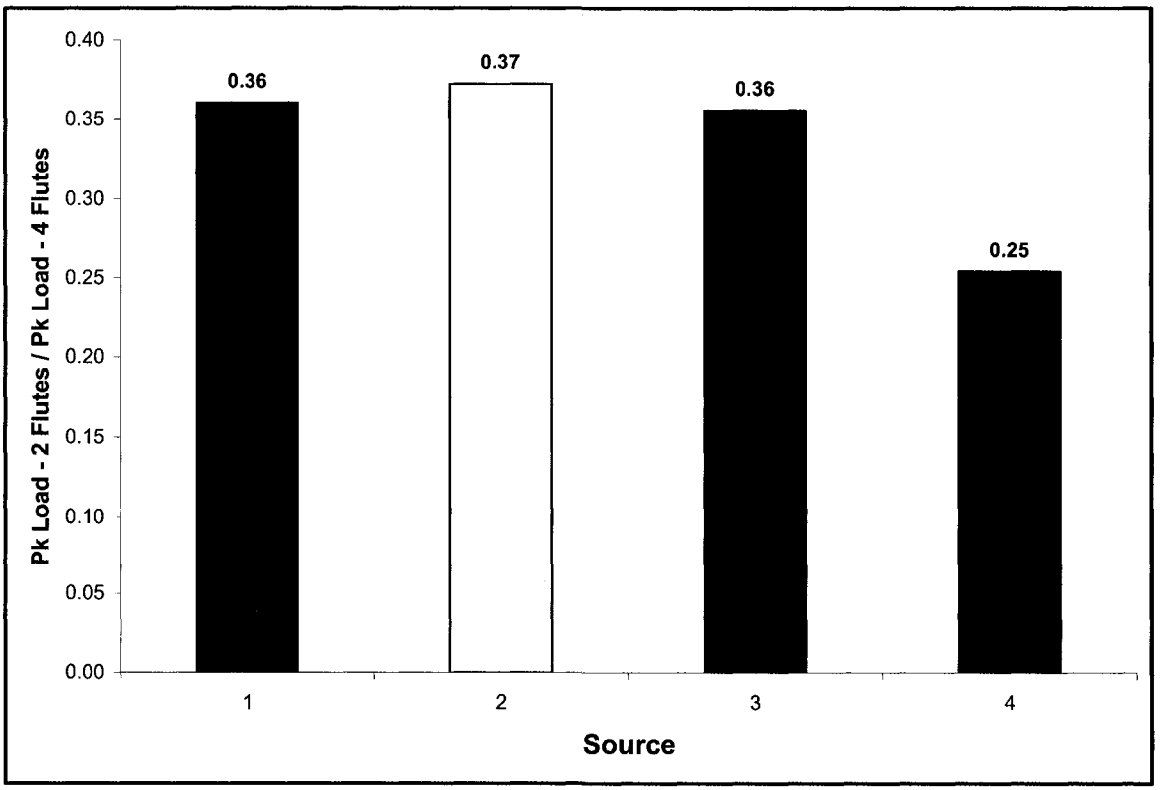

Figure 5.28: Peak load 2 flutes/ peak load 4 flutes for sources 1-4

5.7 Attachment Condition Verification – Failure Plane Analysis

Figure 5.29 illustrates the overall breakdown of failure planes when comparing the change of failure planes from the 4 flute attachment condition to the 2 flute attachment condition.

Table 5.3 illustrates the source-by-source breakdown of failure planes from the 4 flute attachment condition to the 2 flute attachment condition.

As discussed in section 5.6, the experimental setup for the two-flute condition placed a stress concentration on the insulation facer. Based on this experimental setup there are two expectations. The first expectation should be that specimens tested with the two flute attachment condition could fail more frequently around the facer. The second expectation should be that there should be no major failure plane shift from the four and two flute attachment condition.

Both of these observations hold true. No new failure planes were encountered – all failure planes for the two-flute condition had already been encountered previously with the four flute condition. An examination at a source-by-source level may help clarify the mechanisms leading to failure.

Source 1 failure planes (illustrated in Figure 5.30) change from facer delamination to facer rupture when the attachment condition goes from two flutes to four flutes. This is to be expected because under the four flutes condition, the deck remains plane, and the facer delamination which is a brittle planar failure, while the facer rupture occurs due to the onset of peeling forces due to the presence of the deck acting as a stress concentration. Source 2 (Figure 5.31) results in a negligible change in failure plane. The poor performance of Source 2 under both the two flute and four flute condition results in negligible change in failure planes. It is a catastrophic failure regardless of the attachment condition.

Source 3 (Figure 5.32) provided some interesting results that reinforce the hypothesis presented herein. Exactly half of each sample of specimens from the four and two flute condition exhibited facer delaminations and adhesive failures. The adhesive failures for the four flute condition occurred above the top face of

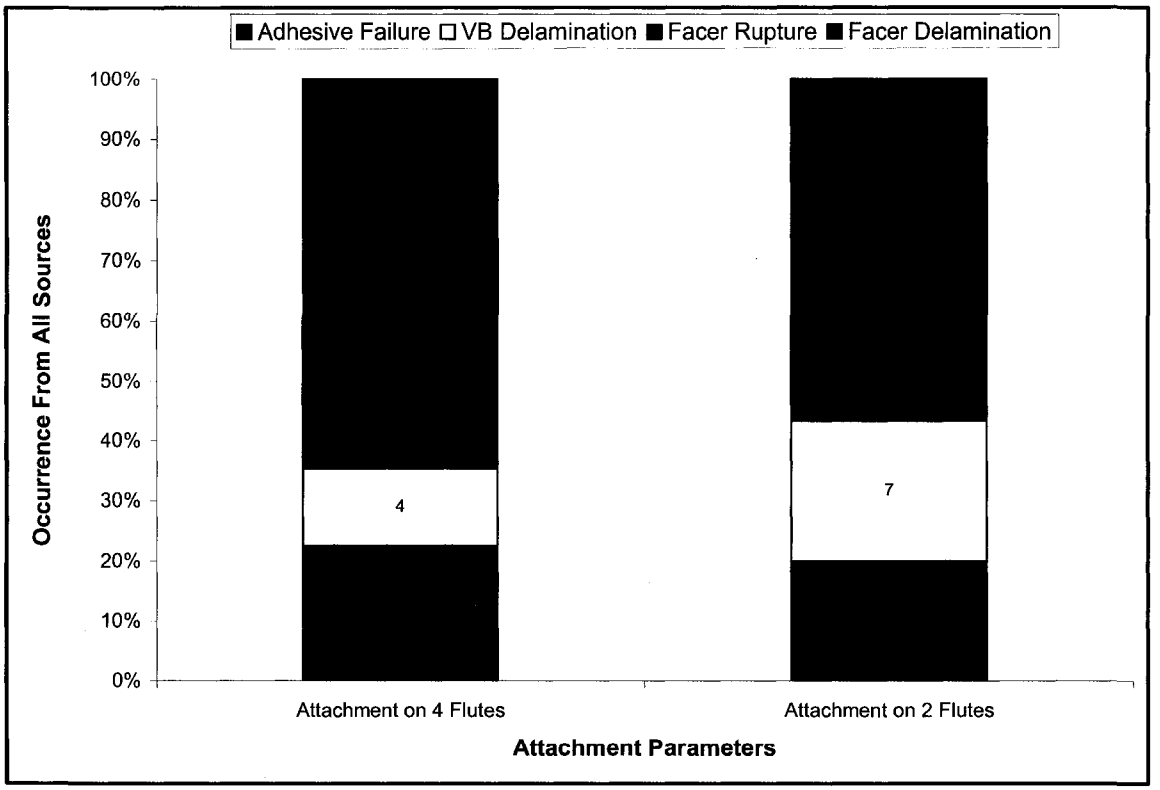

Figure 5.29: Comparison of failure planes of specimens with the four and two flute attachment condition

End Condition	Source 1		Source 2		Source 3		Source 4	
	Failure Plane	Freq	Failure Plane	Freq	Failure Plane	Freq	Failure Plane	Freq
4 Flutes	Facer Delamination	5	Facer Rupture	8	Facer Delamination	4	VB Delamination	4
	Facer Rupture	2			Adhesive Failure (SD - VB)	4	Adhesive Failure (SD - VB)	2
	Adhesive Failure (SD-VB)	1					Facer Delamination	1
2 Flutes	Facer Rupture	4	Facer Rupture	7	Facer Delamination	4	VB Delamination	7
	Facer Delamination	2	Adhesive Failure	1	Adhesive Failure (CB - BS)	4		
	Adhesive Failure (SD-VB)	1						

Table 5.3: 4 flute & 2 flute attachment condition failure plane breakdown for sources 1 – 4

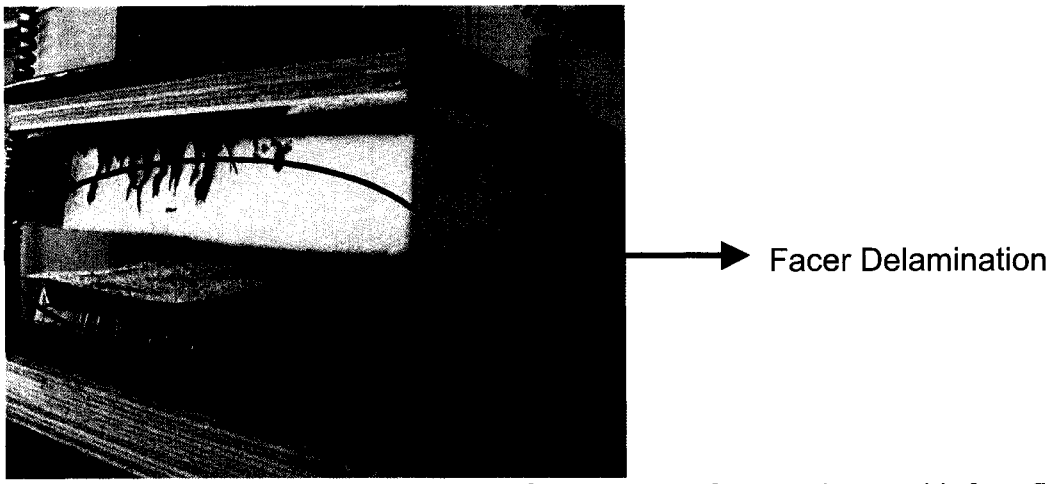

Figure 5.30a: Illustration of typical failure plane for specimen with four flute attachment condition from Source 1

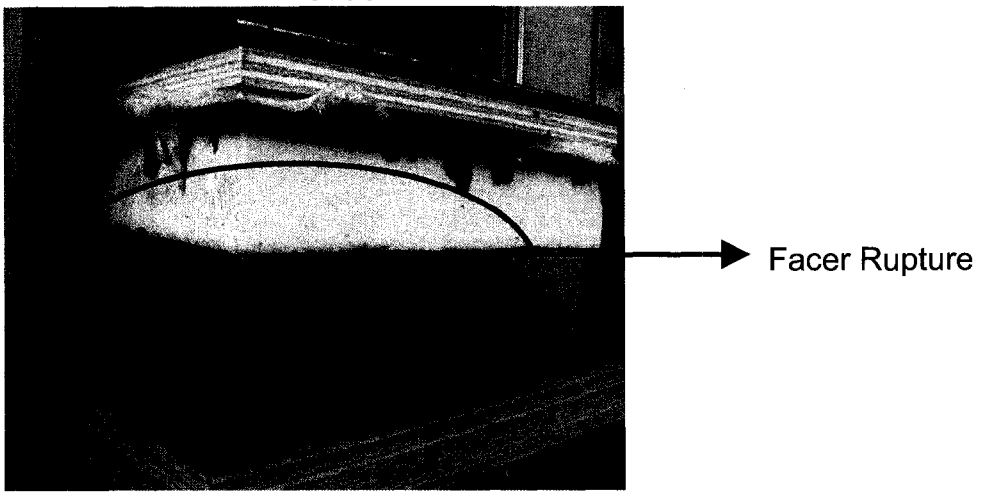

Figure 5.30b: Illustration of typical failure plane for specimen with two flute attachment condition from Source 1

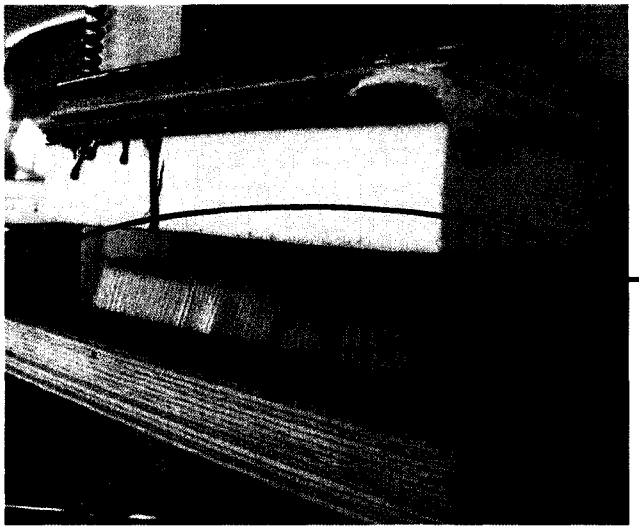

Figure 5.31a: Illustration of typical failure plane for specimen with four flute attachment condition from Source 2

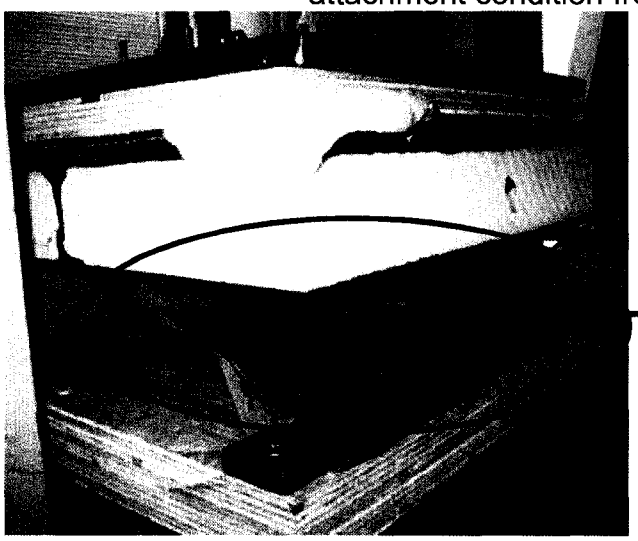

Figure 5.31b: Illustration of typical failure plane for specimen with two flute attachment condition from Source 2

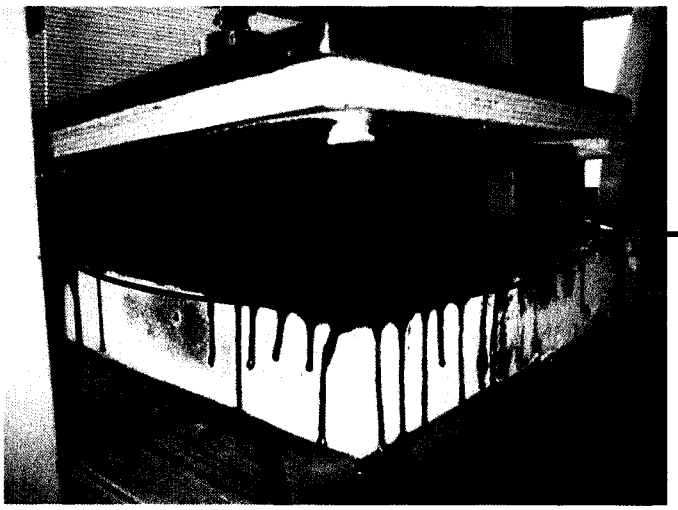

Figure 5.32a: Illustration of typical failure plane for specimen with four flute attachment condition from Source 3

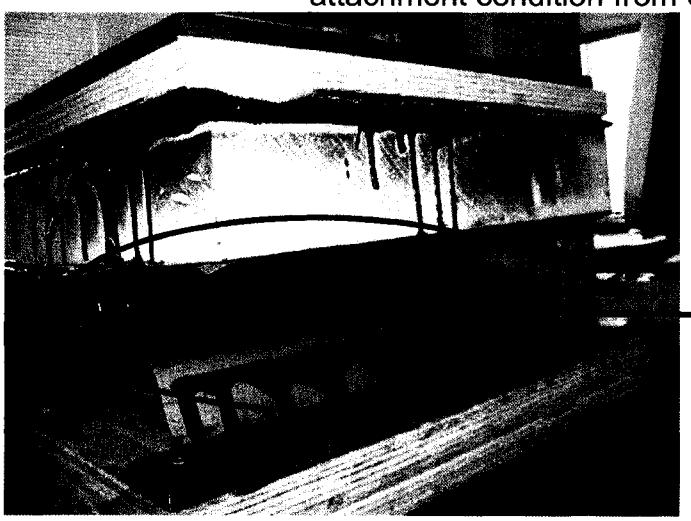

Figure 5.32b: Illustration of typical failure plane for specimen with two flute attachment condition from Source 3

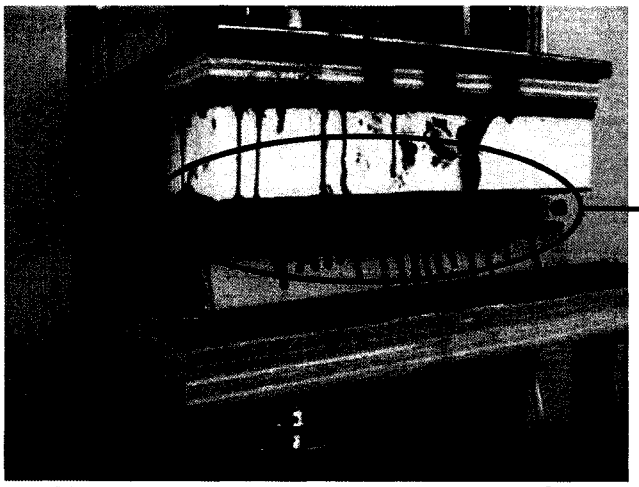

Figure 5.33a: Illustration of typical failure plane for specimen with four flute attachment condition from Source 4

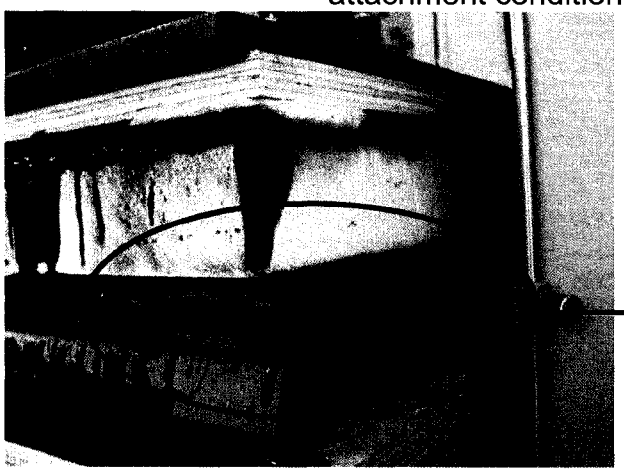

Figure 5.33b: Illustration of typical failure plane for specimen with two flute attachment condition from Source 4

the insulation, while for the two flute condition all adhesive failures occurred at the deck level.

Source 4 (5.33) shows that under the two flute condition the only failure that was observed was the vapour barrier delamination – with the four flute condition there was a mixture of facer, adhesive and vapour barrier delaminations. The two-flute attachment condition brings the failure planes closer to the deck – reasserting the deck stress concentration hypothesis proposed earlier.

All of these failure planes help to illustrate that no major failure plane shift was observed when the attachment condition is changed from the four flute to the two flute condition. Based on observations however, the four flute attachment condition is a worthwhile benchmark for the sake of comparison and should be emulated due to its superior results.

5.8 Development of Test Method – Conclusion

This chapter summarized tests that were conducted in order to adequately specify the key parameters required for characterizing the pullout resistance of AARS specimens. It was shown in this chapter that:

- The appropriate pullout rate should be 6.35 mm/min.
- Specimen plan dimensions should be 300mm x 450mm.
- The location for testing should be overtop of structural steel joists.

By fixing these variables, the following chapter will evaluate component pullout resistance of AARS specimens.

Chapter 6: Applications of the Present Test Method

6.1 Introduction

In chapter 5 of this thesis the present studied identified and developed the key variables that required specification for the development of a pullout test. Justification was provided for the selection of a pullout rate of 6.35 mm/min and the selection of the 300 x 450 mm specimen size. It was shown that the optimum fixation condition for conducting pullout tests was with all flutes fastened. After concluding these experiments a test method was drafted as shown in Chapter 7 for possible adoption by the American Society for Testing and Material (ASTM) or Canadian Standards Association (CSA).

The present test method was applied to ascertain the influence of other critical variables on pullout performance. This chapter will address some of these other variables and how they affected pullout performance of AARS specimens. Sections 6.2 & 6.3 present the results of experiments that were performed to assess the optimal material combination. Sections 6.4 & 6.5 present the results of experiments that were performed to compare the pullout performance of specimens constructed on steel and concrete decks. Finally sections 6.6 & 6.7 will present the results of experiments conducted to determine the effects of a specific alternative adhesion pattern. In each pair of sections mentioned above, a failure plane analysis is preceded by an empirical analysis. Section 6.8 will provide a summary of the applications of the test method. Please note, that in this Chapter, Source 4 exhibited anomalous behaviour under certain configurations. Where applicable, this will be mentioned as part of the discussion.

6.2 Effect of Insulation & Coverboard – Comparative Analysis

When assessing the pullout resistance of AARS it should be noted that the pullout resistance depends critically on the constituting materials. Substitution of different components in AARS can result in different pullout resistance because

the elastic response, yield strength, and all other physical properties can differ from one material to another. This section will summarize the results of pullout tests that were conducted on 96 specimens in order to characterize the pullout behaviour of different possible material combinations that are commonly used in AARS in Canada. Components that are being substituted are locations where failure has been most frequently observed to occur at full scale such as in the insulation and the coverboard. Figure 6.1 shows a breakdown of all the experimental variables that need to characterize the pullout behaviour of different combinations of AARS construction materials. Note that the test variables that were developed in the previous chapter are kept constant in this analysis.

The four types of materials that were tested in this section were two types of insulation facers – an acrylic facer (AF) and a paper facer (PF) – and two types of coverboard – an asphalt core board (ACB) and a fiberboard (FB). Each source constructed four samples (PF & ACB, PF & FB, AF & ACB, AF & FB) to test all four possible combinations of insulation and coverboard. The parameters were setup in a manner similar to the way the setup was used for specifying the deflection rate – the same thickness of insulation, the same deck, and the same specimen size were all identical global parameters as shown in Figure 6.1.

After conducting all 96 pullout tests, the peak load, displacement at peak load and elastic energy calculations were all extracted or calculated from the raw data and plotted to compare the performance of material combinations. In figure 6.2 the sample average peak load of the four different material combinations is compared for sources that employed partial adhesion, with partial adhesion as defined previously in section 3.2.2.

Unless otherwise specified, the broken red line represents the overall material combination average from the given sample averages for a given material combination. Based on the results presented in Figure 6.2, it appears that if the peak load measurement is a barometer for pullout resistance, PF & ACB and AF & ACB appear to be superior material combinations, with PF & ACB exhibiting slightly superior performance than AF & ACB. It also seems that the behaviour of the PF & ACB material combination exhibits more consistent

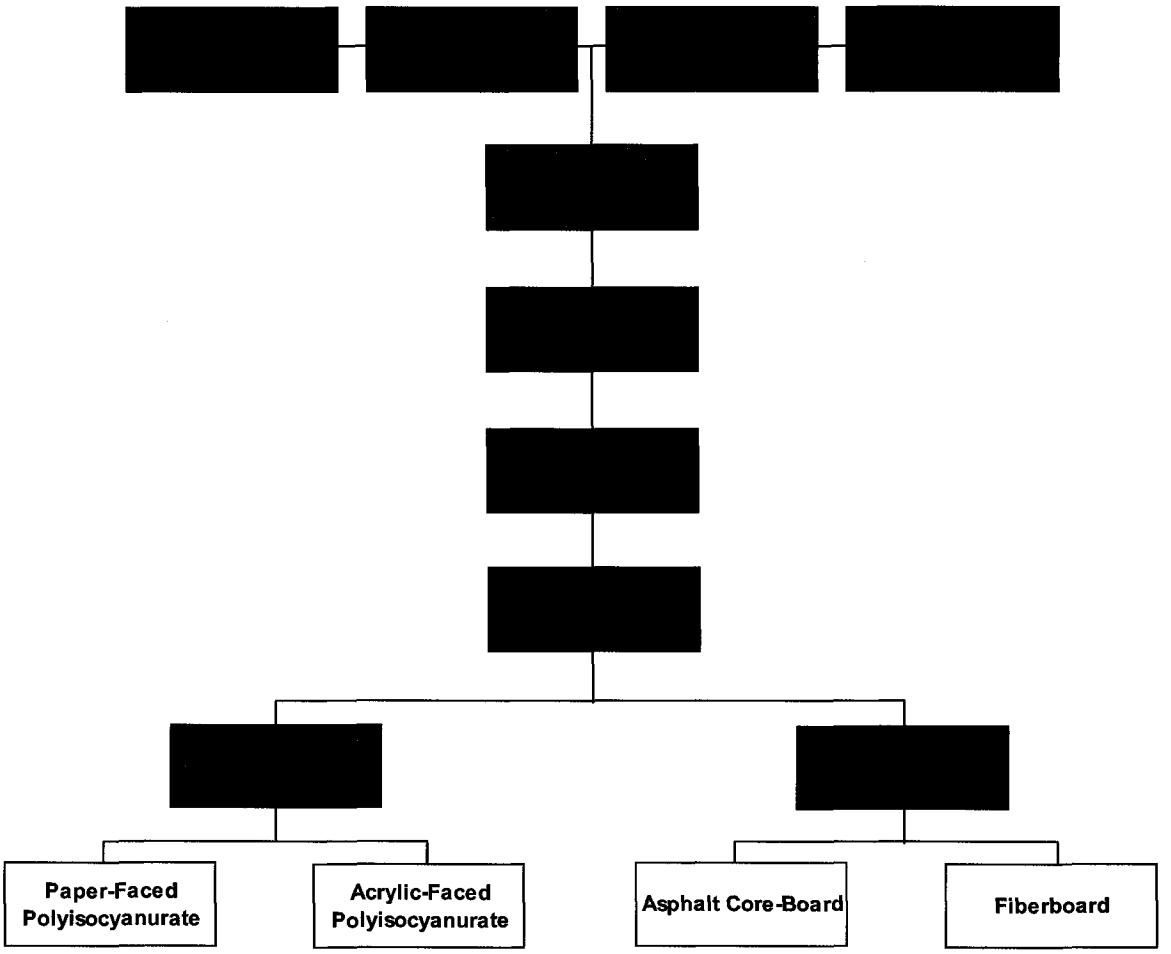

Figure 6.1: Test matrix for optimum material combination determination

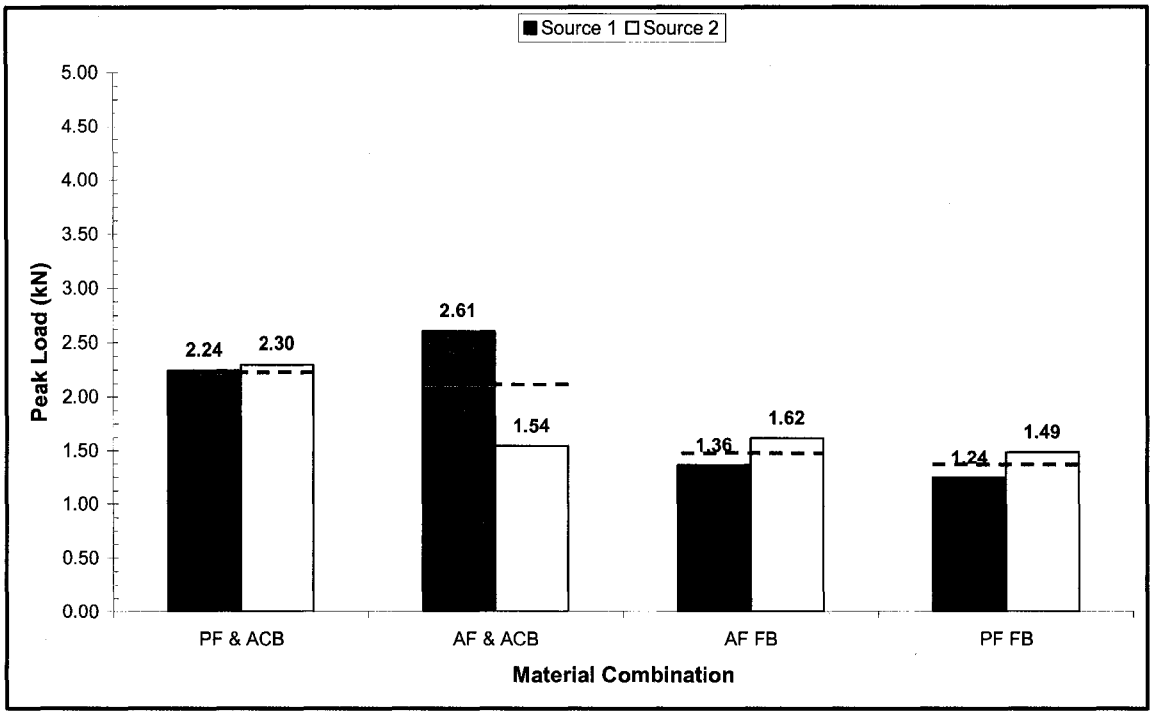

Figure 6.2: Sample average peak load pullout performance of 4 different material combinations with partial adhesion

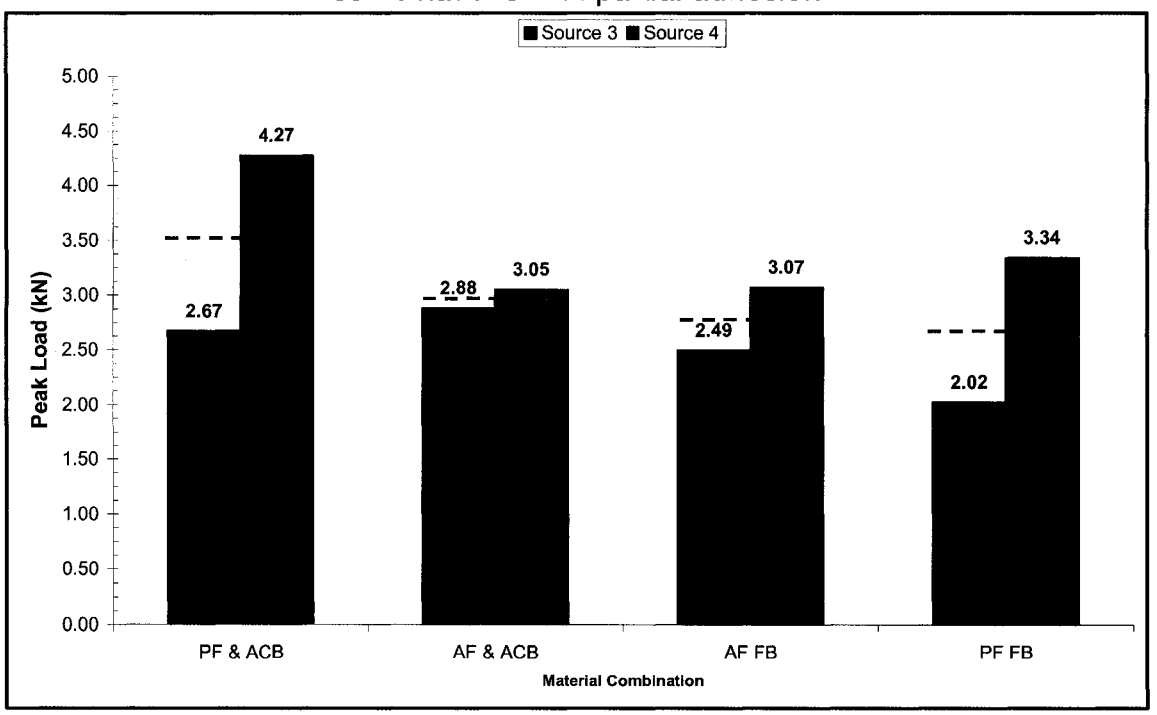

Figure 6.3: Sample average peak load pullout performance of 4 different material combinations with full adhesion

performance due to the proximity of the results from Sources 1 & 2 when compared to the proximity of the results for AF & ACB.

When the coverboard is changed from ACB to FB there is a significant loss in pullout resistance as shown by the combinations of AF & FB and PF & FB. The relative proximity of the results from specimens constructed with FB indicates that this is a particularly poor performing material.

In figure 6.3, the sample average peak load of the four different material combinations is compared for sources that employed full adhesion, with full adhesion as defined in section 3.2.2.

Note that partial adhesion was applied for Source 3 when specimens were constructed with ACB in order to be reflective of Source 3's current practice. It should also be noted that the extraordinary pullout performance of Source 4 (4.27 kN) unduly affects the overall PF & ACB material combination average. Figure 5.26 from the previous chapter tested identical specimens from Source 4 with identical test parameters and resulted in a sample average peak load of 3.14 kN. Based on these observations the real pullout resistance of Source 4 probably lies between the results presented in Figure 5.26 and those presented in Figure 6.3. Provided that this assumption is true, the material combination sample average pullout resistance of PF & ACB should be close to the material combination pullout resistance of AF & ACB. Figure 6.3 already explicitly illustrates that the material combination pullout resistance of AF & FB and PF & FB are fairly close to one and other and the pullout resistance of these combinations are only marginally less than the pullout resistance of the PF & ACB and AF & ACB material combinations.

Based on these observations it would appear that peak load pullout performance would appear heavily dependent on the coverboarding materials – if asphalt core board is used higher loads on pullout tests can be observed as opposed to if fiberboard was applied as the coverboarding material. Overall it appears that the PF & ACB is the best performing material combination with respect to pullout resistance and is followed closely by AF & ACB. The performance of PF & ACB seems to perform the most consistently, regardless of

adhesion application, although some arguments could show that AF & ACB is the more consistently performing combination.

Sample average deflection at peak load has been presented in Figure 6.4 for all sources, including both the effects of full & partial adhesion.

The results of figure 6.4 reflect the same order of performance shown in Figure 6.2 and Figure 6.3. Figure 6.4 represents a measurement of the malleability of the material combination. (PF & ACB> AF & ACB> AF & FB> PF & FB) However the results seem to infer that given the conditions imposed on these pullout tests, there is a finite amount of work that can be put into a specimen prior to failure. The PF & ACB material combination is an example that supports this hypothesis. For all four sources with PF & ACB, the range at which failure occurs is a value of 6.5 +/- 0.5 mm. based on the deflection at peak loads of the four sources of 7.08, 6.01, 6.41, and 6.88 mm. This data may indicate that the development of standards may depend heavily on the amount of deflection that can occur before failure as opposed to the amount of force alone that can be put into a specimen before failure.

Other material combinations, like PF & FB, exhibit deflection threshold trends in behaviour – the deflection at failure for this material combination for all four sources is 3.98, 4.43, 4.88, and 5.28 mm. This would yield a failure deflection of approximately 4.60 +/- 0.65 mm. Specimens that were tested with AF exhibit similar overall trends based on the results of Figure 6.4. However, due to the typically successive nature of the failures from specimens that were constructed with AF, there is a higher degree of scatter for specimens constructed with this material.

In figure 6.5, elastic energy calculations have been performed and are based on the guidelines provided in section 4.3.2 of this investigation. This figure displays the elastic energy material average of the PF & ACB - FA (1 source), PF & ACB – PA (3 Sources) AF & ACB - FA (2 sources), AF & ACB – PA (2 Sources) AF & FB with full (2 sources) and partial (2 sources) adhesion and PF & FB with full (2 sources) and partial (2 sources) adhesion.

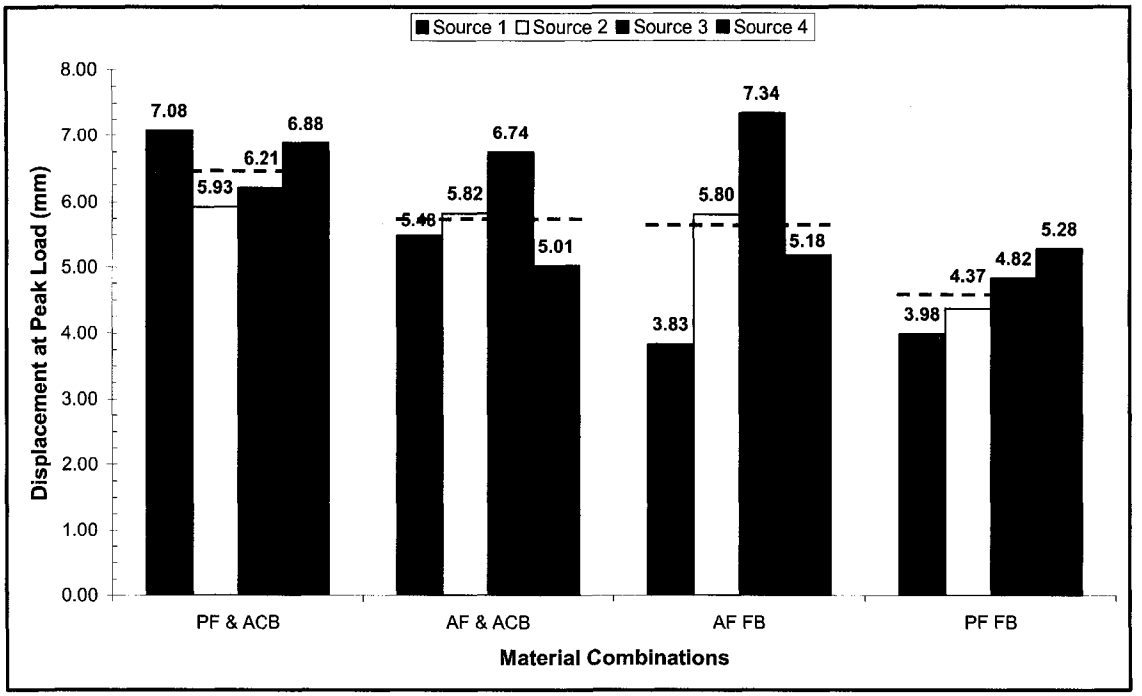

Figure 6.4: Sample average deflection at peak load pullout performance of 4 Different Material Combinations

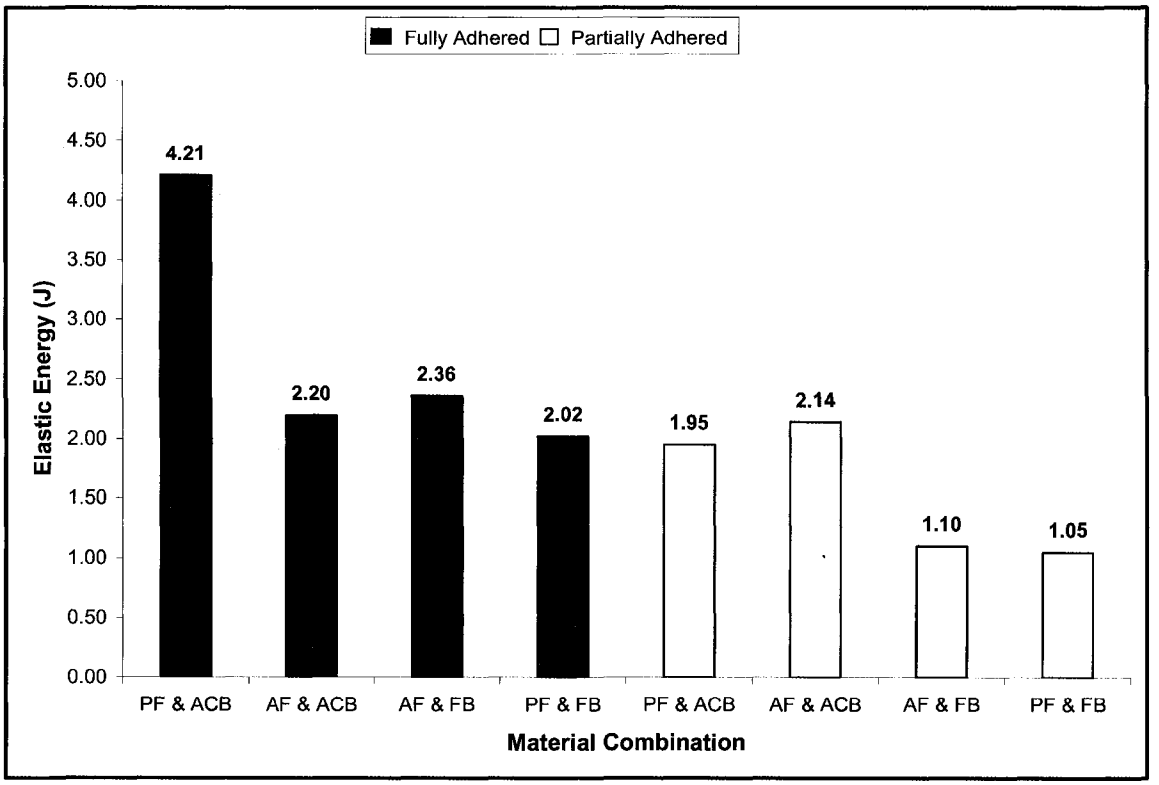

Figure 6.5: Material combination elastic work sample average

By combining the results of figures 6.2 -6.4, as shown in figure 6.5, there is a definitive trend that develops and is simplified by the following (excludes insulation) (ACB – FA > ACB – PA ≈ FB – FA > FB – PA)

The first remark is that for all material combinations with ACB, and for those with full adhesion with FB, the minimum amount of elastic work that can be put into a specimen ranges from 2.0-2.5J. This is an interesting conclusion. This measurement is a very specific range over which consistent behaviour is observed and it is independent of material, source and application. For specimens constructed with FB with partial adhesion, there is a decrease in the amount of work that can be put in and a drop-off of the order of magnitude 2. Figure 6.5 illustrates the susceptibility of FB to premature failure when exposed to pullout testing under partial adhesion and reasserts the arguments from the preceding discussion regarding: (ACB – FA > ACB – PA ≈ FB – FA > FB – PA)

This conclusion has been compared with full scale data by Current et al. (2007), Murty et al. (2008) and Murty et al. (2008). In figure 6.6, full scale performance of AARS systems tested to the CSA A123.21-04 standard and the corresponding pullout performance have been compared. Full scale wind uplift performance is measured by the test pressure sustained by the system. For example Source 1 tested a system with fiberboard and paper faced insulation under partial adhesion application conditions and was able to sustain a 1.44 kPa (30 psf) test pressure, but failed under a subsequent loading sequence. Corresponding pullout tensile stresses were calculated using peak load measurements to reflect their magnitude over the entire surface area of the test specimen (in this case 300 x 450 mm). From figure 6.2, the sample average peak load for Source 1 for the PF & FB material combination is 1.24 kN and translates into a peak stress of 9.19 kPa. This procedure was repeated for Sources 2 and 3. Source 4 sustained a test pressure of 120 psf and the test was stopped. What is important to note is the relative performance of the source and material combination measurements in Figure 6.6 and although no empirical relationship has been established between the two tests, good performance (Ex: Source 4 – PF & ACB) was observed for both wind uplift and pullout testing and vice versa.

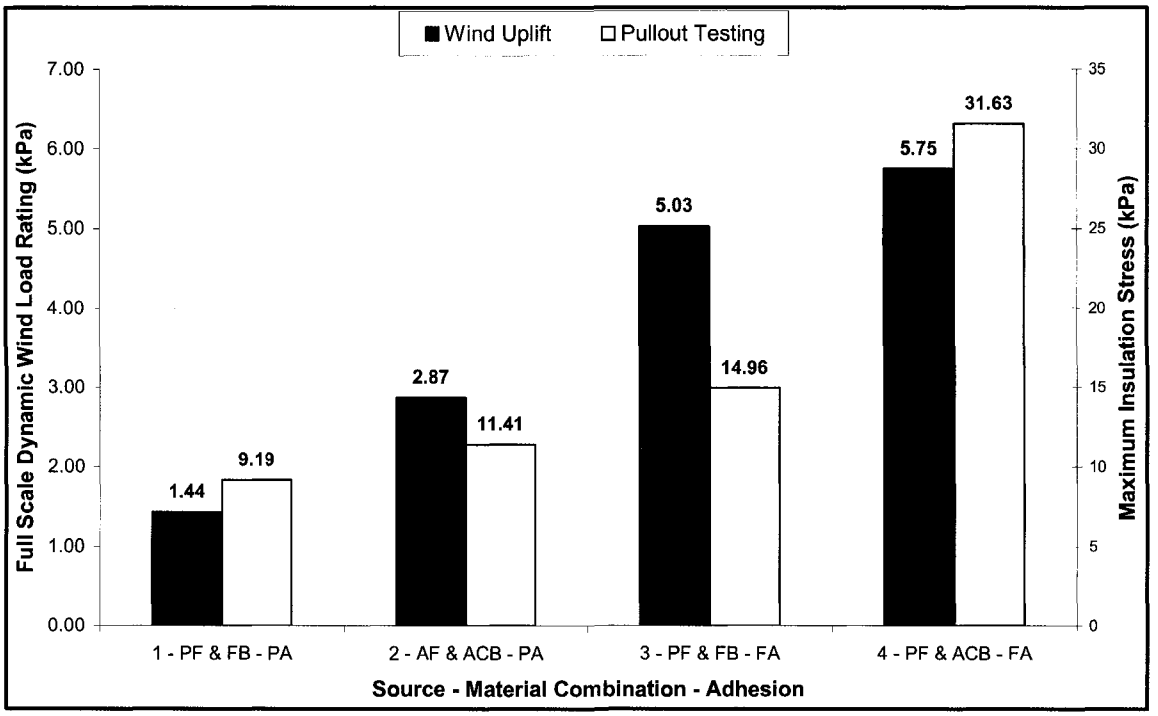

Figure 6.6: Comparison of Pullout and Wind Uplift Testing

6.3 Effect of Insulation & Coverboard – Failure Plane Analysis

Substitution of different materials into the AARS specimens may lead to different failure planes. Figure 6.7 illustrates the breakdown of failure planes from all sources based on material combination. Table 6.1 is also presented as resource to illustrate a source by source overview of the failure planes encountered for the 96 experiments that were conducted to characterize pullout performance of AARS specimens.

A conclusion from Section 6.2 was that there were empirical results that supported the theory of a strong correlation between sample average peak load and the type of coverboard material that was used for pullout testing. A review of the failure planes confirms this hypothesis. In referring to Table 6.1, whenever a specimen was constructed with ACB, with PF or AF, the failure plane was consistent on a source by source basis. None of these failure planes will be illustrated explicitly here. Similar failure planes have already been illustrated in figure 5.8 – 5.11. From Table 6.1, note the frequency of facer delamination with respect to the AF & ACB material combination. In the preceding section, there was mention of the PF & ACB material combination exhibiting the most consistent results. With respect to failure plane occurrence, it appears that the AF & ACB material combination exhibits superior consistency.

Specimens constructed with FB tended to have more variable failure planes and is most clearly illustrated by the material combination of AF & FB for Source 2, but overall it is quite apparent that loss of cohesion of the coverboard is observed when fiberboard is applied. Results from section 6.2 also suggested that the FB is a weak link in the AARS construction when it is used as a substitute for ACB. Intuitively, the expectation would be that failure would occur on the FB and Figure 6.8 illustrates that this is in fact true. Out of 48 specimens tested with FB, 40 of them failed in the coverboard. Figure 6.8 illustrates failure planes from the predominant failure plane from the PF & FB material combination for each of the four sources.

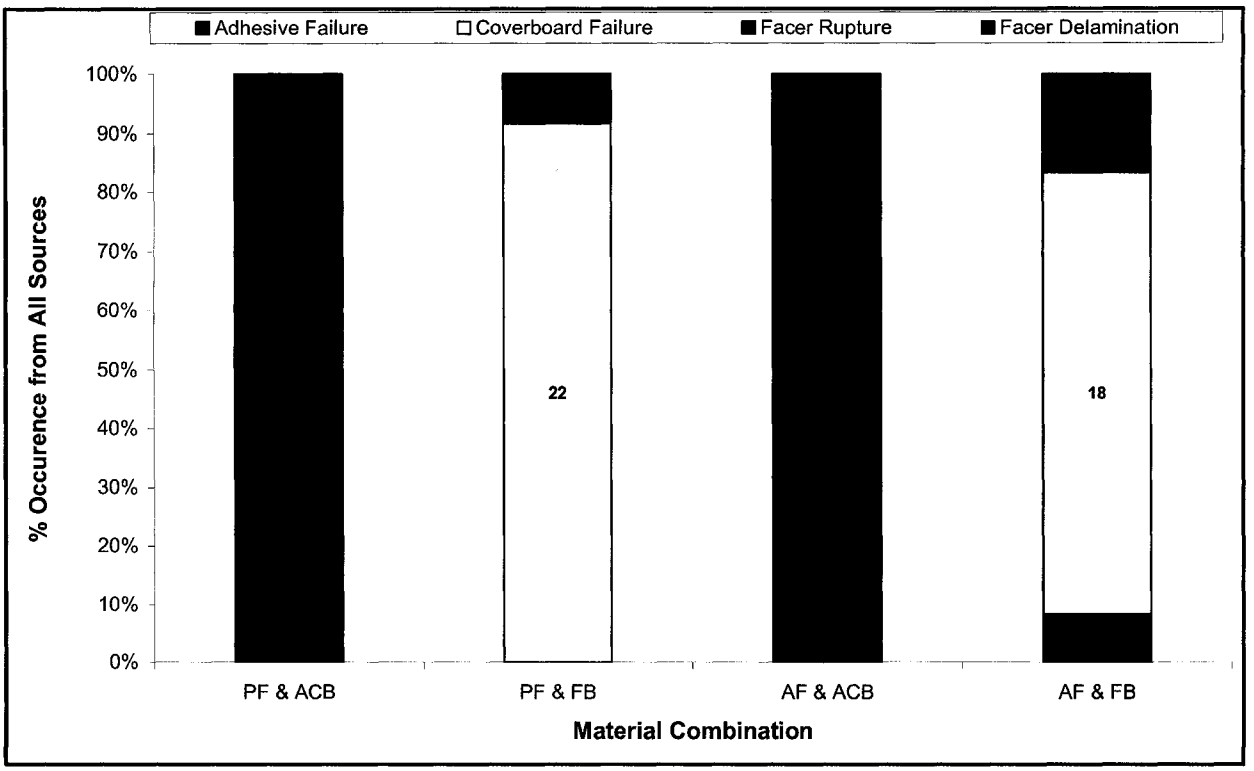

Figure 6.7: Failure plane occurrences for sources 1-4 for different material combinations

Material Combination	Source 1		Source 2		Source 3		Source 4	
	Failure Plane	Freq	Failure Plane	Freq	Failure Plane	Freq	Failure Plane	Freq
PF & ACB	Adhesive Failure	6	Facer Rupture	6	Facer Rupture	6	Facer Delamination	6
AF & ACB	Facer Delamination	6	Facer Delamination	6	Facer Delamination	6	Facer Delamination	6
PF & FB	Coverboard Failure	6	Coverboard Failure	4	Coverboard Failure	6	Coverboard Failure	6
			Facer Rupture	2				
AF & FB	Coverboard Failure	6	Adhesive Failure	2	Coverboard Failure	5	Coverboard Failure	6
			Facer Delamination	2	Facer Rupture	1		
			Facer Rupture	1				
			Coverboard Failure	1				

Table 6.1: Comparison of failure planes for different combinations of materials of PF, AF & ACB, FB for sources 1 – 4

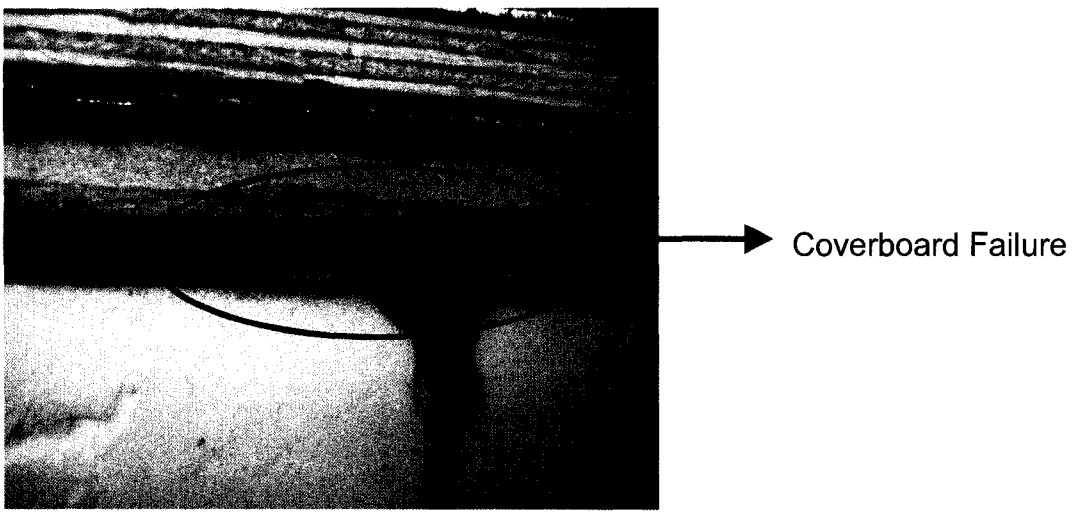

Figure 6.8a: Illustrations of typical failure planes from Source 1 for the PF & FB material combination

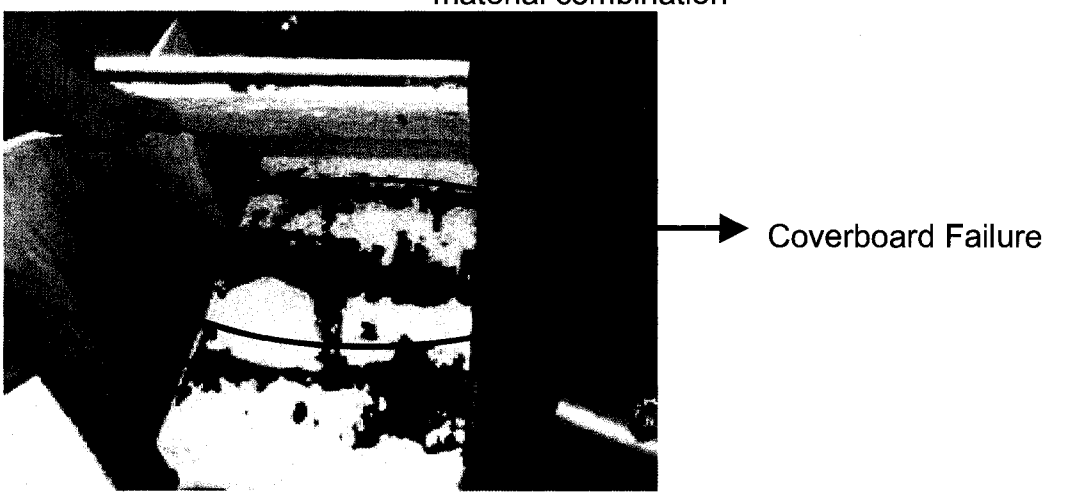

Figure 6.8b: Illustrations of typical failure planes from Source 2 for the PF & FB material combination

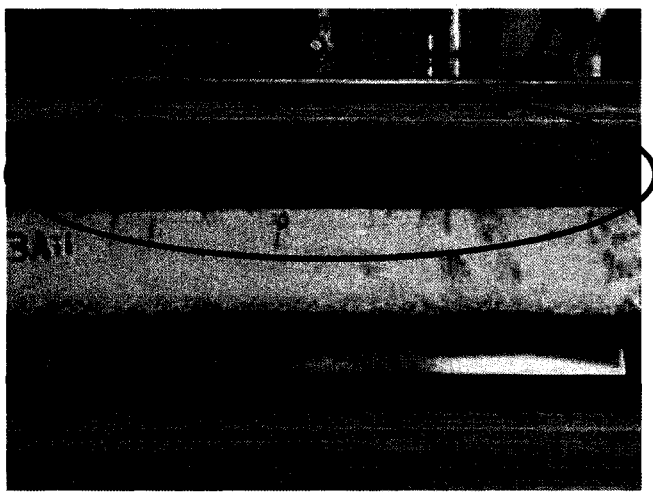

Figure 6.8c: Illustrations of typical failure planes from Source 3 for the PF & FB material combination

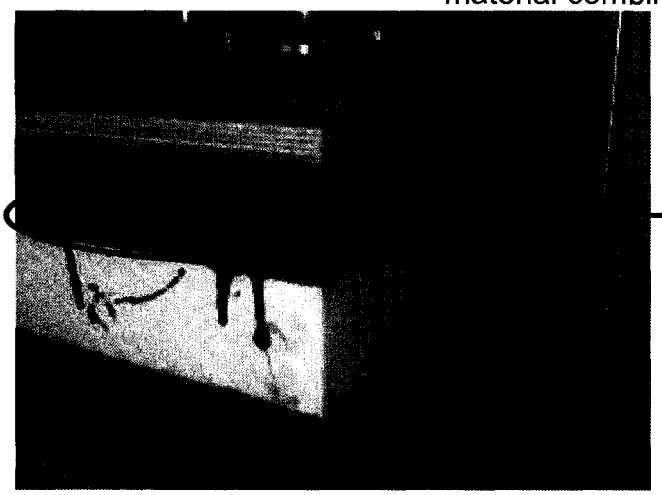

Figure 6.8d: Illustrations of typical failure planes from Source 4 for the PF & FB material combination

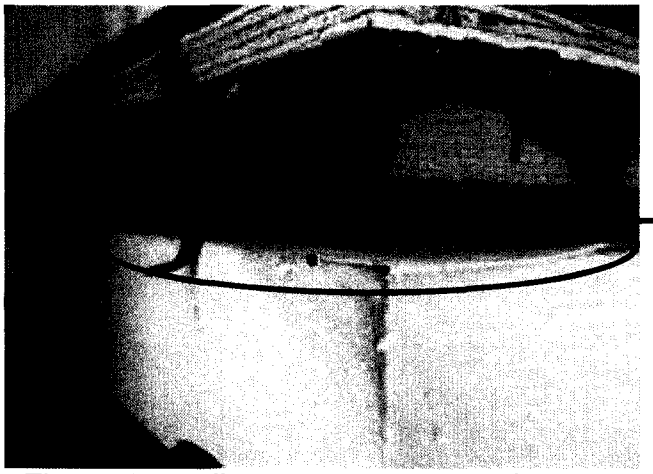

Figure 6.9a: Illustrations of typical failure planes from Source 1 for the AF & FB material combination

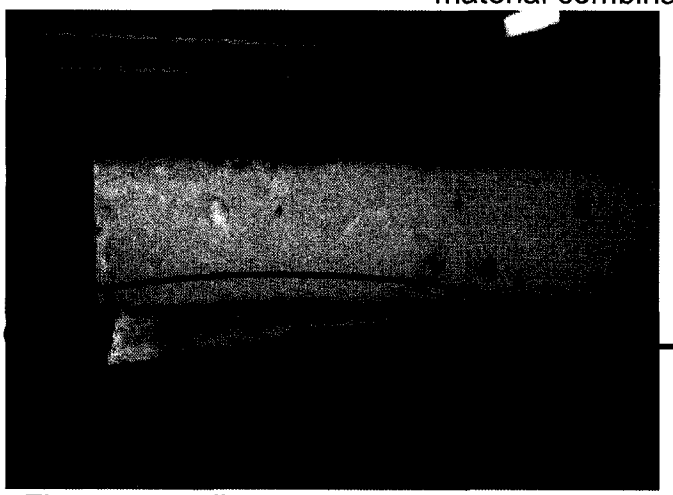

Figure 6.9b: Illustrations of typical failure planes from Source 2 for the AF & FB material combination

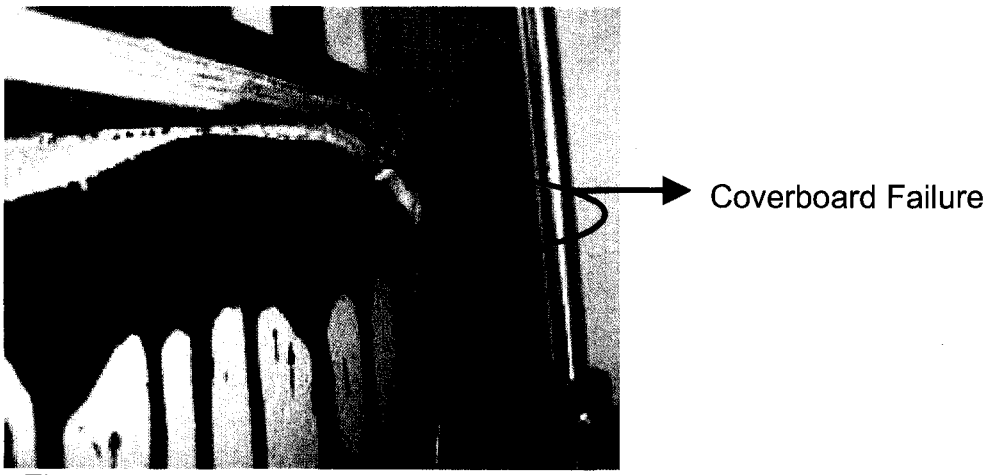

Figure 6.9c: Illustrations of typical failure planes from Source 3 for the AF & FB material combination

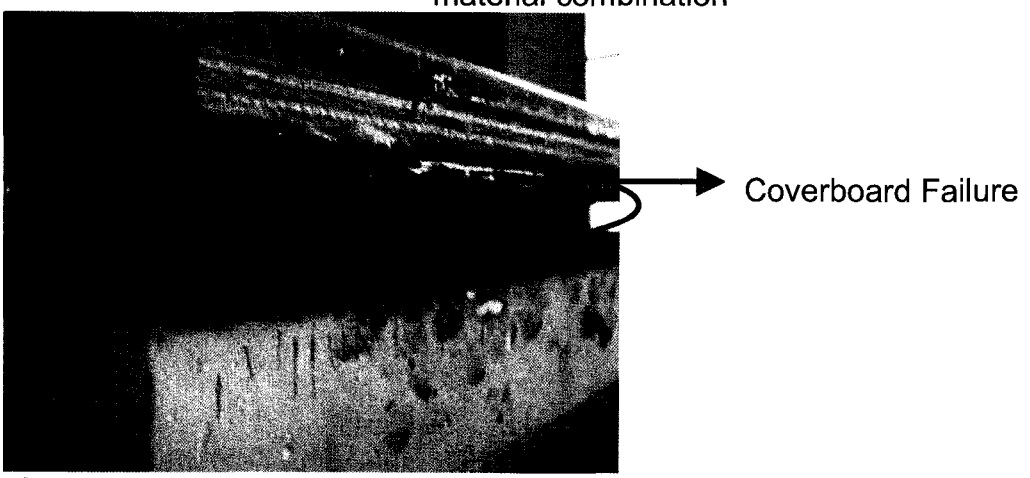

Figure 6.9d: Illustrations of typical failure planes from Source 4 for the AF & FB material combination

Note that the failure occurs in the coverboard regardless of whether the construction materials have been partially adhered. (Example: Figure 6.8a & b) or the construction materials have been fully-adhered (Example: Figure 6.8c & d) Likewise, the same sort of behaviour is exhibited to a lesser degree in Figure 6.9 which illustrates the predominant failure plane of one specimen from each of the 4 Sources of the AF & FB material combination.

Once again Figure 6.9 reasserts the arguments presented in the preceding paragraph that stated that coverboard failure occurs regardless of whether the construction materials have been adhered fully or partially. The failure planes of the AF&FB material combination from Source 2 do not follow this typical pattern of behaviour as illustrated in Figure 6.9b.

6.4 Effect of Deck – Comparative Analysis

As demonstrated in the preceding section, the type of components used in AARS play a significant role in the pullout response and performance. Likewise, the deck plays a similar role in determining the pullout response. This section will summarize the results of experiments that were conducted in order to characterize the different pullout behaviour of two different decks that are commonly used in AARS. Specimens from each of the 4 sources were constructed with a concrete deck, and these results were then compared to the data on steel deck with PF & ACB that were examined in the preceding section.

In figure 6.10, a breakdown of all the experimental variables has been provided in characterizing the different pullout behaviour between specimens with concrete and steel decks. Figure 6.11 illustrates the peak load results from these pullout tests and presents the results based on the deck on which specimens were constructed – steel or concrete.

While the specimens constructed on concrete decks for Sources 1 & 3 outperform the same specimens built on steel decks, the specimens from Sources 2 & 4 exhibit the exact opposite behaviour – significantly superior performance on the steel deck. What should be remarked is the relative proximity

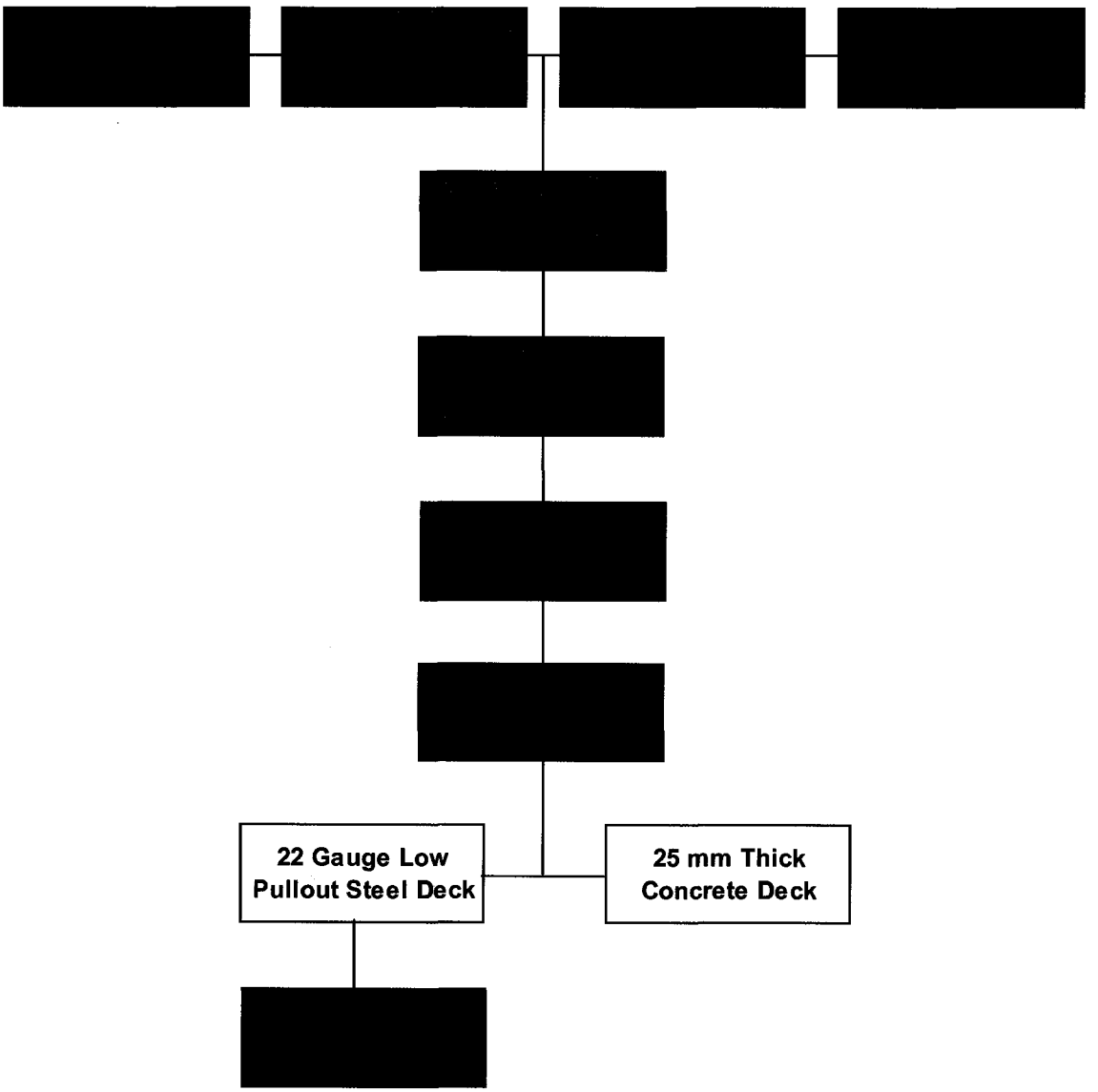

Figure 6.10: Test matrix for optimum deck material determination

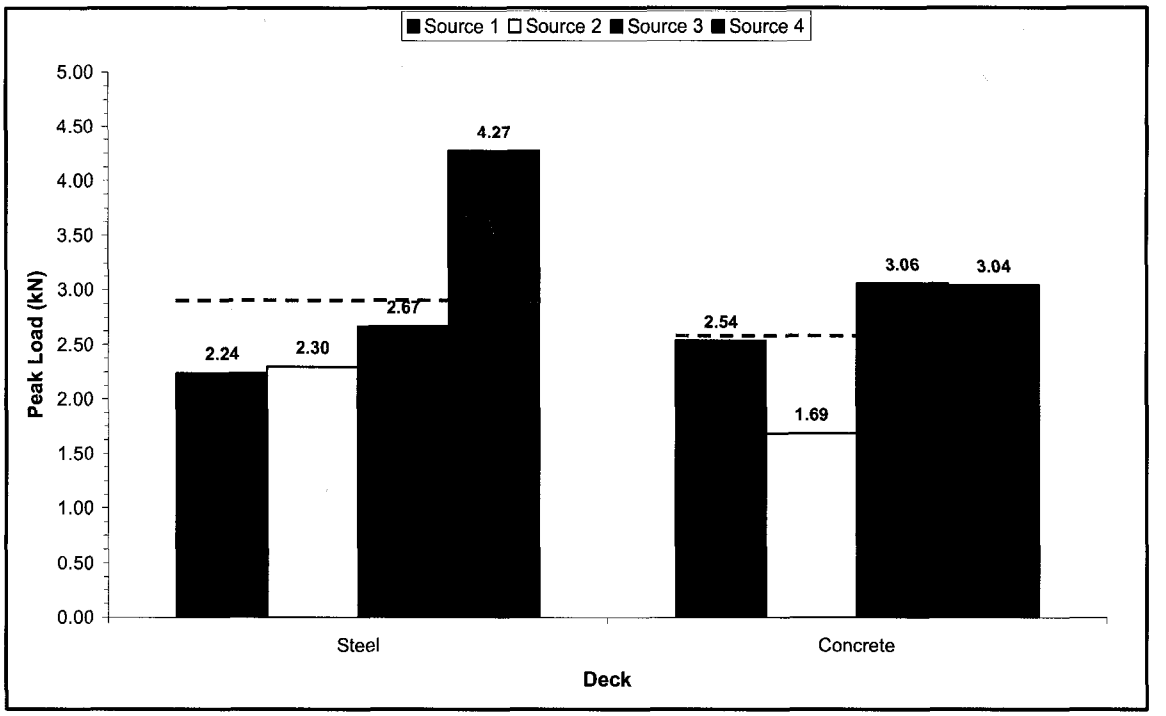

Figure 6.11: Sample average peak load pullout performance of 2 different types of decks

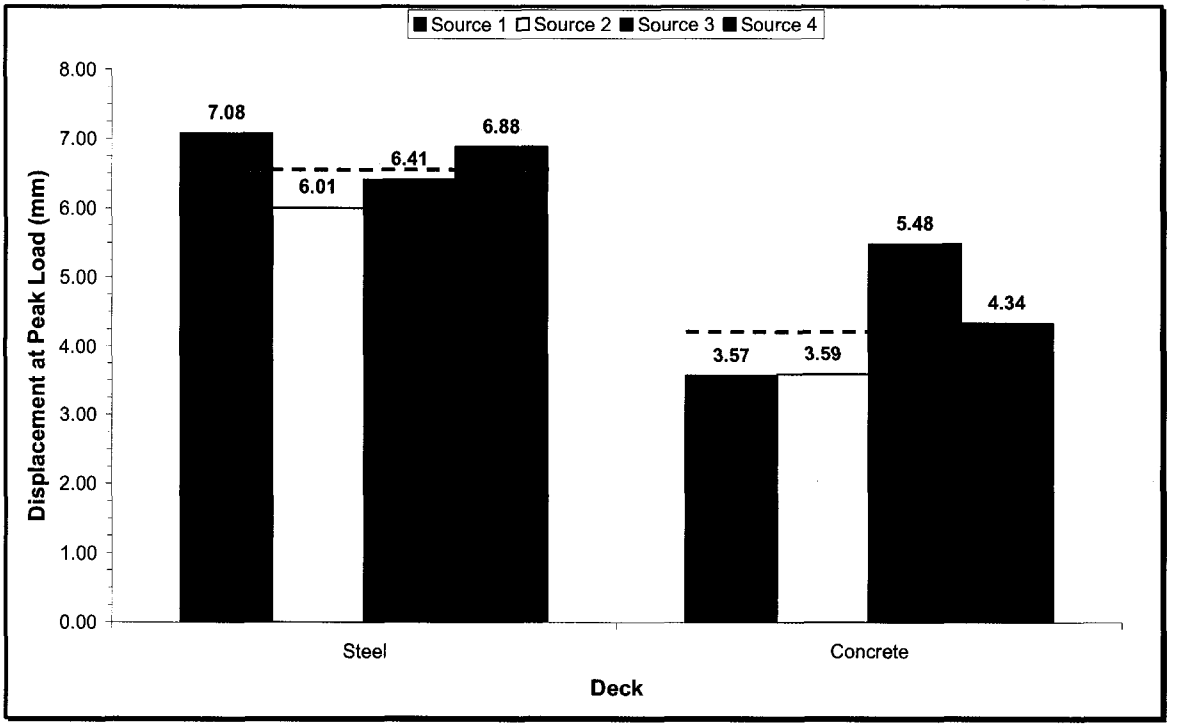

Figure 6.12: Sample average deflection at peak load pullout performance of 2 different types of decks

for steel and concrete deck specimens. (2.24 kN & 2.54kN for Sources 1 & 2.67kN & 3.06 kN for Source 3) This contradicting behaviour can be further explained by analysis of deflection and energy measurements.

In Figure 6.12, the deflection at peak load measurements have been tabulated and presented on a source-by-source basis. These results exhibit a more definitive pattern. In section 6.2 it was stated that for specimens constructed to a size of 300 x 450 mm tested with a pullout rate of 6.35 mm/min on steel deck with asphalt core board and paper facer there was a predictable limit of how much deflection could be incurred before failure occurred. Comparisons of the PF & ACB combination yielded a nominal deflection at peak load of the order of 6.5±0.5mm. The poorer performing PF & FB material combination yielded a nominal displacement at peak load of 4.60±0.65mm.

By extrapolating this argument, the conclusion is that the steel deck specimens performed better than the concrete deck specimens since the steel deck specimens were able to incur significantly more deflection prior to failure when compared to the specimens constructed on the concrete deck. This seems to be a superior way for characterizing the behaviour of AARS specimens built on concrete deck. It appears that the deflection at failure should be approximately 4.5 ±1.0 mm, based on the deflection at peak load measurements for specimens constructed with concrete decks. This is a substantially lower range than the range that was provided for specimens built on steel decks (6.5±0.5mm). A possible explanation follows. Specimens constructed on steel deck can deform more than those constructed on concrete decks because the more elastic behaviour of the steel deck allows some of the work that is placed into the specimen to be manifested as deflections on the deck. Concrete decks, are much more rigid and do not allow the dissipation of energy in such a manner. The result of which is a lower amount of deflection that can incur prior to failure. To confirm this hypothesis, a comparison of elastic energy plots between specimens constructed on steel decks and specimens constructed on concrete decks has been performed.

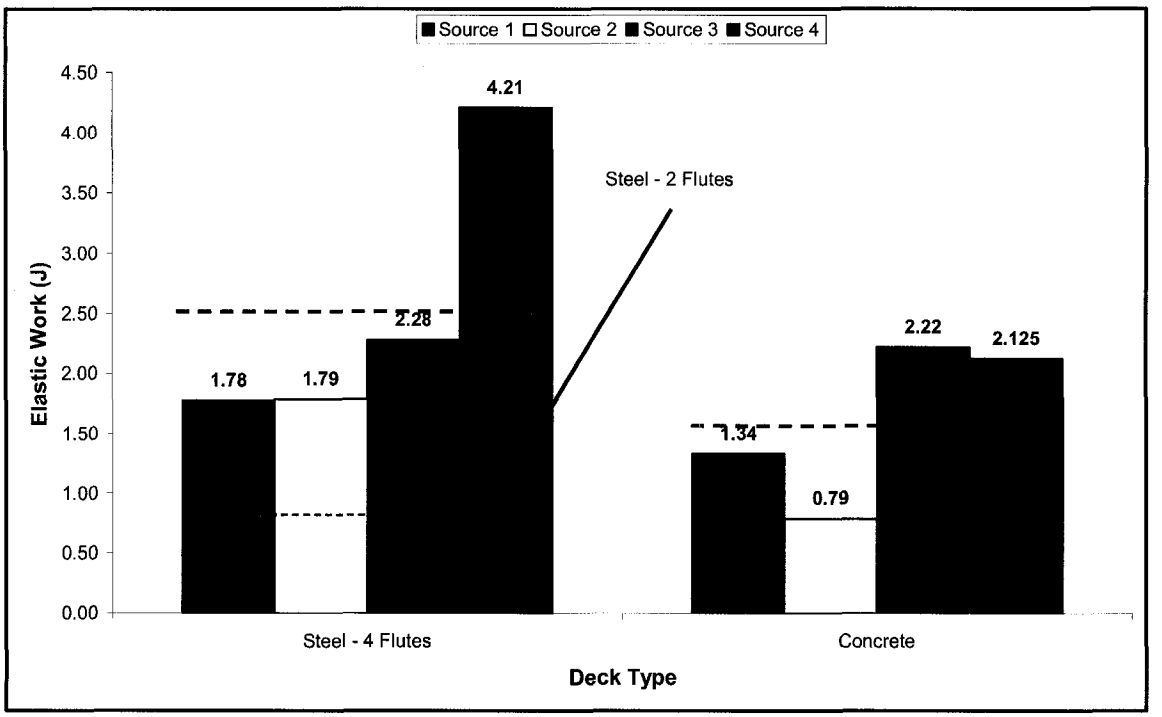

Figure 6.13: Sample Average Elastic Work Measurements for 2 Different Types of Decks

In figure 6.13 elastic work measurements have been plotted for the steel deck specimens attached on 4 flutes and the concrete decks. It is apparent from figure 6.13 that steel deck specimens outperform the concrete deck specimens. Even if the results of the steel deck specimens from Source 4 bloat the results for the steel deck overall deck average, steel deck still outperforms concrete decks by a significant margin. What should also be remarked about the results of Figure 6.13 is that the elastic energy calculations for steel deck specimens include both work that is used to cause failure (work used to break adhesive bonding or work used to cause cohesive failure) and work that is put into a specimen to cause deck deformations. Since steel decks dissipate work put into the specimens during pullout tests, they consistently should outperform concrete deck specimens. For comparison, calculations of elastic work from specimens attached with two flutes have been shown. Steel deck specimens attached on 2 flutes under perform when compared to the other conditions. Average elastic work for specimens was 0.802 J as shown in Figure 6.13. This is because the driving force to failure for these specimens has changed because of the change in attachment condition. This change in driving force to failure has been studied by Wu (2008) and reflects the lower magnitude in performance of steel deck specimens attached on 2 flutes when compared to the results of specimens attached on 4 flutes and concrete decks.

6.5 Effect of Deck – Failure Plane Analysis

Table 6.2 compares the failure planes of steel deck specimens and concrete deck specimens tested under the same conditions on a source by source basis while Figure 6.14 illustrates a breakdown of failure planes based on specimens with concrete and steel deck.

There are one of two possible outcomes that will be observed when the deck changes from steel to concrete. The failure can become more brittle as a stress concentration is placed on the insulation facer because of the lack of ductility of the concrete deck. The other possible outcome of switching decks can

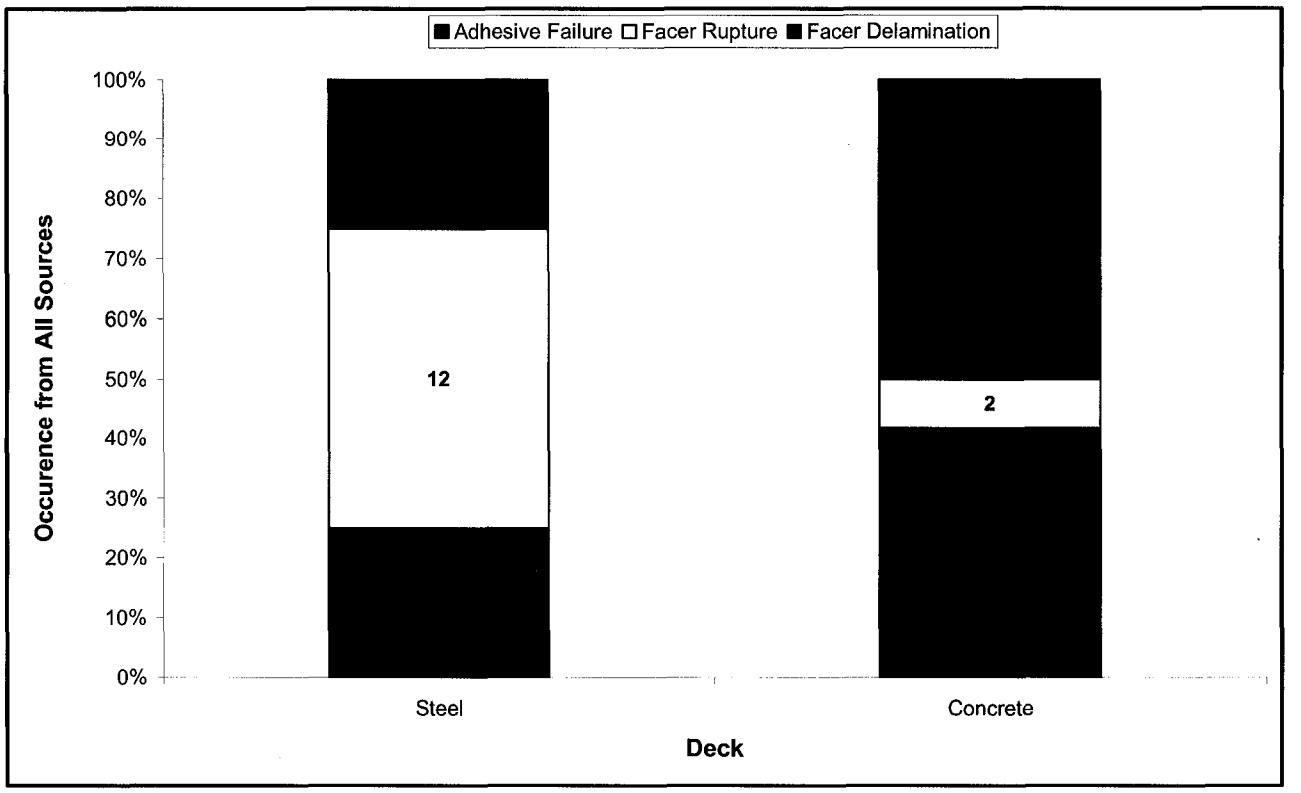

Figure 6.14: Failure Plane Occurrences for Sources 1-4 for Different Decks

Deck	Source 1		Source 2		Source 3		Source 4	
	Failure Plane	Freq	Failure Plane	Freq	Failure Plane	Freq	Failure Plane	Freq
Steel	Adhesive Failure	6	Facer Rupture	6	Facer Rupture	6	Facer Delamination	6
Concrete	Facer Delamination	7	Adhesive Failure	4	Adhesive Failure	5	Facer Delamination	4
					Facer Rupture	1	Adhesive Failure	1
					Facer Delamination	1	Facer Rupture	1

Table 6.2: Comparison of Steel Deck and Concrete Deck Failure Planes for Sources 1 - 4

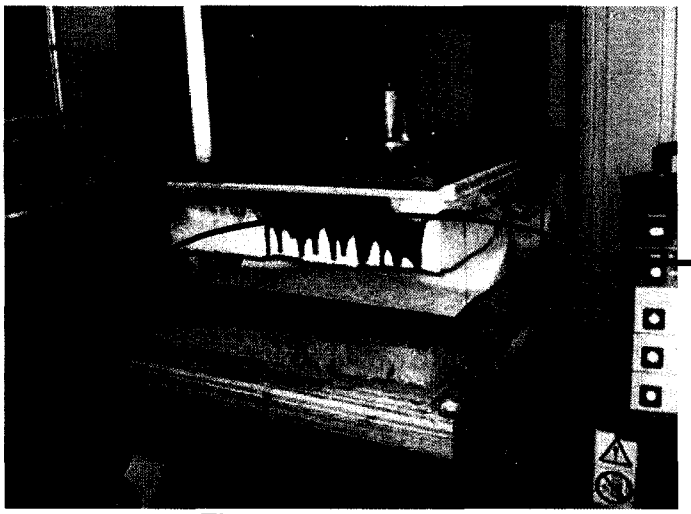

Figure 6.15a: Source 1 concrete deck specimen failure

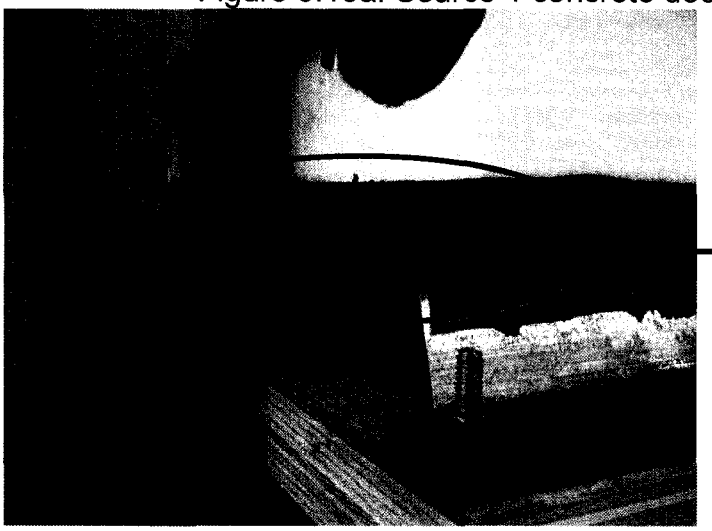

Figure 6.15b: Source 1 steel deck specimen failure

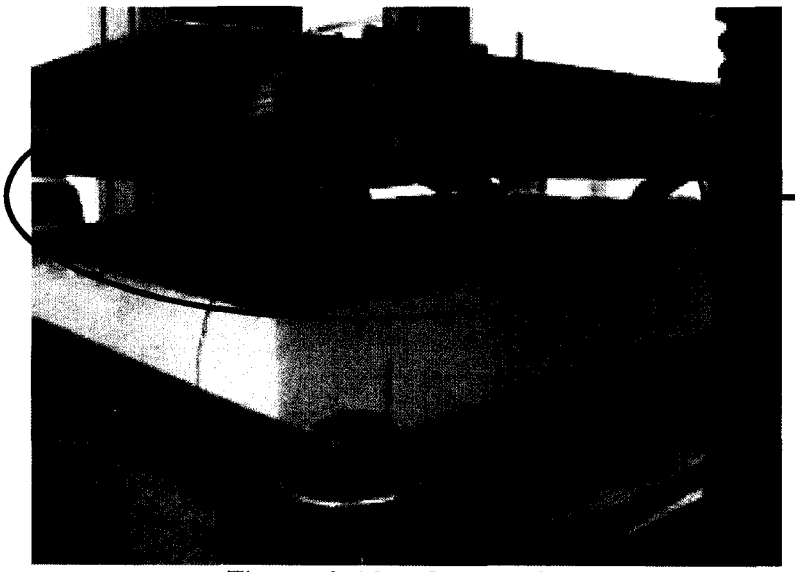

Figure 6.16a: Source 2 concrete deck specimen failure

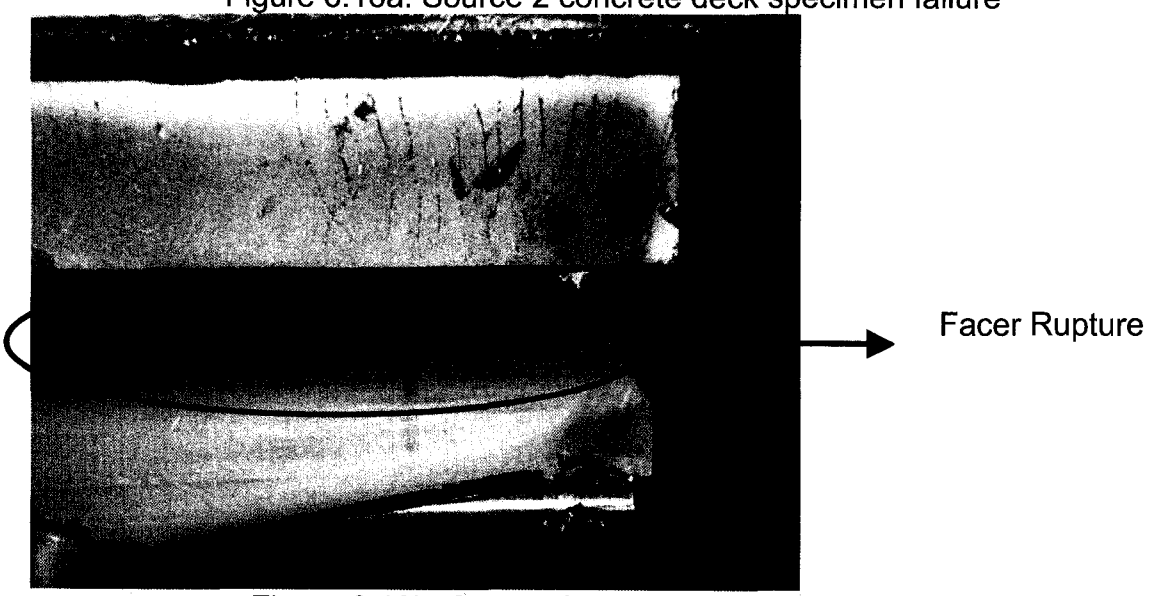

Figure 6.16b: Source 2 steel deck specimen failure

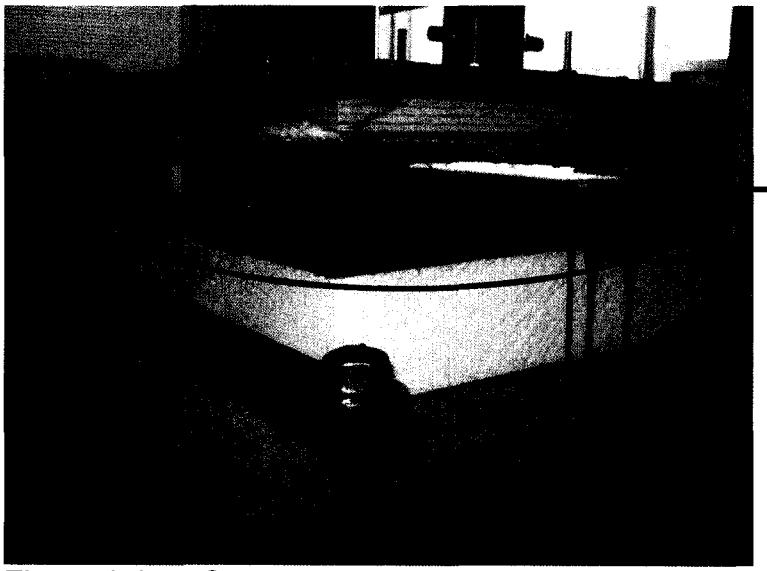

Figure 6.17a: Source 3 concrete deck specimen failure

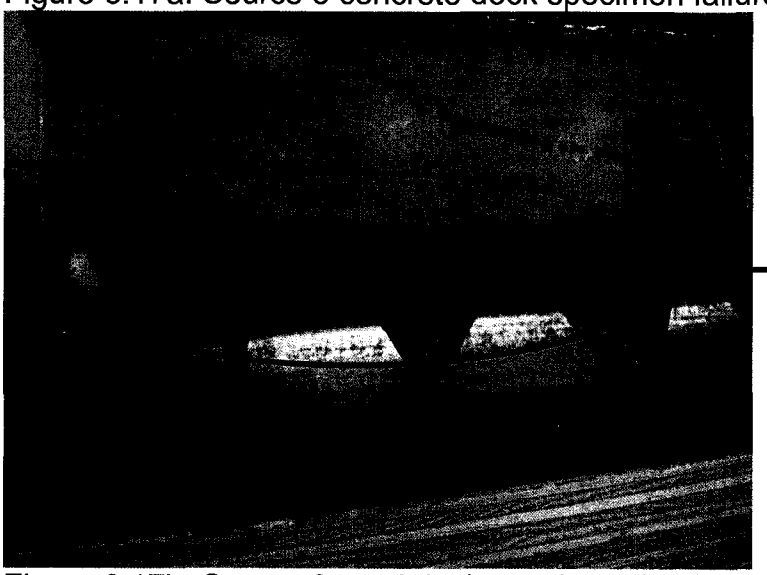

Figure 6.17b: Source 3 steel deck specimen failure

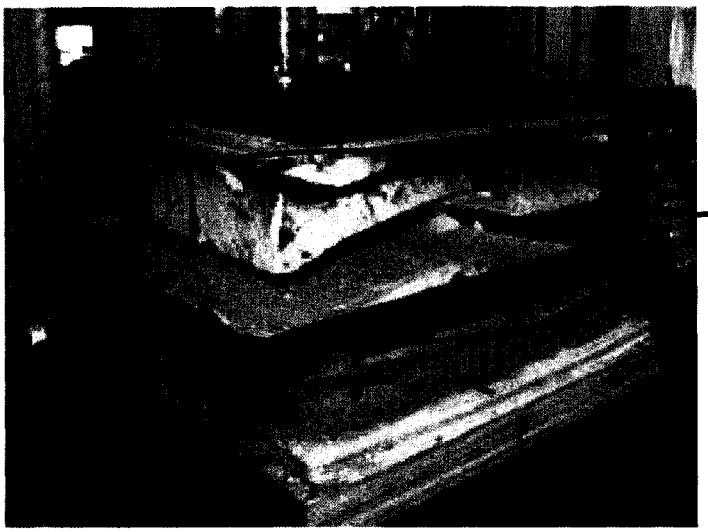

Figure 6.18a: Source 4 concrete deck specimen failure

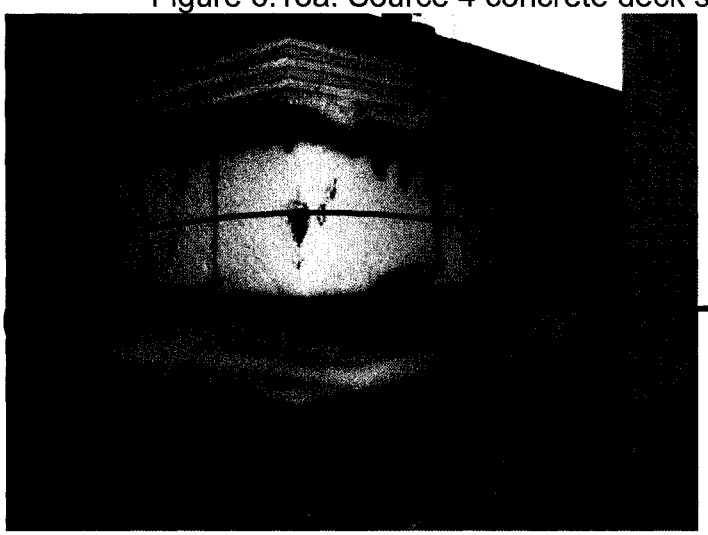

Figure 6.18b: Source 4 steel deck specimen failure

result in a more successive failure as adhesive or cohesive failure occurs in the coverboard before the facer can delaminate.

Figures 6.15 – 6.18 illustrate the predominant failure plane of concrete and steel deck specimens. Please note that the illustrations provided of steel deck specimens are repeated from earlier in this study. Source 1 (illustrated in 6.15) failures planes are typically successive as they evolve from adhesive failure to facer delamination. Sources 2 & 3 (illustrated in figure 6.16 & 6.17) become more catastrophic as the failure plane has changed from facer rupture to adhesive failure. Due to the fact that full adhesion was applied for Source 4 (illustrated in figure 6.18), the change in failure plane was negligible. However there was an increase in scatter in the occurrence of failure planes for specimens constructed on concrete deck. This scatter was also reflected in the empirical data.

Based on the arguments presented above, the steel deck exhibits superior pullout performance when compared to the concrete deck. The combination of (slightly) superior results with respect to peak load measurements, deflection at peak load measurements, and elastic energy provide the empirical justification for this conclusion.

6.6 Effect of Deck-VB Adhesion – Comparative Analysis

Another variable of interest that industrial partners wished to capture was how the effect of alternative adhesion patterns on steel deck specimens affected the pullout performance of AARS specimens. This is a useful test for several reasons. Typically, in the field, the possibility exists not to fully-adhere all flutes of the steel deck. This is done as a cost savings initiative to save on both labour and material. Thus, it was of interest to determine the specific effect of altering the adhesion pattern between the deck and the vapour barrier. It would also be of interest to see if intentionally placing less adhesive between two components would result in a failure plane close, or closer, to the location of where less adhesive was applied. To accomplish this end, four additional samples were constructed and compared with the four samples already referred to in section

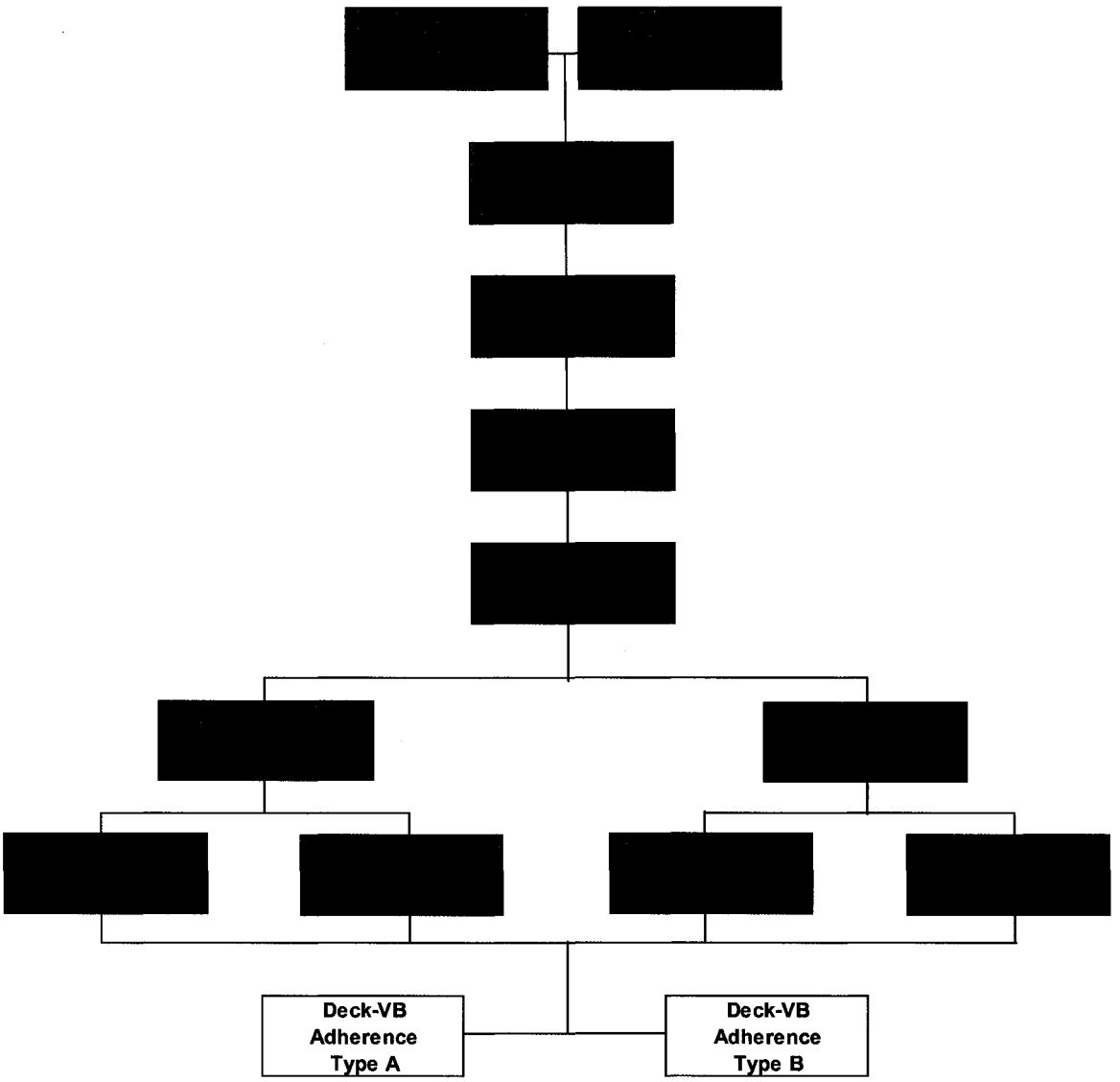

Figure 6.19: Test matrix for deck-VB adherence relationship determination

6.2 as the PF & ACB, AF & ACB, PF & FB, and AF & FB material combinations. They were sized at 300 x 450 mm with steel deck, and tested with a pullout rate of 6.35 mm/min. The second set of samples was a new set of specimens identical to the first in every way, except that adhesive was only placed in between the steel deck and the vapour barrier on the outer two flutes, and not all three flutes. The difference in between construction of Type A and Type B specimens has been explicitly illustrated in Figure 3.6, with figure a showing Type A specimens and figure b illustrating Type B Specimens. Since Sources 1 & 2 use auto-adhering vapour barriers, these two sources were excluded from this investigation. However, Sources 3 & 4 apply a vapour barrier that is adhered with its own adhesive and the Type A and Type B differentiation can be made with these sources. The results of 48 experiments are analyzed in this section and Figure 6.19 illustrates the breakdown of the experimental variables. Peak load measurements for both types of adhesion patterns have been captured and are compared in figure 6.20. In the following figure, 6.21, the peak load of Type B has been divided by the peak load of Type A and then material combinations have been averaged.

In figure 6.20, there is nothing out of the ordinary – Type B specimens follow the same relative trends (or follow them closely enough) that their counterpart Type A specimens follow. The peak loads of Type B specimens fail to reach the same level that the Type A specimens reach – as expected. Also in reference to figure 6.20, it appears that peak load failure range of specimens of the Type B configuration is more finite than it is for specimens of Type A configuration. Based on figure 6.21, it appears that Type B specimens only attain 50-70% of the peak load of Type A specimens, depending significantly on the type of materials employed for specimen construction.

Due to the fact that Type B specimens have less adhesive in an area adjacent to the deck (which under loading deflects significantly) the expectation is that the displacements at peak load would exceed those of the Type A specimens. This is because the lack of restraint at this level will permit more excessive deformations than was observed with Type A specimens. It should

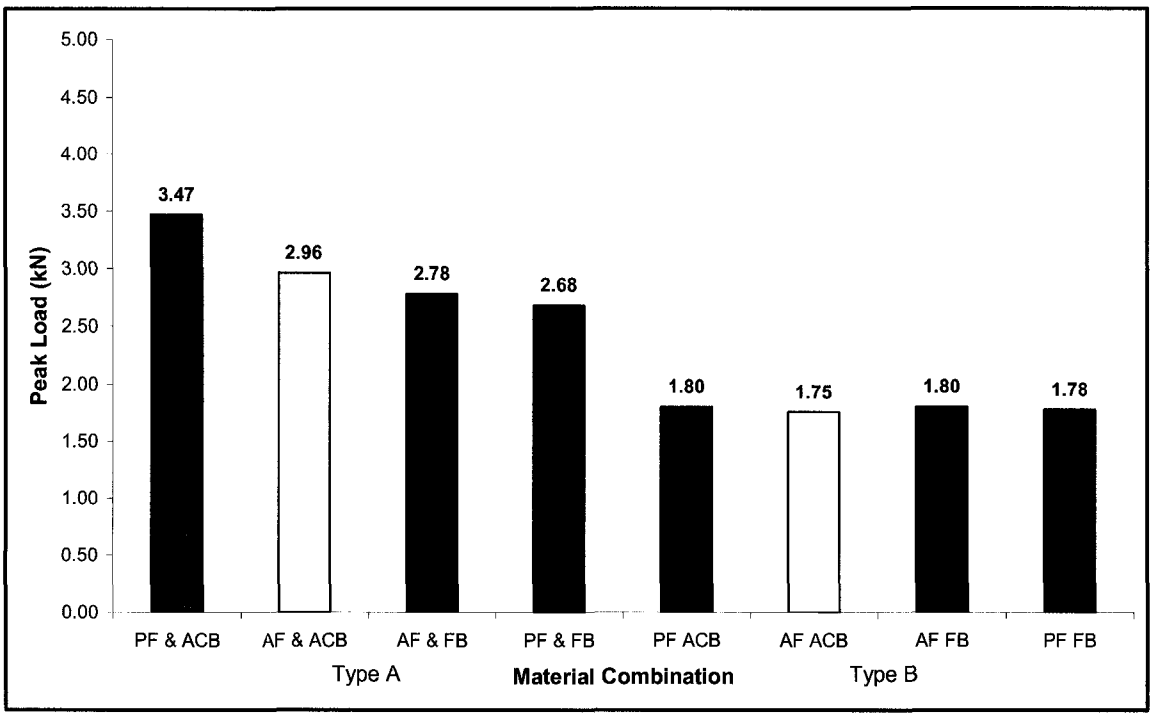

Figure 6.20: Peak load pullout performance of different adhesion patterns of different materials

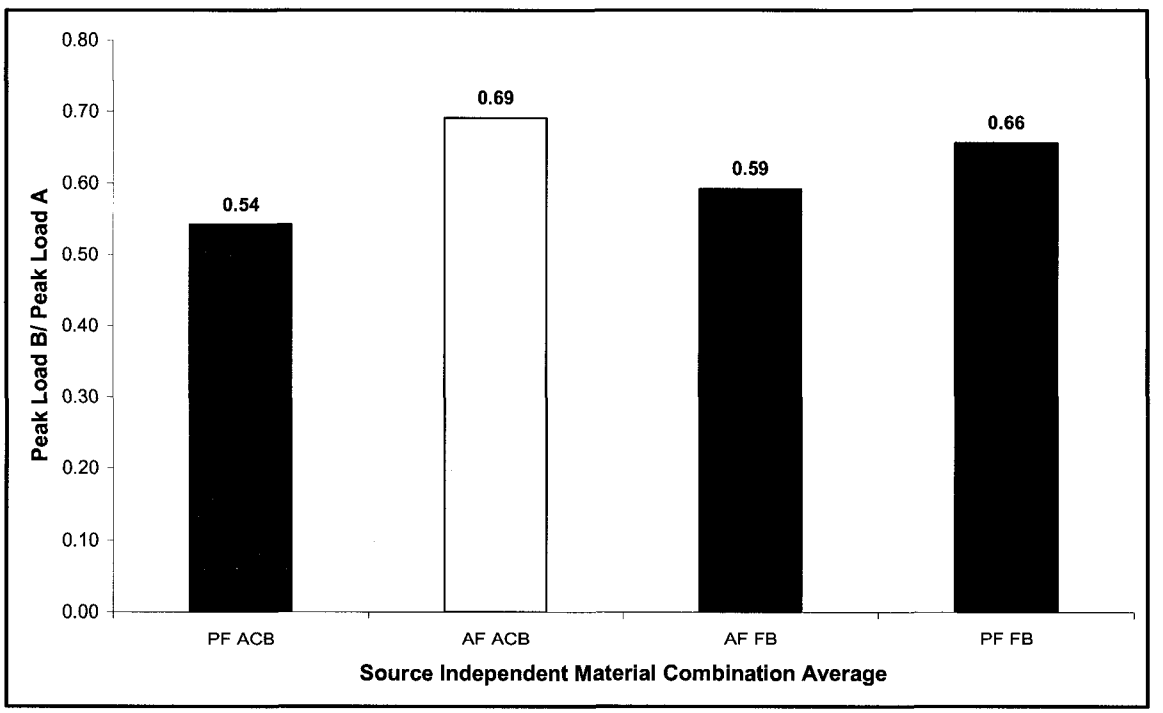

Figure 6.21: Peak load pullout comparison of Type B/ Type A

also account for the difference in peak loads attained between Type A and Type B specimens. Figure 6.22 presents the deflection at peak load average from Sources 3 & 4 of both Type A specimens and Type B specimens for all material combinations.

Under the new adhesive conditions, the new adhesive pattern permits more deflection prior to failure as expected. Also relative material combination trends are reflected in a similar fashion. (ie: for Type A: PF & ACB> AF & ACB < AF & FB > PF & FB, and is the same order for Type B) It also seems that the most ductile of all material combinations is the PF & ACB material combination as a deflection at peak load measurement in excess of 9.00 mm for both Source 3 and 4. On the whole, it appears that Source 3 generally exhibits more ductility than Source 4. There also appears to be a better "compatibility" of the Source 3 adhesive with the acrylic facer. The next step in this discussion is to combine the results of the measurements from the two previous figures. The elastic energy for these experiments have been calculated and in figure 6.23, the elastic energy of Type A adhesion has been divided by the elastic energy of Type B adhesion for specimens constructed with like materials.

The results of Figure 6.23 provide interesting results. For 6 of the 8 trials with Type B adhesion (from both sources) elastic energy decreases when compared to Type A adhesion. A practical explanation for this physical behaviour can be described as less adhesion will mean less contact area and as a result less work required to break adhesive bonding or induce cohesive material failure. However, specimens constructed by Source 3 with Type B adhesion and FB as a coverboarding material, the elastic energy actually increases. An explanation for this behaviour is a little less forthcoming. It is possible that in removing adhesive from the middle flute of the specimen a stress concentration has been placed on the specimen in the area around the deck – a stress concentration that nullifies the typically weak performance of specimens with FB. It is possible that this stress concentration "shields" the FB from premature failure.

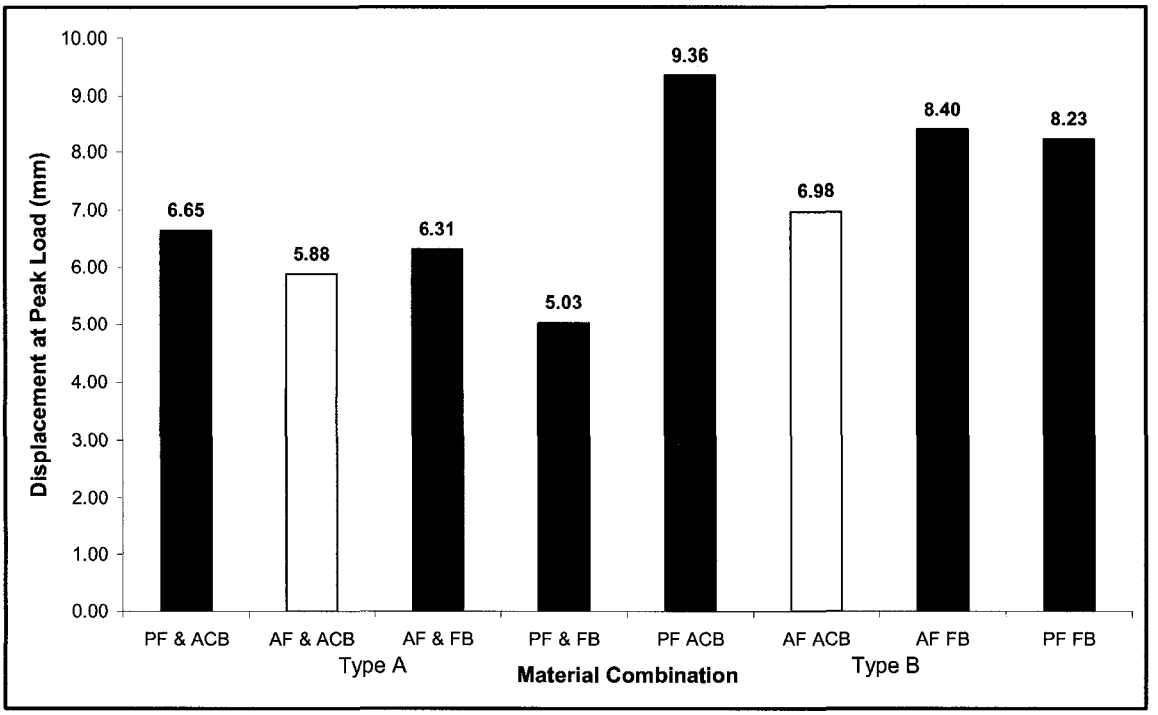

Figure 6.22: Deflection at peak load pullout performance of different adhesion patterns for different materials

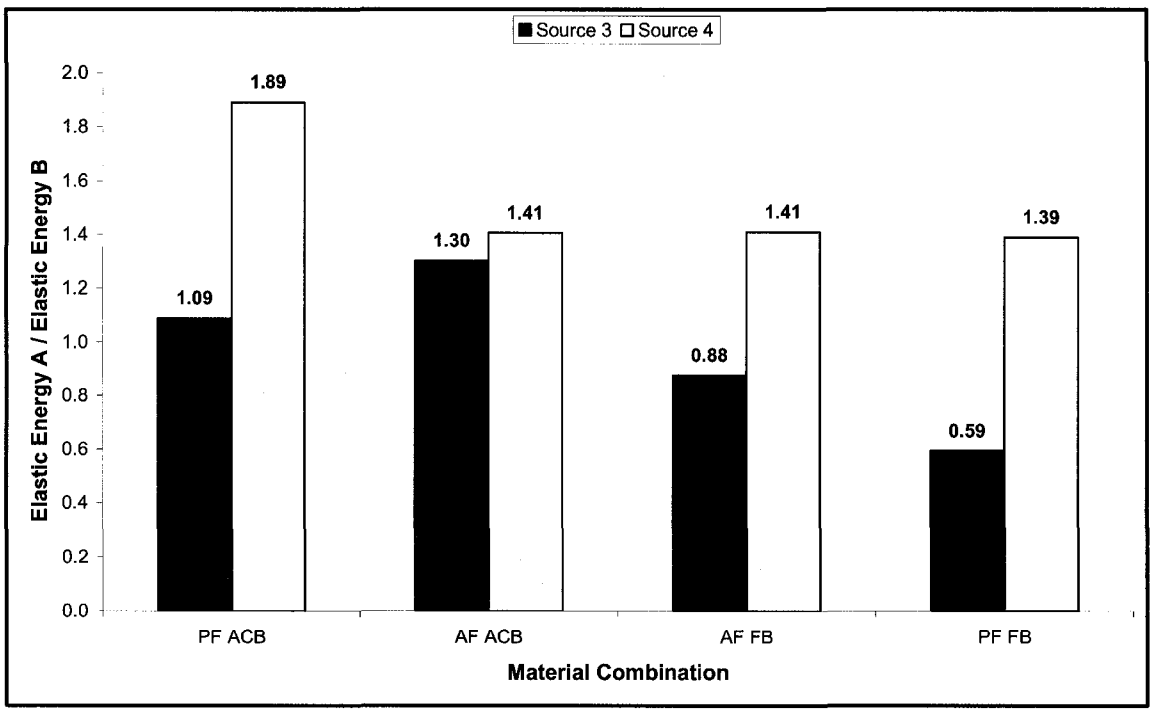

Figure 6.23: Comparison of Elastic Energy of Type A & B Specimens

6.7 Effect of Deck-VB Adhesion – Failure Plane Analysis

An overview of the failure planes for all Type A and Type B laboratory experiments are summarized in Table 6.3. Figure 6.24 has also been provided to compare the failure planes of Type A and Type B constructed specimens. The hypothesis is that with the change in adhesion types from A to B, the failure plane will shift towards the material that is causing the stress concentration – the steel deck.

However, this hypothesis aside, the two most important questions that should be answered are whether or not changing the adhesive pattern on specimens constructed with FB cause the failure plane to occur surreptitiously. The next question that should be posed is whether or not changing the adhesive pattern to Type B will result in the exact same failure plane that was encountered for Type A.

Of the 12 trials performed on specimens with Type B adhesion from Source 3 and constructed with fiberboard, only 3 coverboard failures were encountered. These failures were encountered when the fiberboard was combined with the paper-faced insulation. The rest were failures on the facer. Of the 12 trials performed on specimens with Type B adhesion from Source 4 and constructed with fiberboard, none had any occurrence of a failure in the coverboard. All failures were either on the facer or due to vapour barrier delaminations. In the previous section, it was observed that the elastic energy increased for Source 3 constructed with Type B adhesion was applied as opposed to Type A adhesion. In examination of the failure planes of Table 5.3, it is noted that the failure planes for Type A specimens constructed with FB were predominantly coverboard failures. The Type B on the other hand encountered 9/12 failures on the facer, with 3 more coverboard failures. This change in failure plane can account for the weaker pullout performance of the Type A specimens.

Based upon these observations it would appear that under the Type B adhesion test conditions, facer failure and vapour barrier delaminations become a weaker link in the overall construction than the cohesive coverboard failures

Material Combination	Source 3				Source 4			
	Type A		Type B		Type A		Type B	
	Failure Plane	#	Failure Plane	#	Failure Plane	#	Failure Plane	#
PF & ACB	Facer Rupture	6	Facer Rupture	5	Facer Delamination	6	VB Delamination	4
			Facer Delamination	1			Facer Delamination	2
PF & FB	Coverboard Failure	6	Coverboard Failure	3	Coverboard Failure	6	VB Delamination	4
			Facer Rupture	2			Facer Delamination	2
			Facer Delamination	1				
AF & ACB	Facer Delamination	6	Facer Delamination	5	Facer Delamination	6	Facer Delamination	6
			Adhesive Failure	1				
AF & FB	Coverboard Failure	5	Facer Delamination	6	Coverboard Failure	5	Facer Delamination	6
	Facer Delamination	1			Facer Delamination	1		

Table 6.3: Failure plane comparison for Type A & B Construction for Sources 3 & 4

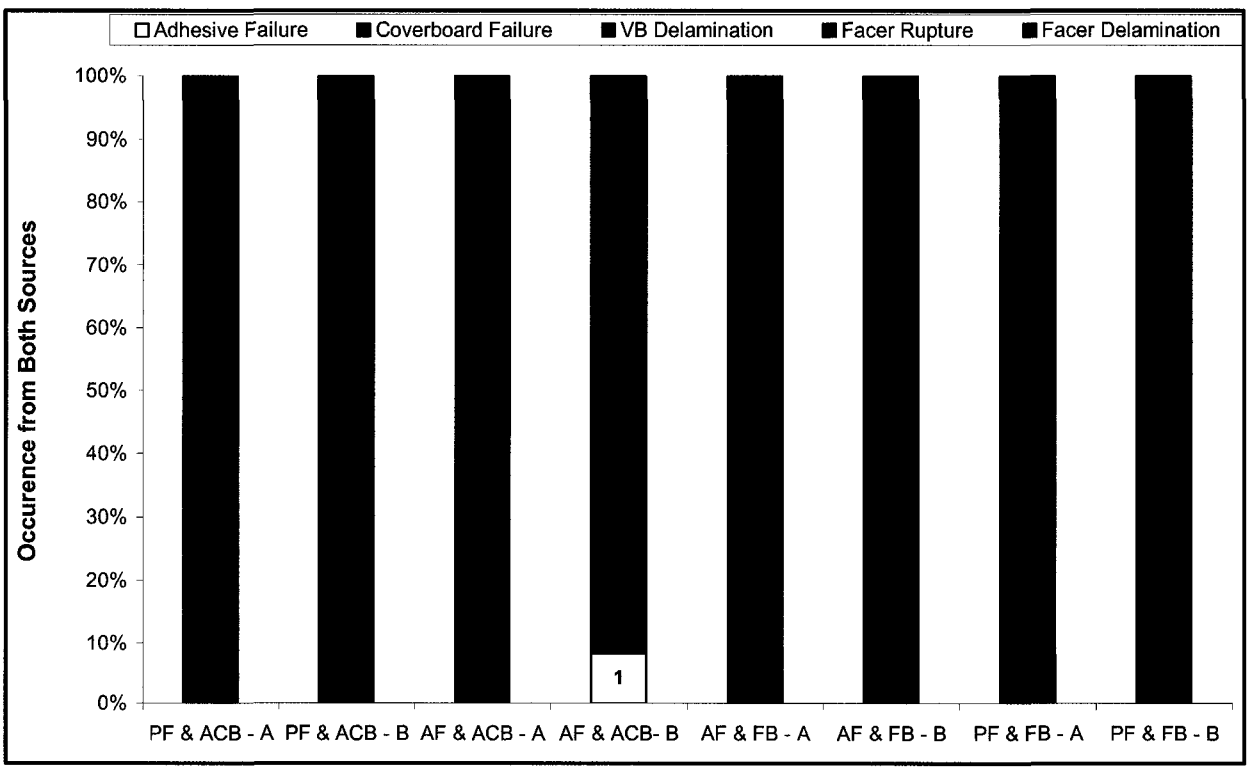

Figure 6.24: Failure Plane Occurrences for Sources 3-4 for Type A and Type B Adhesion

are with Type A construction. Observed phenomena concur with this hypothesis in that analysis of failure planes "shifting" towards the deck.
The next question that requires answering is the question of which failure planes do not change, or have the most insignificant changes, due to a change in adhesive pattern. For Source 3, the failure plane does not change when ACB is used. Regardless of adhesion pattern, the facer ruptured when combined with the paper facer (6/6 for Type A, 5/6 for Type B) and the facer delaminated (6/6 for Type A, 5/6 for Type B) when combined with the acrylic facer. When combined with the acrylic facer for Source 4, under both Type A and Type B conditions all 6 observations for both resulted in facer delaminations.

6.8 Conclusions on Applications of the Test Method

Based on the results of this chapter several conclusions can be drawn. It was determined that the most consistent performing material combination of the four combinations studied was the PF & ACB combination. However AF & ACB showed the potential to exhibit similar consistency. Both of these combinations were superior to the AF & FB and PF & FB combinations – particularly when partial adhesion was applied between the insulation and the fiberboard. Observations confirmed the susceptibility of fiberboard to premature failure when partial adhesion was applied. The resulting conclusion that was drawn was that the type of coverboard that was employed played a significant role in pullout response.

Pullout experiments on specimens constructed with concrete decks exhibited more ductile failure than pullout experiments constructed with steel decks. This was due to the fact that steel deck deformations placed stress concentrations on the insulation facer – the result of which was a more brittle failure. It appeared that a more realistic approach for evaluating specimens constructed on concrete decks was to evaluate the amount of deflection that had incurred when the peak load was attained. Finally elastic energy calculations (area tabulated underneath the force-extension curve), determined that more work was required for failure of steel deck specimens than for concrete ones,

however this only proves that the work put into a steel deck specimen is the work caused to cause adhesive or cohesive failure as well as the work required to undergo deck deformation.

A different adhesion pattern between the deck and the vapour barrier brought around a few expected and unexpected observations. As expected, peak load measurements dropped on the order of 50-70% from the Type A application to the Type B application. As a result of the new adhesion pattern, failure planes tended to shift towards the location of where less adhesive had been applied. In Type B application, deflection at peak load measurements tended to increase. Elastic energy measurements on the whole dropped for six out of the eight source-material combinations, however when FB was applied for Source 3 elastic energy measurements increased. The hypothesis here is that the removal of adhesive from the Deck-VB level results in a stress concentration at this level that shields the typically weak FB from premature pullout failure.

In the following chapter, a standard test method for pullout evaluations of AARS specimens will be presented.

Chapter 7: Standard Test Method for the Pullout Resistance of Roofing Components Bonded using Cold Adhesives

One of the main objectives of this thesis is to draft a standard test method for the pullout resistance of AARS. A standard test method is presented in this chapter. Experimental results obtained in this thesis and input received from participating industrial partners formed the basis for this standard development. The draft is written following the format requirement of the ASTM standards. The format includes the scope, test apparatus, test conditions, procedures for the preparation of specimens and reporting of the test results. It is expected that this draft will be submitted to standard development organizations such as ASTM and CSA. Then this draft will undergo consensus process. Upon completion, this standard method will serve as a regulatory guide for Canadian roofing community in testing the pullout resistance of various AARS materials.

7.1 Introduction

The purpose of this test method is to determine the pullout resistance of roofing components bonded using cold adhesives. The proposed method described herein requires the use of tensile testing apparatus available in material science laboratories and universities. The accuracy of the test results will depend on the conditions under which the bonding process is carried out. Unless special arrangements have been agreed upon between the manufacturer and the purchaser, the manufacturer of the adhesive shall prescribe bonding conditions. In order to ensure that complete information is available to the testing agency, the manufacturer of the adhesive shall furnish numerical values and other specific information for each of the following variables:

(1) Procedure for preparation of the surfaces prior to application such as surface cleaning, drying and special surface treatments if any.

(2) Complete mixing directions for the adhesive.

(3) Conditions for the application of the adhesive, including the rate of spread or thickness of the film, number of coats to be applied – either on one or both of the component surfaces, and the conditions of drying.

(4) Assembly conditions before the application of pressure, including temperature and length of time.

(5) Curing conditions, including the amount of pressure to be applied, the length of time under pressure, and the temperature and relative humidity of the assembly while under pressure. It should be stated whether this temperature and relative humidity is that of the glue line, or of the atmosphere at which the assembly is to be maintained.

(6) Conditioning procedure before testing, unless a standard procedure is specified, including length of time and relative humidity.

(7) Range may be prescribed for any variable provided it is acceptable to both the manufacturer and the purchaser of the adhesive.

7.2 Scope

1.2.1 This test method covers the determination of the pullout resistance of roofing components with adhesive bond under specified conditions of preparation and testing

1.2.2 The values stated in SI units are to be regarded as the standard. The values given in parentheses are for information only.

1.2.3 This standard does not purport to address all of the safety concerns, if any, associated with its use. It is the responsibility of the user of this standard to establish appropriate safety and health practices and determine the applicability of regulatory limitations prior to use.

7.3 Referenced Documents

ASTM Standards:

- D 907 Terminology of Adhesives;
- D 2095-96: Standard Test Method for Tensile Strength of Adhesive by Means of Bar and Rod Specimens;
- D 7234-05: Standard Test Method for Pull-Off Adhesion Strength of Coatings on Concrete Using Portable Pull-Off Adhesion Testers;
- D 5179-02: Standard Test Method for Measuring Adhesion of Organic Coatings to Plastic Substrates by Direct Tensile Testing

ISO Standards:

- 15509: "Determination of the bond strength of engineering plastic joints"

European Standards:

- 1348: 2007 "Tensile Adhesive Strength of Ceramic Tiles After Conditioning"

SPRI Standards:

- FX1: 2006 "Standard Field Procedure for Determining the Withdrawal Resistance of Roofing Fasteners"
- IA-1-2005: 2005 "Standard Field Test Procedure for Determing the Mechanical Uplift Resistance of Insulation Adhesives over Various Substrates" IA-1-2005

FM Standadrds:

- FM I 52: 2007 "Field Uplift Tests"

7.4 Terminology

Many of the definitions used in this test method are more clearly explained in ASTM D 907

7.5 Summary of Test Method

This test method purports to quantify the pullout resistance of AARS. Tests are performed in a controlled environment with small modifications to standard laboratory tensile testing equipment. Tests are to be conducted at a fixed rate of deflection of 6.35mm/min. A test area of 300 x 450 mm is required and all flutes of steel deck have to be fastened.

7.6 Significance and Use

This test method is useful for acceptance and quality control testing. Adherends, application procedure, and sample conditioning shall be as agreed upon by the manufacturer and the user of the adherends and the adhesive.

7.7 Apparatus

7.7.1 Testing Machine

The testing machine shall have a load weighing system conforming to the requirements of Practice E 4. It shall have the capability of constant rate of extension (CRE) with a crosshead speed of 6.35 mm/min (0.25 in./min). Data acquisition capabilities from the machine will be required to determine the force-displacement response from the tested specimens. Any properly calibrated Instron machine, or similar machine, will suffice to perform this test method.

7.7.2 Specimen Mounting Platform

The specimen mounting platform is a flat, fixed, and rigid base that test specimens will sit on while the pullout test is performed. The platform should be a minimum of 75mm thick, 350 mm wide, and 600 mm long. Four pairs of holes 6.5 mm in diameter should be drilled along the perimeter of the platform with a center

to center distance of 125 mm along the 600 mm dimension as shown in Figure 7.1.

7.7.3 Specimen Mounting Platform Housing

The specimen mounting platform housing is a housing that is attached directly to the platform and creates a fixed rigid connection between the testing machine and the platform. The bottom clevis housing is illustrated in Figure 7.2, but any similar connection rigidly securing the specimen mounting platform will suffice.

7.7.4 Fixating Strips

The Fixating strips are 350 mm long x 25 mm wide x 12.5 mm thick steel strips. They have 6.5 mm diameter holes that can be superimposed over the holes on the platform to rigidly secure specimens while performing pullout testing. The fixating strips for steel deck specimens are illustrated in Figure 7.3.

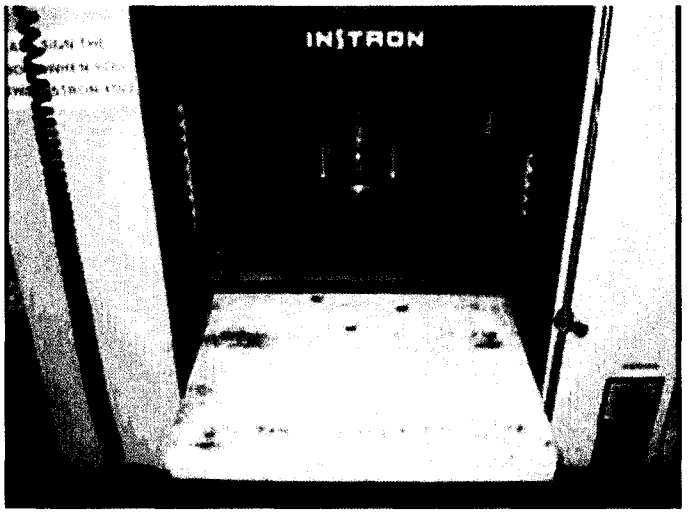

Figure 7.1: Attachment of Specimen Mounting Platform & Stress Plate

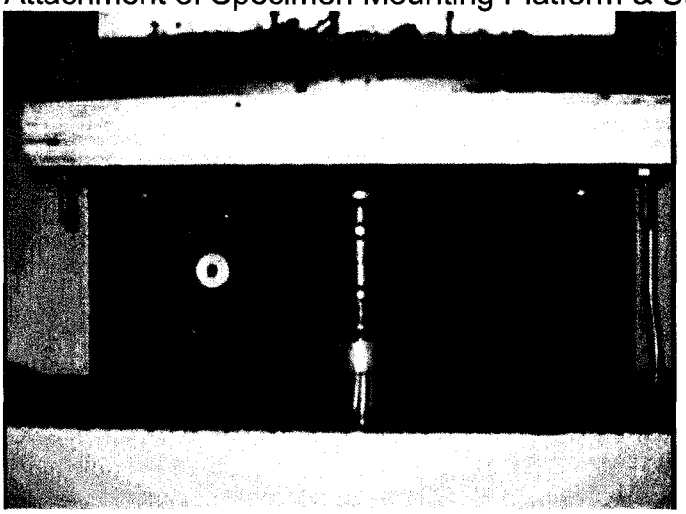

Figure 7.2: Rigid Connection of Specimen Mounting Platform

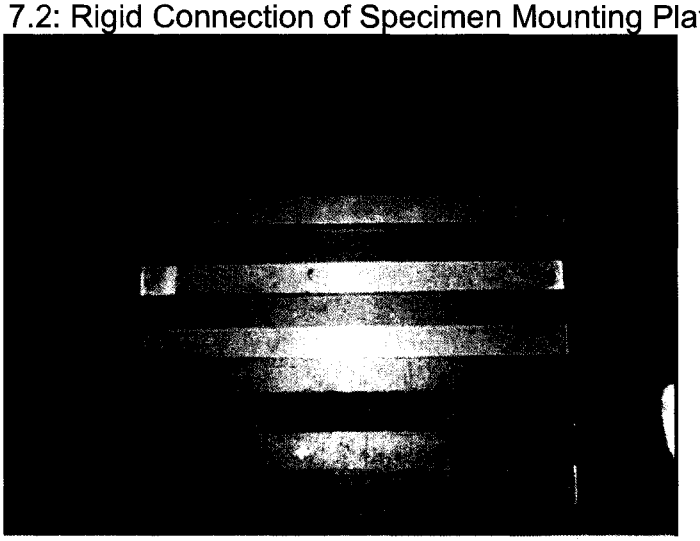

Figure 7.3: Steel Deck Fixating Strips

7.7.5 Stress Plate & Attachment Housing

The stress plate is a 300 mm wide x 450 mm long x 130 mm thick steel plate that will be superimposed overtop of the test specimens while testing is performed. Countersunk holes for 10 25 mm #10 Robertson wood screws are drilled into the plate to attach the specimen to the tension plate. The attachment housing will be rigidly and securely attached to the Instron machine. A pin member will be used to attach the tension plate and specimen to the movable crosshead of the tensile testing machine. The stress plate, and attachment housing assembly is illustrated in a plan view of Figure 7.4.

NOTE 1: There are 14 countersunk holes in the tension plate as shown in Figure 7.4. There are 8 holes in the corners of which 4 of these holes are redundant.

7.8 Specimen Preparation

- A minimum of six specimens per condition are constructed with steel deck, vapour barrier, insulation, coverboard, base sheet and cap sheet as per manufacturers agreed conditions. Cold adhesives will be used to bond all construction materials and a minimum of 28 days is required for adhesives to cure. Deviations from this procedure are permitted but must be agreed upon prior to the construction of test specimens;
- Upon completion of adhesive curing, the cap sheet is cleaned of loose-lying debris and a plywood dummy 300 mm x 450 mm is superimposed over the specimen and glued directly onto the cap sheet. The optimum glue to be used can be a two-part epoxy and polyurethane expanding adhesive, however any adhesive that exhibits similar physical properties to the epoxy-polyurethane mix is acceptable. A 24 hour cure time is required for the dummy adhesive, however follow the prescribed manufacturer's instructions for cure time and optimal curing conditions.

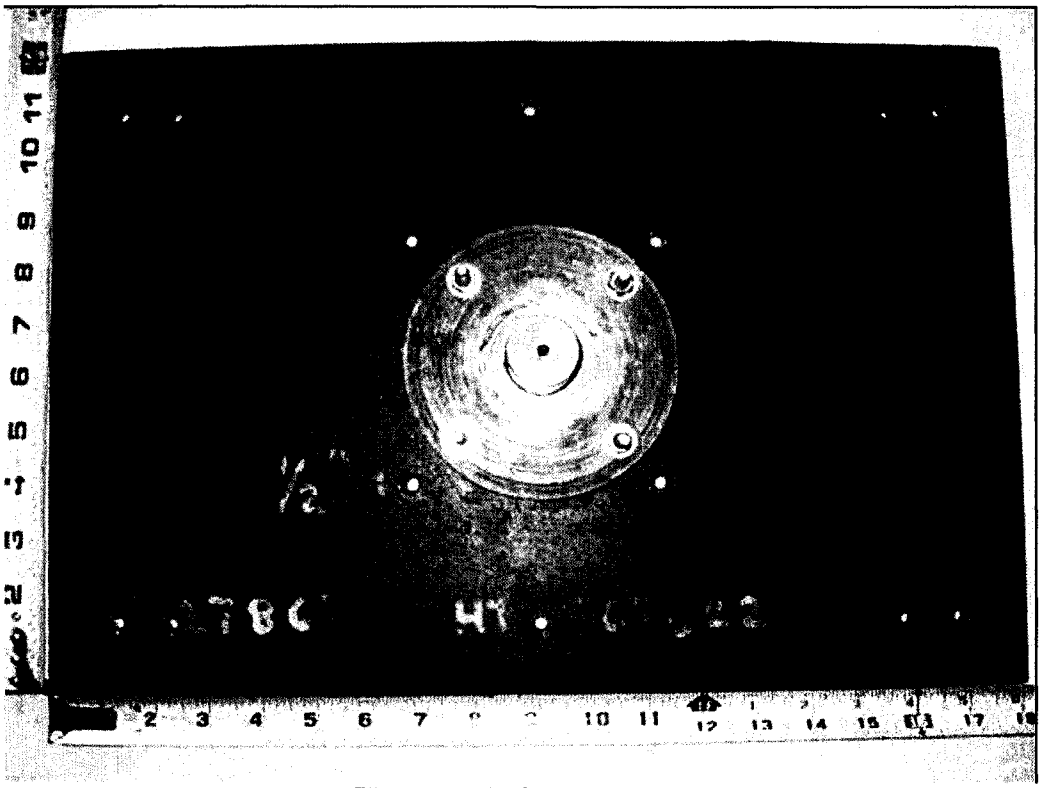

Figure 7.4: Stress Plate

Figure 7.5: Instron Frame with AARS pullout testing equipment installed

7.9 Test Method

- An overview of the experimental setup without a specimen installed is illustrated in Figure 7.5;
- Center the first specimen to be tested on the platform and align holes in the specimen mounting platform with the male flutes on the steel deck of the test specimen;
- Place fixating strips through the male flutes and superimpose holes on the strips with the holes on the platform. Place 75 mm long bolts through the strips and the platform. Secure the specimen with appropriately sized nuts and tighten with a ratchet;
- With the specimen rigidly secured to the platform, jog the crosshead so that the stress plate sits overtop of the plywood specimen. Remove the stress plate from the attachment housing by removing the pin that secures it in place. Jog the crosshead up approximately 300mm;
- Fasten the tension plate to the plywood dummy with 10, 25 mm wood screws. Jog the crosshead back to its original position and replace the pin in the attachment housing to re-secure the connection;
- Manually remove the slack in the test setup by jogging the crosshead until the load reading is +/- 10 N. Manually set the gauge length to zero;
- Run the test until catastrophic failure has been achieved. Carry the test method out backwards to remove the specimen from the test frame and repeat for the required number of repetitions.

7.10 Calculation

The following parameters should be determined.

- A force-deflection curve;
- The peak load obtained during testing;
- The deflection observed at peak load.

7.11 Report

Report the following information:

- Complete identification of the adhesive tested including type, source, etc.
- Compete description of the test specimen, including all of the materials used to construct the specimen. Take particular note of the type of coverboard material, and insulation facer type.
- Description of bonding process, including method of application of adhesive, glue-line thickness, assembly methods, curing time, temperature and relative humidity.
- Testing temperature.
- Type of test machine.
- Number of pullout tests performed, including average value obtained, maximum, minimum and standard deviation of the sample.
- Description type of failure mode for each individual specimen. The failure mode is pre-defined by test operator or manufacturers

Chapter 8: Conclusions & Future Objectives

8.1 Introduction

As exemplified by the findings of chapter 2, many standards exist today for quantifying pullout performance of materials for both wind and other loading applications. However, none of these standards relate to wind-induced uplift failure related directly to adhesive roofing systems. As a result, the undertaking of an experimental review of AARS performance when subjected to pullout loading was required.

In chapters 1 & 2, the necessity and justification for a test method for evaluation of AARS was outlined. In chapters 3 & 4, definitions were provided for the constituents of AARS, test equipment and a broad plan to accomplish the objectives outlined in Chapter 1. In Chapter 5, the key variables that needed specifying in order to develop a standard test method were specified. In Chapter 6 the parameters of the proposed test method were applied to different AARS configurations to determine the effect of a specific variable on overall pullout performance. Chapter 7 presented a proposed test method based on the findings of Chapter 5. In this chapter, a summary of the results will be presented in section 8.2, highlighting the key findings of this experimental endeavour. Having highlighted the major contributions, in section 8.3, a critical assessment of the work presented in this thesis will be presented as well as the areas where possible errors may have been incurred. Finally, areas of possible future research and the reasons why it is necessary for this research to be undertaken will be presented in section 8.4.

8.2 Summary of Research

Based on the literature survey of Chapter 2, three variables required specification in order to develop the test method shown in Chapter 7. The first that required specification was the rate at which deflections or stresses were

induced. Based on a series of experiments that were conducted at 1.27, 2.54, 6.35, and 12.7 mm/min, 6.35mm/min was selected. These reasons are:

- Regardless of the construction protocol (full or partial adhesion) and source, 6.35 mm/min corresponds to a local maximum peak load with respect to other pullout rates.
- Normalized sample standard deviation of peak load is a minimum at 6.35 mm/min.
- 6.35 mm/min exhibits the most consistent location of failure plane when compared to the three other pullout rates.

After specifying the pullout rate, the specimen size required specification. After undertaking experimentation with specimen sizes of 300 x 450 mm and 300 x 900 mm, it was determined that 300 x 450 mm exhibited superior results and should be the specimen size: Reasons for its selection include:

- 300 x 900 mm specimens failed over the course of a larger range with respect to the 300 x 450 mm specimens.
- 300 x 450 mm specimens were able to deflect significantly more before the onset of catastrophic failure which lead to the assumptions that 300 x 450 exhibited more ductile failure
- The failure planes of 300 x 450 mm specimens exhibited less dependence on construction protocol than 300 x 900 mm specimens.

In addition to the two preceding variables, it was also important to determine whether there was evidence supporting the notion that there was a discernible difference between different fixation conditions and overall pullout results. Comparisons of results of different fixation conditions resulted in similar trends in both quantitative measurements and in failure planes.

With the key variables specified and empirical evidence supporting their selection, the next step was to apply the test method in order to further characterize pullout behaviour of AARS. Of specific interest, was to characterize the pullout behaviour of different AARS materials. At the completion of a series of

experiments by testing four different material combinations, the lessons learned include:

- The PF & ACB material combination exhibits superior performance but AF & ACB also exhibits good pullout performance as well.
- PF & FB and AF & FB exhibit extremely poor performance. This performance is even worse when partial adhesion is applied.
- The latter two observations lead to the conclusion that coverboard plays a significant role in the pullout behaviour of AARS.
- With respect to AF & PF, the only consensus is that PF exhibits superior consistency than AF with respect to deflection at peak load measurements.
- By combining the effects of load and displacement and calculating elastic work, there are three broad ranges over which failures occur. There is the performance of fully adhered PF & ACB (excellent, > 4.0 J), there is also the performance of all other fully adhered material combinations and partially adhered combinations with ACB (good, 2.0 – 2.5 J) and the performance of partially adhered FB (inadequate, 1.0 – 1.1 J)

After completing analysis of the data of different material combinations, different decks were tested under pullout testing. Key lessons include:

- Steel deck attained marginally higher peak loads than concrete deck
- When comparing deflection at peak load, steel deck vastly outperformed concrete decks, and as a result exhibited superior elastic energy performance as well.
- Much of the physical interpretation of the data is predicated on the fact that steel deck calculations are measurements of the deformation of the steel decking.
- Empirical analysis of concrete deck specimens illustrate a large degree of scatter, scatter that is also found in failure plane analysis in a significant number of both adhesive failures and facer delaminations – indicative of opposites in the spectrum of failure.

Finally, different adhesion patterns were tested. Different adhesion patterns resulted in:

- A range of 60-80% reduction in pullout strength when comparing Type B adhesion with Type A adhesion
- Failure planes shifting in the specimen closer to the location where adhesive was deliberately omitted.

These correspond to the major findings of this research endeavour.

8.3 Critical Review of Research

At the completion of an experimental investigation it is necessary to reflect upon the work and to use the lessons learned to critically assess the quality of the experimental work. Overall there were a few areas hindsight would have assisted in providing results with superior clarity.

Perhaps the greatest shortcoming of the test is the amount of inherent eccentricity built into the results. Numerous factors conspire to prevent testing from being true pullout testing: different layers of construction materials with beads of adhesive applied in between, full adhesion, the shifting of specimens during adhesive curing. There are numerous factors conspiring to render it impossible to quantify how much is pure pull tension, and how much is bending and shearing due to the configuration. There is no way to quantify this, and it remains a significant shortcoming of this investigation.

As mentioned in section 5.4, in the application of partial adhesion, neither measurements were taken of the characteristic dimensions of the beads of adhesive, nor were observations taken to qualitatively describe them. This is a major shortcoming of this experimental work . In the absence of this information it is impossible to predict the behaviour of the adhesive joint. In future analysis it is imperative that at minimum, observations of the amount and location of the adhesive be noted.

Another shortcoming of this study is the lack of different sizes tested. Only two sizes were tested with one common width (300 mm). The facilities could have accommodated specimens of a length between 450 and 900 mm, while still working within the 100 mm center to center flute spacing of steel decking. Also no size corroboration was performed with concrete deck specimens although this was performed with specimens constructed on steel deck.

8.4 Future Research

Since the research work presented herein is only part of a pilot investigation, there is still abundant room for further research, particularly expanding the data pool of findings of Chapter 6.

One of the variables that was specified in many of the standard test methods, but not tested in this study was the temperature at which specimens were conditioned, cured or tested. Due to seasonal variances in temperature, it may be of interest to populate Time-Pullout Performance curves similar to those found in figure 5.4 for pullout rate.

Logistical issues and limitations of the Instron machine realistically prevented testing of specimens that exceeded a width of 300 mm. The development of equipment and peripherals to test specimens with sizes that exceed this dimension would greatly enhance the nature of how specimen size affects pullout performance. The lack of testing equipment to facilitate larger specimens is a major impediment at the moment.

Pullout testing has been performed on at least two possible decks, insulation facers, and coverboard materials. However, roofing technology is constantly evolving and new techniques and materials are constantly being developed or modified. The effects of another deck like tongue and groove plywood should also be analyzed. A material similar to gypsum board, densedeck is frequently used as a coverboard and should be tested with different types of insulation. Finally, a tinfoil faced insulation should also be tested and

with these multiple combinations of deck and materials, it will be easier to characterize AARS pullout performance.

Bibliography

Standards

American Society for Testing and Materials (1996), "Standard Test Method for Tensile Strength of Adhesive by Means of Bar and Rod Specimens", ASTM D 2095-96, USA

American Society for Testing and Materials (2005), "Standard Test Method for Pull-Off Adhesion Strength of Coatings on Concrete Using Portable Pull-Off Adhesion Testers" ASTM D 7234-05, USA

American Society for Testing and Materials (2002), "Standard Test Method for Measuring Adhesion of Organic Coatings to Plastic Substrates by Direct Tensile Testing", ASTM D 5179-02, USA

European Standards (2007), "Adhesives for tiles – Determination of tensile adhesion strength for cementitious adhesives", BE EN 1348

Factory Mutual Global (2007) "Field Uplift Tests", FM 1-52.

The International Organization for Standardization (2001), Determination of the bond strength of engineering plastic joints", ISO 15509

Single Ply Roofing Industry (2005), "Standard Field Test Procedure for Determing the Mechanical Uplift Resistance of Insulation Adhesives over Various Substrates" ANSI/SPRI IA-1-2005

Single Ply Roofing Industry (2006) "Standard Field Test Procedure for Determining the Withdrawal Resistance of Roofing Fasteners" ANSI/SPRI FX-1-2006

Resources

Baker, M., (1964) "New Roofing Systems." Canadian Building Digest 49, National Research Council Publication

Baskaran, A., Desjarlais, A., Roodvoets and D., "Hurricane Katrina Wind Investigation Report, Powder Springs, Georgia: Roofing Industry Committee on Weather Issues", Inc. pp. 183, August 01, 2007 (NRCC-50024)

Baskaran, A. and Lei, W. (1997), "New Facility for Dynamic Wind Performance Evaluation of Roofing Systems", Proceedings of the Fourth International Symposium on Roofing Technology, (Gaithersburg, MD., USA, September 17, 1997), pp. 168 -179.

Baskaran, A., Molleti, S., Sexton, (2006) M. "Wind performance evaluation of fully-bonded roofing assemblies" Journal of Construction and Building Materials 22, pp 343-363

Banks D. (2000) "The suction induced by conical vortices on low-rise buildings with flat roofs", Ph.D. Thesis, Department of Civil Engineering, Colorado State University, Fort Collins, Colorado,

Banks, D., Meroney, R.N., Sarkar p.P., Zhao, Z., Wu, F. (2000) "Flow visualization of conical vortices on flat roofs with simultaneous surface pressure measurement", Journal of Wind Engineering and Industrial Aerodynamics. 84 pp 65-85

Current, J, Murty, B., Wu, J., Baskaran, A., Tanaka, H. "Wind uplift resistance data for adhesive applied roofing systems - Part 1," pp. 1-236, January 01, 2007 (IR-876)

Garcia, R., (1997) "Roofing Materials", Kirk-Othmer Encyclopedia of Chemical Technology. John Wiley & Sons, Inc.

Kirby, J., (2006) "Getting Stickier". Professional Roofing: June 2006.

Molleti, S. (2006), "Performance Evaluation of Mechanically Attached Roofing Systems.", PhD. Thesis, University of Ottawa, Ottawa, Canada

Murty, B.; Current, J., Wu, J., Baskaran, A.; Tanaka, H. "Wind uplift resistance data for adhesive applied roofing systems - Part 2," pp. 1-180, January 01, 2008 (IR-877)

Murty, B., Current, J., Davelay, C., Baskaran, A., Tanaka, H. "Wind uplift resistance data for adhesive applied roofing systems - Part 3," pp. 1-120, August 01, 2008 (IR-878)

Phalea, T., "Design and Analysis of Single-Ply Roof Systems", 1993

Wu, J (2008) "Development of a Peel Test Procedure for Adhesive Applied Roofing Systems." M.A.Sc. Thesis, Department of Civil Engineering, University of Ottawa, Ottawa, Ontario.

Websites

www.allsteel-buildings.com (March, 2009)
http://cmroof.com/ (March, 2009)
www.ddinstallations.com (March, 2009)
www.milleniumadhesives.com (March, 2009)
www.reliantroofingsystems.com (March, 2009)
www.yourguardianroof.com (March, 2009)